

STUDY OF AN INTERNAL COMBUSTION ENGINE TO BURN HYDROGEN FUEL
AND BACKFIRE ELIMINATION USING A CARBURETOR FUEL DELIVERY
METHOD

by

Shahriyar Garmsiri

A Thesis submitted in Partial Fulfillment
of the Requirements for the Degree of
Masters of Applied Science in Mechanical Engineering

Faculty of Engineering and Applied Science Program
UOIT (University of Ontario Institute of Technology)

April 2010

© Copyright by Shahriyar Garmsiri (2010)

ABSTRACT

Hydrogen appears to be a clean and sustainable fuel for transportation vehicles, including internal combustion engine vehicles. In this research, a 1986 GMC Sierra truck with a 350CID 5.7L V8, 4 barrel carbureted Chevrolet gasoline engine is converted to burn hydrogen as a sustainable and environmentally benign fuel with a shorter energetic cycle. It demonstrates that the problems of backfire can be eliminated using several less expensive methods, such as employing cold spark plugs with reduced spark gap and low temperature cooled valves along with the introduction of water vapor to the mixture.

In the experiments, the internal combustion engine was tested for two fuels: (i) octane 95 gasoline, and (ii) gaseous hydrogen at 99% purity. The vehicle underwent dynamometer tests using both the gasoline and hydrogen fuels for performance comparisons. A comprehensive thermodynamic analysis, through energy and exergy, of the engine is conducted for both cases: (i) with the octane 95 gasoline fuel and (ii) with hydrogen gaseous fuel. The performance results through energy and exergy efficiencies are compared for possible improvements.

The mileage and energy efficiencies calculated and tested using this engine showed that it is more efficient operating on gasoline fuel rather than hydrogen. This is explained fully in the thesis as to the properties of hydrogen and gasoline fuels that differ, and the particular vehicle technology makes this difficult to achieve a reasonable mileage and efficiency.

*To my father, mother, and brothers,
my beloved family for all their support*

ACKNOWLEDGEMENTS

This thesis would not have been made possible without the supervision of my advisor Professor Dr. Ibrahim Dincer, who has been supervising my progress with this project. All his efforts are appreciated, who has shown complete trust in this project. Furthermore, I would like to thank Dr. Vinh Quan and Dr. Ebrahim Esmailzadeh for their guidance, support and faith in this thesis is highly appreciated. I would like to thank the members of the ATW Automotive, for providing me with useful information in regards to converting a vehicle to natural gas and hydrogen, and special thank goes to Ray Wolting and his staff Rob and Ralph for sharing their knowledge in the automotive field of applications.

I would like to thank Ron Wensel for providing his expertise and knowledge in the 1980's style Chevrolet trucks. Also acknowledgements go to Mr. G. Rymal Smith for donating a hydrogen tank for testing purposes on this project. Furthermore, I would like to thank OCE for providing funding in this research as well as CNE for allowing the opportunity to make this research possible. Acknowledgements go to Stephen Wilcox, airport manager at the Oshawa Municipal Airport for providing space to store some of the project vehicles. Many thanks go to Marc Hubert, Project Coordinator of Hydrogen on the Hill Project for providing some information on the Hydrogen powered Ford E450 shuttle bus. Lastly, I would like to acknowledge Bob Walduck from Princess Auto with his vast knowledge in Carburetor engines and guidance in identifying parts and the safety precautions while converting the GMC Sierra truck using hydrogen via the carburetor. Lastly I would like to thank Othman J. Jaber and Pouya Saneipour for their help, support and contribution for the experimental setup.

TABLE OF CONTENTS

PRELIMINARY SECTIONS

Abstract	ii
Dedication	iii
Acknowledgement	iv
Table of Contents	v
List of Symbols	vii
List of Tables	ix
List of Figures	x
CHAPTER 1: INTRODUCTION.....	1
1.1 Preamble	1
1.2 Benefits of burning hydrogen	2
1.2.1 Clean	2
1.2.2 Safe	3
1.3 Multiple Sources	4
1.4 Hydrogen Storage	5
1.5 Environmental Impacts	5
1.6 Economic Factors.....	6
1.7 Security of Fossil Fuel Resources.....	6
1.8 Motivation and Objectives of Thesis	6
1.8.1 Thesis Approach and Process Synopsis	8
1.9 Theoretical Background – Engine History	9
CHAPTER 2: LITERATURE REVIEW	12
2.1 Literature Review and Patent Search.....	12
2.2 Literature Review on Engines.....	12
2.2.1 HEC Engines.....	12
2.2.2 Patent Search.....	13
2.2.3 Literature Publication Review	14
CHAPTER 3: EXPERIMENTAL SETUP	29
3.1 Introduction.....	29
3.2 Engine Modifications and Parts Installation	30
3.2.1 Engine Fluid Drain, Parts Removal and Installation	30
3.2.2 Tank Mount and Fuel Line Installation	34
3.2.3 Combustion Aspects of Hydrogen in SI Engine	35
CHAPTER 4: EXPERIMENT ANALYSIS	37
4.1 Air Mass Estimation	37
4.2 Kinetic Modeling of the Pre-flame Reactions	38
4.3 Standardized Equation for Hydrogen Gas	39
4.4 Thermodynamics of ICE.....	41

4.5 Analysis of the Gas Exchange Stage	45
4.6 Energy and Exergy Analyses	48
4.6.1 Experimental Setup and Testing Procedure	49
4.7 Fuel Economy and Engine Characteristics	58
4.8 Fuel Economy Calculation for Gasoline Fuel	58
4.9 Fuel Economy for Hydrogen Fuel	61
4.10 Engine Characteristics	68
CHAPTER 5: PARAMETRIC STUDY.....	80
5.1 Parametric Contributing in the Design for Water Injection.....	80
5.2 QFD House of Quality	83
5.2.1 Interactions between Parameters.....	83
5.2.2 Formulation of Rigidity Index	85
5.2.3 Decision Making Sequence.....	87
5.3 TRIZ Methodology	89
5.3.1 39 Design Parameters	89
5.3.2 40 Inventive Principles	89
5.3.3 Axiomatic and Contradiction Matrix	90
5.4 Six Sigma Methodologies	91
5.5 Regression Analysis, DOE, and ANOVA	92
5.6 Failure Mode-Effect Analysis.....	95
5.6.1 FMEA Analysis and Poke-Yoke method.....	95
5.6.2 Poke-Yoke approach.....	97
5.7 Detailed Design.....	100
5.8 Designs for Excellence (X).....	101
5.9 Axiomatic Design	103
5.9.1 Axiom 1	104
5.9.2 Axiom 2	104
CHAPTER 6: CONCLUSIONS AND RECOMMENDATIONS FOR FUTURE WORK	105
6.1 Conclusions.....	105
6.2 Future Work	107
REFERENCES.....	109
APPENDIX A	123
APPENDIX B	124
APPENDIX C	125
APPENDIX D	128

NOMENCLATURE

$A(t)$	Throttling area [m ²]
AF_{ratio}	Air fuel ratio
$B_i^*(T)$	Temperature dependent pressure virial coefficient [K]
b	Specific fuel consumption [lb/bhp.h]
c	Specific heat [J/(kg K)]
c_d	Discharge coefficient
c_p	Specific heat at constant pressure [J/ (kg K)]
c_v	Specific heat at constant volume [J / (kg K)]
CV	Calorific value [kJ/kg]
D	Diameter valve [m]
D_i	Diameter intake valve [m]
\dot{E}	Energy flow [J/s]
$\dot{E}x_{\text{dest}}$	Exergy destruction [W]
ex	Specific exergy [kJ/kg]
$E_{\text{displacement}}$	Engine size [L]
G	Gibbs energy [W]
h	Specific enthalpy [J/kg]
h_c	Specific enthalpy of in-cylinder gas [J/kg]
H_{ib}	Specific enthalpy of backflow gas [J/kg]
H_e	Specific enthalpy of exhaust gas [J/kg]
i_o	Unit gear ratio
i_g	Final gear ratio
k	Heat transfer coefficient [W/ (m ³ K)]
K_b	Kinetic constant direct reaction speed [m/s]
K_f	Kinetic constant inverse reaction speed [m/s]
L	Length of intake valve [m]
$\dot{m}_\alpha(t)$	Mass air flow [kg/s]
M	Molar mass [g/mol]
\dot{M}_i	Inlet valve mass flow rate [kg/s]
\dot{M}_{ib}	Inlet valve mass backflow rate [kg/s]
\dot{M}_e	Exhaust valve mass flow rate [kg/s]
\dot{M}_{eb}	Exhaust valve mass backflow rate [kg/s]
N	Normalization constant
n_A^a	Concentration of species and stoichiometric coefficient a
n_p	Engine speed [RPM]
P_{ambient}	Ambient pressure [kPa]
P_{final}	Final pressure [kPa]

P_{initial}	Initial pressure [kPa]
$P_{\text{in}}(t)$	Inlet pressure [kPa]
P_e	Power output [W]
P_w	Aerodynamic power [W]
P_f	Frictional power loss [W]
P_m	Manifold pressure [kPa]
\dot{Q}	Heat flow [W]
\dot{Q}_{ev}	Heat transfer rate to the exhaust valve area [W/m ²]
\dot{Q}_{loss}	Heat loss rate [W]
R	Gas constant [J/kg K]
r	Rolling resistance coefficient
St_v	Stanton number [N_{st}]
\dot{S}_{gen}	Entropy generation [J °C]
T	Temperature [K]
u	Specific internal energy [J/kg]
u_a	Vehicle speed [km/hr]
v	Specific volume [m^3 /kg]
V	Volume [m^3]
V_m	Manifold volume [m^3]
v_a	Ambient air velocity [m/s]
V_d	Displacement [m^3]
\dot{V}	Volumetric flow rate [m^3 /s]
\dot{W}	Power [W]
\dot{W}_{sh}	Shaft work [W]

Greek Symbols

γ	Angle[°]; heat ratio
Δm	Vibe parameter
λ_v	Volumetric efficiency [%]
ρ	Density [kg/ m^3]
ψ	Outflow function
$\omega_e(t)$	Exhaust swirl [rad/s]
Θ	Angle around tube bend [°]
η_m	Mechanical efficiency [%]
η_{th}	Thermal efficiency [%]
η_v	Volumetric efficiency [%]

LIST OF TABLES

Table 1.1: Combustion reaction characteristics of different fuels	3
Table 3.1: Natural gas conversion diagram for carburetor type engines	30
Table 3.2: Properties of hydrogen and gasoline.....	36
Table 4.1: Technical specifications of 5.7L engine	51
Table 4.2: Emission test results running on gasoline fuel.....	76
Table 4.3: Emission test results running on hydrogen fuel.....	76
Table 5.1: Design parameters chosen for analysis.....	82
Table 5.2: Rigidity matrix parametric analysis.....	86
Table 5.3: Quality characteristics vs. demand quality	86
Table 5.4: Customer requirement quality demand.....	87
Table 5.5: Ranked rigidity index percentage	87
Table 5.6: TRIZ Matrix.....	90
Table 5.7: Water pump and solar panel data information.....	91
Table 5.8: Factor analysis using ANOVA method	92
Table 5.9: Regression analysis using factors	93
Table 5.10: FMEA analysis	99

LIST OF FIGURES

Figure 3.1: Vacuum lines removed and capped on carburetor	31
Figure 3.2: TN2 regulator	32
Figure 3.3: Gas Mixer assembly	32
Figure 3.4: Hose connected from regulator to mixer	33
Figure 3.5: Relay with all wires connected.....	33
Figure 3.6: Four mount brackets with welded screws on the brackets	34
Figure 3.7: Hydrogen test tank with brackets	35
Figure 4.1: Typical location of a mass air flow sensor	38
Figure 4.2: Closed thermodynamic system in a piston.....	42
Figure 4.3: Open thermodynamic system in a piston	43
Figure 4.4: Energy balance on the in-cylinder gases with various terms	46
Figure 4.5: Energy balance of the backflow zone	46
Figure 4.6: Energy balance on the exhaust gas zone	47
Figure 4.7: Typical inlet valve with various distances identified.....	48
Figure 4.8: 1976 Chevrolet small block 350 5.7L V8	50
Figure 4.9: Layout of the experimental apparatus	50
Figure 4.10: Layout of the experimental apparatus in 1986 GMC Sierra 1500	51
Figure 4.11: Engine on hydrogen components	52
Figure 4.12: Engine on hydrogen components	52
Figure 4.13: Illustration of engine on gasoline fuel operations	53
Figure 4.14: Illustration of engine on hydrogen fuel operations	53
Figure 4.15: Energy efficiency of engine operating on gasoline fuel.....	56

Figure 4.16: Energy efficiency of engine operating on hydrogen fuel	56
Figure 4.17: Exergy efficiency of engine operating on gasoline fuel.....	57
Figure 4.18: Exergy efficiency of engine operating on hydrogen fuel.....	57
Figure 4.19: Specific fuel consumption map of a V8 engine	59
Figure 4.20: Time vs. pressure of hydrogen usage in a 5.7L V8.....	62
Figure 4.21: Brake specific fuel consumption for gasoline fuel.....	63
Figure 4.22: Brake specific fuel consumption for hydrogen fuel	64
Figure 4.23: Gasoline mass air flow rate in 5.7L V8 engine	65
Figure 4.24: Hydrogen mass air flow rate in 5.7L V8 engine	66
Figure 4.25: Gasoline mass fuel flow rate in 5.7L V8 engine	66
Figure 4.26: Hydrogen mass fuel flow rate in 5.7L V8 engine	67
Figure 4.27: Air fuel ratio for both gasoline and hydrogen fuel.....	67
Figure 4.28: 1986 GMC Sierra 1500	68
Figure 4.29: 1976 Chevrolet small block 350.....	69
Figure 4.30: -barrel Rochester quadrajjet M4MED carburetor	69
Figure 4.31: Dynamometer test results for gasoline fuel.....	70
Figure 4.32: Dynamometer test results for gasoline fuel.....	72
Figure 4.33: Hydrogen and gasoline fuel net power output graph	74
Figure 4.34: Hydrogen and gasoline fuel torque output graph.....	74
Figure 4.35: Brake mean effective pressure for both gasoline and hydrogen	75
Figure 4.36: Water nozzle location.....	76
Figure 4.37: Water nozzle demonstration.....	77
Figure 4.38: After-market headers.....	78

Figure 4.39: Spark plug wire modification.....	79
Figure 5.1: House of Quality QFD chart.....	84
Figure 5.2: Rigidity Index graph.....	88
Figure 5.3: Water pump.....	91
Figure 5.4: Solar panel.....	91
Figure 5.5: Main effect plot for A.....	94
Figure 5.6: Main effect plot for total value.....	94
Figure 5.7: Main effect plot for means.....	95
Figure 5.8: Water pump and water storage.....	96
Figure 5.9: Water pump and water storage enclosure.....	100
Figure 5.10: Water storage and pump location.....	100
Figure 5.11: Pump mounted to the bottom of the tank.....	102
Figure 5.12: Power cable and sealant.....	102
Figure 5.13: Water tank with open top.....	103

Chapter 1

INTRODUCTION

1.1 Preamble

In today's high energy demand to run the high tech equipments, which have made the living conditions much easier, there still exist a struggle to keep the high pollution trend low, while keeping up with the high energy demand, and this has become a great issue in today's society. This is specially seen in the automotive transportation sector, which has created a big environmental impact. According to Natural Resources Canada (NRC) [1] a study done in 2003, it shows that the energy usage of the automotive transportation sector has been about 29% of the overall energy consumption. Meanwhile, in the study [1] conducted by the NRC showed that the automotive sector has been one of the major contributions to the greenhouse gases (GHG) producing 34% of the overall GHG produced annually.

Thus many engineers and researchers have been developing alternative methods of providing this high energy demand while considering the environmental impact. Many researchers have concluded that by using hydrogen as energy carrier can help reduce the greenhouse gases being produced to help contribute to a cleaner environment. This can be achieved through the use of renewable alternative sources of electric production such as solar, wind, and water energy, which can be used to produce hydrogen and use this hydrogen as a source of energy transfer through the use of fuel cells and also as a source of fuel in the automotive internal combustion engine applications.

Using hydrogen as a fuel there are several advantages [2], it has a carbon neutral property when obtained from renewable sources of energy, and a shorter energetic cycle than the fossil fuel. There are several benefits of burning hydrogen as a source of fuel, and some of these include:

- cleanliness,
- safety,
- multiple sources,
- environmental,
- economic, and
- security of fossil fuel resources.

In the next section the above mentioned benefits are fully explained in detail.

1.2 Benefits of Using Hydrogen as a Fuel

1.2.1 Clean

Hydrogen when produced from a renewable source of energy is a clean fuel. During the combustion process in an Internal Combustion Engine (ICE), when the hydrogen fuel is burned it produces water vapors. The heat generated during this stage is enough to keep the nitrogen emissions extremely low. The emissions produced are sufficiently low that the hydrogen powered Internal Combustion Engines can still pass Super Ultra Low Emission Vehicle (SULEV) emissions standard one of the strictest in the United States of America [3].

1.2.2 Safety of Hydrogen as a Transportation Fuel

Public perception about the safety of hydrogen is a major issue facing this alternative clean source of fuel. While hydrogen has many safety issues to be addressed, the perception such as the Hindenburg and the hydrogen bomb clouds hydrogen's safety as a fuel [4]. The Hindenburg disaster was believed that hydrogen was the main reason, although the primary cause for this disaster was the highly flammable coating used on the zeppelin. These perceptions can be allayed through education and hydrogen awareness outreach programs. The hydrogen material safety data sheet, which explains the characteristics of hydrogen as odorless, colorless, and does not cause harm when exposed to Skin, eye and ingestion; furthermore, the combustion reaction characteristics in different fuels are compared in Table 1.1.

Table 1.1: Combustion reaction characteristics of different fuels

<i>Characteristic</i>	<i>Hydrogen</i>	<i>Natural Gas</i>	<i>Gasoline</i>
Lower heating value kJ/g	120	50	44.5
Self-ignition temperature (°C)	585	540	228-501
Flame temperature (°C)	2,045	1,875	2,200
Flammability limits in air (vol%)	4 -75	5.3 - 15	1.0 - 7.6
Minimum ignition energy in air (uJ)	20	290	240
Detonability limits in air (vol%)	18 -59	6.3 -13.5	1.1 -3.3
Theoretical explosive energy (kg TNT/m ³ gas)	2.02	7.03	44.22
Diffusion coefficient in air (cm ² /s)	0.61	0.16	0.05

Source: [5]

In addition to the safety concerns that consumers have regarding hydrogen fuel, when working with hydrogen there are important technical considerations to be focused on. The amount of energy needed to ignite hydrogen is similar to natural gas, however, it is one-tenth of the energy required to ignite gasoline fuel. Hydrogen has properties that

are more beneficial than gasoline, it is nontoxic and it is difficult to gather a high enough concentration of hydrogen to combust. This is so, due to its low density and buoyant nature, unlike gasoline, when leaked, it can puddle at the source and build the emitted fumes, leading to an explosive scenario.

1.3 Multiple Sources

There are multiple ways of producing hydrogen using both traditional and renewable sources of energy. Electrolysis is one method of hydrogen production that uses electricity to split up the water molecules (H_2O) into Hydrogen (H_2) and Oxygen (O_2) gases. One advantage of electrolysis is that the process can be done using renewably-sourced electricity, so that the produced hydrogen is the energy carrier. Another method includes the hydrolysis of water with another compound such as methane, ammonia, ethanol, and alkali metal hydrides can be used to produce hydrogen.

Other methods of hydrogen production under development include thermo chemical water-splitting using solar energy, and nuclear power, using high temperature water splitting, specifically using waste heat from the plant has the capability of producing massive amounts of hydrogen while drastically cutting carbon emissions are being strongly promoted as solutions. Other clean sources of hydrogen would incorporate energy conversion from solar panels, wind turbines, biomass and biological energy.

1.4 Hydrogen Storage

Hydrogen can be stored in many ways, in gaseous, liquid and solid form. Hydrogen can be stored in gaseous form using steel tanks that can support up to 0.5 -1% by weight hydrogen storage and can hold hydrogen gas at a pressure of up to 35 MPa (5,000 psi). Furthermore, hydrogen can be stored in composite tanks in gaseous forms; which have a higher storage capacity compared to the steel tanks. 7% by weight and pressures of up to 69 MPa (10,000 psi), composite tanks weigh less than steel tanks. Hydrogen can be stored in liquid form, or formally known as cryogenic, this is a condensed gas which takes place for hydrogen to be liquefied at 20.28K (-252.87°C) temperature.

Lastly, hydrogen can be stored in a solid state form, it is considered to be stored in a solid state form, as the hydrogen is stored using hydrides. Some applications are metal hydrides, Alkali metal hydrides, Sodium borohydrides, carbon nanotubes, and zeolites, which the molecules would chemically bond with the hydrogen molecules when cooled and the hydrogen can be extracted when heated.

1.5 Environmental Impacts

There are enormous long-term environmental benefits of using hydrogen as a fuel, when burned it produces few pollutants. Hydrogen is a carbon-free fuel, and when produced using renewable sources of energy, the process can become carbon-neutral and even carbon- free. Hydrogen can lead to reduction of greenhouse gases (GHG) and many toxic pollutants.

1.6 Economic Factors

For over a hundred years, hydrogen has been produced and used for industry, as the technology required to make this available wide-scale is available. With the existing technology to run vehicles using the hydrogen fuel is very costly to manufacture. To aid with the transition to hydrogen technology vehicles, these technologies need to be able to compete with the existing technologies that have been mass-produced for many years.

To aid this transition, measures may include:

- financial incentives,
- positive regulatory frameworks,
- effective codes and standards,
- creating demand,
- reducing costs, and
- improving availability,

1.7 Security of Fossil Fuel Resources

Fossil fuels are incredibly valuable resources; the efficiency that these resources are used will determine the life expectancy of them. Transitioning to a hydrogen fuel economy ensures the availability of crude oil and its products upon which so many industries depend, for longer.

1.8 Motivation and Objectives of Thesis

There exists a problem with the use of hydrogen as a source of fuel in an internal combustion engine. Backfire is referred to the sudden burn of unburned fuel in the

exhaust; back flash (backfire/post ignition) is referred to the burnings of hydrogen fuel mixture in the intake manifold. There are many sources that lead to the back flash, of such relating to the engine temperature and spark timing, this is all related to the chemical properties of hydrogen and its ignition parameters. Of the several methods of this back flash elimination, a few methods are suggested and tested. One of the suggested methods is the water injection method, which delivers a mist-like amount of water into the intake manifold mixing with hydrogen before it mixes with the oxygen, this can be achieved through the implementation of a fluent water nozzle. This method would reduce the chances of the back flash (backfire/post ignition) occurring, although not completely eliminating it. Thus for this project a water injection kit is developed specifically for this 1986 GMC Sierra 5.7L V8 4-barrell Rochester carbureted engine. In the following chapters, an engineering design approach has been made in developing this water injection kit, and other means of eliminating the back flash/backfire occurring in the intake manifold.

In this thesis, the energy and exergy analyses of the engine are calculated using the octane 95 gasoline and hydrogen gaseous fuels. The engine tested and some conditions are assumed to remain constant, such as the atmospheric temperature and pressure. Also this analysis is done for major components of the system, and not the individual components, such as the water pump, water fan, radiator, carburetor, etc., as the individual components change the energy and exergy analyses over time, due to wear, grade of fuel inconsistency, as well as the weather conditions varying from time to time. Thus, these analyses are done for one set period time and conditions also the major components are analyzed for the calculations to remain consistent as much as possible.

1.8.1 Thesis Approach and Process Synopsis

In this thesis a complete elimination of backfire was achieved. The processes examined to achieve this elimination are studies performed on the fuel delivery, spark ignition, and combustion cycle for this engine. The process of fuel delivery was considered and from the literature review, it is known that a fuel injected operation is more favorable than the conventional carbureted method. Carburetor technology is outdated and mechanical and thus for this reason a carburetor is disadvantageous for the hydrogen gaseous fuel.

If the fuel was distributed through a venturi setup, it would be controlled by a throttle body, versus relying on the mechanical components and butterfly of the carburetor. When the engine is first started, a very rich air/fuel mixture is required because cold fuel vaporizes slowly. The "choke" at the top of the carburetor provides the rich mixture by closing and "choking off" the carburetor's air supply. The choking effect also creates an area of low pressure inside the throat of the carburetor that helps to pull additional fuel through the main metering circuit. At idle there isn't enough air flowing through the venturi to pull fuel through the venturi discharge nozzle. By temporarily choking off the air supply, however, a manifold vacuum rather than venturi vacuum helps to draw the extra fuel through the main metering circuit. In this thesis in the experimental setup, the choke proved to show some signs of improvement in the backfire elimination. In a fuel-injection, the fuel can be controlled using a control system logic fuel map to inject the amount of fuel required for the combustion process.

The spark plug wires, spark plugs, and the distributor are analyzed to improve the elimination of backfire. The spark plug wires are modified and different designs are

sought, as the spark plug wires picked up excess charge from the distributor during the exhaust stroke, which led to the ignition of the unburned pocket of hydrogen fuel from the exhaust stroke. The traditional spark plugs were replaced with platinum spark plugs and their gaps were reduced for shorter ignition and an ability to withstand high flame temperatures during the combustion stroke. In advancing the distributor, although mechanical, it is easy to allow more ignitions to occur for the faster flowing gaseous fuel to ignite quicker and reduce the fuel buildup in the intake manifold that leads to backfire.

Lastly, aftermarket exhaust headers were installed for faster exhaust travel and possible future works in turbo-charging and water re-circulation for water injection. By introducing water into the combustion process, the water vapor makes the hydrogen air fuel denser and allows for a more complete burn in the combustion process, improving fuel economy, total backfire elimination and increased power from the engine. The quality and quantity of water coming from the exhaust and the power increase with the water injection through a two-fluid nozzle will be analyzed and further corrosion prevention studies are required. For this reason a parametric study was done for the water injection system to be deemed feasible. Furthermore energy and exergy analyses were done to compare the performance and efficiencies of this engine operating on gasoline and hydrogen fuels.

1.9 Theoretical Background – Engine History

The engine can be dated as early as 1680, where people such as Christian Huygens were trying to develop an engine. Christian Huygens was the first to use combustible substances such as gun powder to run his version of the engine; he designed the engine but never built it [6]. In 1769, a French Engineer and Mechanic, Nicolas

Joseph Cugnot was given recognition for the very first self-powered vehicles using a steam engine. This invention was first used as a military tractor in the French military [7]. However, it was a German Engineer, Nikolaus August Otto that got a patent in 1876, and he called this the Otto cycle, which was a gasoline-powered four stroke engine, the inventor was also credited as the co-inventor of the internal combustion engine, originally designed by Jean Lenoir [8]. Jean Joseph Etienne Lenoir, a Belgian born French engineer, the inventor of the first internal combustion engine which consisted of a single cylinder with a storage battery for the electric ignition system were first fuelled by coal gas in 1863 [7]. In 1886 Karl Benz obtained a patent for an automobile that used gasoline in an internal combustion engine [10]. Karl Friedrich Benz, a German engineering pioneer of the automobile unveiled his Benz-3-wheeler in 1885, it was powered by a single cylinder, water cooled, fueled by the vapor of ligroin or benzene [11]. It was Gottlieb Daimler who patented a carburetor in 1887 that he used to build his 1885 prototype [9]. Daimler's improvements made to the internal combustion engine along with his colleague Wilhelm Maychin in the 1880's focused on developing the first lightweight high-speed engine to run on gasoline. This then led to the development of an engine with a surface carburetor to vaporize the fuel and mixing with air producing the combustion. Daimler and Maychin's engine could reach 900 revolutions per minute (RPM), and after installing it on a horse carriage they were able to achieve speeds up to 11 MPH, thus the first automobile driven on four wheels [12].

Throughout the past century many changes have been made to the engines to power the automobiles. Of such, the spark ignition engine had been compared to the compression ignition type of engine, powered by diesel, as well as solar-powered electric

motors, battery-powered electric motors and steam-powered engines [10]. The steam powered engines, however had seen a better use for large locomotives. With these many alternative methods of engines operating and powering the vehicles to move, the spark ignition engines are still considered to be the best method. However, with today's high gasoline and oil prices, along with many CO₂ emissions, it now has become the consumer's concern in using alternative methods of fuels and ways of powering the vehicles. Of such one method of reducing the emissions and use the technology available would be the hybrid systems, which use battery and spark ignition engines concurrently in a vehicle. Fuel cell vehicles have been generating interest because they are vehicles powered by means of an electric motor driven by electricity, and this electricity is produced using on board hydrogen fuel tanks. The hydrogen fuel infrastructure is being addressed because some internal combustion engine (ICE) developers consider that an ICE running on hydrogen may be the solution to reduce the emissions. However, the consumers don't want to lose performance on gasoline powered ICE's produce either. Thus, this is the challenge of getting hydrogen powered ICE's to be both powerful to meet the consumer's needs and be efficient enough to be feasible. The spark ignition engines technology has been used in many applications, which require the movement of objects of high weight to transportation purposes.

Chapter 2

LITERATURE REVIEW

2.1 Literature Review and Patent Search

Many Automotive Manufacturers have tried converting existing gasoline engines to burn hydrogen fuel, of such companies that exist are Ford, BMW, General Motors, and many individuals that have tried to apply this concept in the comfort of their own house garage. Ford has a lineup of tugs, shuttle buses, pickup trucks, fuel cells, and engine developments with companies such as Hydrogen Engine Center (HEC). BMW has introduced this type of application in their vehicles which burns Liquid Hydrogen (LH₂) and they also have a dual fuel engine operating on both gasoline and hydrogen gas. General Motors has converted their own Hummer trucks and Chevrolet pickup trucks, along with many Fuel Cell powered vehicles.

2.2 Literature Review on Engines

2.2.1 HEC engines

Hydrogen Engine Center (HEC) has converted an inline-six cylinder 4.9L engine similar to the engine in the airport baggage tug, modified to burn on hydrogen fuel. This type of engine is used for industrial and other types of applications the customers choose to use [13].

2.2.2 Patent Search

There exist some patents in the market today with the conversion of an internal combustion engine using hydrogen fuel, as early as the year 1936 where the development of a hydrogen engine has been attempted. In the patent [14] hydrogen is mixed with a portion of the air in the cylinders to form a combustible mixture which is ignited and burned concurrently with injection over a portion of expansion and in some cases compression stroke. This patent dates back to January 26, 1970 developed by Richard G. Murray, creating an invention that soon after underwent extensive research and finally into practice. There also exists another hydrogen engine development using direct injection in May 2, 1978 by Eisele et al. [15]. These Inventors have developed a combustion process that injects the hydrogen fuel in the internal combustion engine, and supplying the air independently in an air ring rotating about the cylinder axis. The injection of the hydrogen into the air ring takes place in the central area of the air ring while ignition takes place in the transition area between the central hydrogen core and the externally rotating air ring.

In the patent [16], an internal combustion engine using hydrogen as a fuel document, invented by Rudolf Arnold Erren in September 10, 1936 established injecting hydrogen fuel in the cylinder after the oxygen had been introduced in the cylinder. This patent [16], due to the technology at hand in 1936, this engine development could not exceed as the inventor had found that in practice the engine shows inefficient working, sometimes due to insufficient mixing of the hydrogen and other gases. Rudolf Arnold Erren, further explains his patent of mixing the hydrogen fuel with the oxygen in a swirling motion within the cylinder through the design of the cylinder and the inlet valve.

In patent [17], inventor Kenji Watanabe filed his version of the hydrogen engine in September 28, 1982 under the name of internal combustion engine of hydrogen gas. In his patent he illustrates the delivery of the hydrogen gas fuel in the internal combustion engine with a hydrogen gas jet nozzle and water spray jet nozzle in the combustion chamber to directly jet hydrogen gas and water spray. In this process the sprayed water is instantly vaporized to steam by igniting the hydrogen gas. This utilizes the combustion/explosion energy of the hydrogen gas and the steam energy to obtain mechanical dynamic energy.

In a patent [18], inventors Quigley, Jr. et al. filed his version of the hydrogen-oxygen fuel internal combustion engine in October 28, 1966. In his patent he states that the oxygen and hydrogen input into the cylinders have been through separate cam-operated valves. During this process and the Otto cycle, it produces severe detonations, the combusted gas movements would scrub against the cylinder walls, and causing overheating of the combustion chamber walls. Due to the local excessive heat zones in the cylinder walls, a backfire through the manifold is created causing premature ignition of the gases in the intake manifold. To overcome this handicap, the inventors have proposed to supply the combustion chamber with a cold homogeneous mixture of hydrogen and oxygen in order to avoid the pre-ignition problem and reduce the flame speed such that there are no detonations present.

In a patent [19], filed on June 24, 1992, Stanley Meyer, states in his hydrogen gas fuel and management system for an internal combustion engine utilizing hydrogen gas fuel document that there exists some challenges that need to be overcome for the delivery of the hydrogen fuel into the internal combustion engine. He states that hydrogen has

been regarded as efficient, abundant, and potentially non-polluting energy source, however it has not been widely, or practically applied in applications such as an internal combustion engine. Some of the difficulties that hydrogen possesses are the safe transmission of the gas; hydrogen has an inherent volatility and the corresponding rapid dispersion characteristics in the atmosphere. To overcome these challenges his invention was to provide a fuel management and delivery system for the internal combustion engine that utilizes the hydrogen as a fuel. The system includes a safe and effective distribution means for supplying a hydrogen fuel to an internal combustion engine [19]. With the fuel system management it monitors the composition of a fuel gas into the engine such that the hydrogen and oxygen mixture has a ratio of 2:1. Furthermore, by modulating the density of the hydrogen gas fuel with other non-combustible gases to the mixture this allows the burn rate to be similar to that of a fossil fuel mixture.

In a patent [20], hydrogen powered vehicle, internal combustion engine and spark plug for use filed in December 23, 1998 by inventor Herman P. Anderson suggests the structure of mixing the alternative fuel, hydrogen, with oxygen in ambient air to stratify the fuel. The system includes an adapter, in which it contains a housing mounted between the spark plug and the cylinder of the internal combustion engine [20]. The spark plug has ridges or grooves on its outer surface that acts as a mixing structure. When the hydrogen fuel is mixed with ambient oxygen in the chamber it flows over the plug which creates a vortex action as the hydrogen flows over the plug and towards the cylinder of the engine. This invention provides an improved fuel system and also to prove a hotter sparking plug to ignite the fuel. For this system to function correctly, the electrode assembly is redesigned to accommodate the operable sparking communication

with the cylinder and the fuel mixture. This trend of inventors developing and creating new ways of burning alternative cleaner sources of fuel indicates that the engine technology can still be enhanced and more of this technology will be seen in the future.

2.2.3 Literature Review on Backfire Elimination, NO_x emissions

Hydrogen can be produced from many different sources, such as natural gas, biomass, solar, wind and water. Although the potential role of hydrogen in combating global warming appears to be critical, its contribution is currently insignificant in comparison to hydrocarbon-based fuels. The reason is that combustion of hydrogen produces no carbon based compounds such as HC, CO, and CO₂. Hydrogen has special properties so the combustion characteristics of hydrogen are very different from gasoline. The laminar flame speed of a hydrogen air mixture at stoichiometric condition is about 10 times that of gasoline [21]. The wide flammability limit of hydrogen allows the use of very low equivalence ratios which result in reducing nitrogen oxides (NO_x) emissions. The octane rating of hydrogen of 106 RON allows for an increasing compression ratio. Hydrogen is one of the most interesting alternative fuels, and is recently in the centre of attention. Hydrogen is renewable and offers lots of other benefits. The most practical one is its ability to run in bi-fuel conditions.

Hydrogen internal combustion engines have the ability for increasing efficiency [22]. A comprehensive overview of hydrogen engine properties and design features is already done by previous authors and it was concluded that hydrogen internal combustion engines have a high efficiency, are very clean and considerably cheaper than fuel cells [23].

The use of hydrogen as an engine fuel has a great potential for reducing exhaust emissions. With the exception of a little amount of hydrocarbon emissions originating from the lubricating oil, NO_x is the only pollutant emitted, and the life cycle is considered through sensitivity analysis of various vehicle types. Studying and analyzing the behavior in hydrogen ICE and its sensitivity to controllable parameters can help designers to have better understanding over hydrogen characteristics and its combustion in an ICE.

Limited numbers of previous publications have worked on hydrogen-fuelled engine simulation. A two-zone quasi-dimensional engine model for calculating power and NO_x emission was demonstrated by Fagelson et al. [24]. In their work, laminar burning velocity is calculated from a second order reaction with estimated activation energy. Kumar et al. [25] used the same model in order to predict the performance of a supercharged hydrogen engine. They report an overestimation of the rate of pressure rise that can be a consequence of an overestimation in burning velocity. Ma et al. [26] used Wiebe's law in a zero-dimensional model. And for a varying compression ratio and ignition timing the optimum cylinder diameter for a fixed equivalence ratio was calculated. Verhelst et al. [27] preferred a two-zone quasi-dimensional model to multi-dimensional one because of a reasonable accuracy and fast computation on PC system. They developed a complete cycle simulation code for Spark Ignition (SI) engine and they looked thoroughly at the turbulent combustion in a hydrogen-fuelled engine. In another reference [28] a simulation and design tool applicable to hydrogen powered spark ignition engine systems is introduced. The model is applicable to single and multi-cylinder engines under steady state or transient operating conditions. The model is

validated against experimental data for the intake flow model. In a recent publication [29] a 3-dimensional computational fluid dynamic (CFD) modeling of combustion and nitrogen oxide formation in hydrogen-fuelled ICEs has been developed and it was concluded that the mixture heterogeneity is a key parameter to control the combustion spreading and NO_x formation during combustion.

The use of hydrogen as an internal combustion fuel is not a new idea. In the 1820, Cecil developed a "vacuum engine" that used hydrogen as its fuel. In 1854, an English patent was granted to Bursanti and Matteucci for hydrogen-burning, free-piston-type engine, of which Benini built a prototype in 1856 [30]. Otto, used hydrogen in his work with gaseous fuels, when he used gasoline, his first experiments were disastrous that he considered the fuel much too unsafe, until the further development of carburetor made gasoline practical and safe [30].

Erren [31] is a well-known name associated with the development of the hydrogen engine. During the World War 1 era, he converted an airship engine to run on hydrogen, he was also the first to suggest the direct cylinder-wall injection method to reduce backfiring.

There are many benefits in using hydrogen, as it is renewable supply of energy. Hydrogen can be produced from water and burned to produce water, without pollution. Fossil fuels, on the other hand, are limited in supply and burn inefficiently and create pollution [32].

Hydrogen contains 2.5 times the energy of gasoline by weight [33]. Unfortunately, in liquid form gasoline is 10 times as dense as hydrogen [34], which

means that, four times the amount of hydrogen has to be carried for the same amount of output.

Any gasoline engine can be modified to burn hydrogen fuel cleanly [33]. However, the low density of hydrogen requires higher pressures than gasoline for ignition. Generally, the higher compression ratio would indicate a higher thermal efficiency. For comparison purposes, under a given set of conditions such as air-fuel ratio and fuel injection temperature, a calculated compression ratio of 9:1 for a gasoline engine would indicate a compression ratio of 14:1 for a hydrogen engine to achieve the same output power [30]. The calculated efficiencies thereby are about 10% for gasoline and about 30% for hydrogen [35, 36]. The increased efficiency is applicable for low- and part load conditions and lean air-fuel ratios. At high loads and near-stoichiometric air-fuel ratios, nitrous oxide emissions can be high and combustion knock can occur [37]. Knocking is caused by auto-ignition if the compression is too high. Emissions can be lowered by altering the ignition timing and re-circulating the exhaust gases [38]. At near stoichiometric air-hydrogen mixtures due to the high flame velocity and heat release in hydrogen creates a rough combustion. Hydrogen has a strong tendency to detonate, with flammability limits of 4 - 75% by volume in air and low energy of ignition [30], causing pre-ignition and flashbacks.

The topic of greenhouse gas emissions by the transportation sector is the most discussed topic thus far and the need for push towards legislation limiting the fleet average CO₂ emissions [39]. The use of hydrogen as an energy carrier is one option with the potential of lowering these CO₂ emissions. However, affordable fuel cell vehicles have not yet met the right time to enter the market [40]. An interesting alternative and

least expensive method in using hydrogen as a source of fuel would be through the use of ICEs. Hydrogen is a very versatile engine fuel when it comes to load control. The high flame speeds of hydrogen mixtures and its wide flammability limits permit very lean operation and substantial dilution. The engine efficiency and the emission of NO_x are the two main parameters used to decide the load control strategy. The constant equivalence ratio throttled operation has been used mainly for demonstration purposes [41-43]. It is easy to run a lean burn throttle hydrogen engine, however, a significant large decrease in power output is seen. Using a wide open throttle (WOT) operation, it takes advantage of an increase in engine efficiency [44-46], avoiding pumping losses through regulating load with mixture richness. Some of the limitations that the WOT operation have are the misfires, unburned hydrogen gas and decreased stability at very low load, such as idling, as well as NO_x emissions at medium to full load [43,47-50].

For higher loads, flame temperatures quickly exceed the NO_x generation limit. This results in a NO_x limit to WOT operation. One could restrict the mixture richness and use sufficiently lean mixtures to stay below a 10 or 100 ppm NO_x limit, but this implies a large decrease in maximum power output. Alternatively, the engine can be throttled above this limit, using stoichiometric mixtures and thus enabling the use of a conventional three way catalyst for NO_x reduction [47]. The mixture richness is then set slightly rich of stoichiometric so that some unburned H₂ is present in the exhaust for reducing NO_x [52]. Although, this method has a decrease in engine efficiency; another method for NO_x reduction is to use the Exhaust Gas Re-circulation (EGR) to control the load, and recycling the exhaust gas in a proportion that is dependent on the power demand [51,53,54]. This allows for a better efficiency compared to throttling, and by

using EGR it allows for a backfire-free operation at stoichiometric mixtures, enabling a higher power output if NO_x emissions are a boundary condition [16,18]. Water injection can also be used to decrease NO_x emissions from the richer mixtures [48,56], and is more effective than EGR [41] but is mostly considered impractical. Work has been reported using a ‘dual fluid injector’ for Direct Injection (DI) [55], which injects hydrogen and liquid water directly in the combustion chamber, for decreased NO_x. Finding means to maximize engine efficiency is very important for H₂ ICEs considering the H₂ on-board storage challenge. Quantifying the efficiency of H₂ ICEs is useful for assessing the possible vehicle range. Several papers have reported efficiencies of engines operated on hydrogen. Ford [43,51,57] published some results obtained on a dedicated hydrogen engine, where (among others) the compression ratio was optimized to take advantage of the high auto-ignition temperature of hydrogen. Tang et al. [43] mapped the brake specific fuel consumption, both for a constant equivalence ratio, and a throttled strategy as a wide open throttle strategy (regulating load with mixture richness). Brake and indicated thermal efficiencies were shown, as a function of equivalence ratio, for different compression ratios and engine speeds.

Natkin et al. [51] reported brake thermal efficiencies of a comparable engine, with the addition of a supercharger to increase the power output. The supercharged engine reached a maximum indicated thermal efficiency of 50% and a maximum brake thermal efficiency of 37%. The authors also report a relative increase of 15–20% in brake thermal efficiency at the lower loads when using the equivalence ratio to control load (WOT, qualitative control strategy) rather than throttling (quantitative control strategy). Finally, in a joint publication with Westport Innovations and Pacific Northwest National

Laboratory, Ford report an estimated peak brake thermal efficiency of 45% obtained on a single cylinder DI engine [57]. BMW [47,52,58,59] reported efficiency for the different load control strategies. Eichlseder et al. [59] provide a limited comparison of the efficiency of hydrogen versus gasoline operation.

Next to the properties of hydrogen that are beneficial for the efficiency, it is also noted that higher wall heat losses are to be expected for hydrogen, which has a negative effect on the efficiency. Berckmuller et al. [47] showed an indicated thermal efficiency map for a port fuel injected engine, including the wide open throttle strategy, throttled stoichiometric and supercharged stoichiometric strategies. Indicated thermal efficiencies reached 40% at low load and 32% at high load. They also mapped the stoichiometric exhaust gas recirculation (EGR) strategy as an alternative to the throttled stoichiometric approach, which resulted in increased efficiency (roughly 2% points). Rottengruber et al. [52] plotted a similar map, but using direct injection at the higher loads, which enabled higher efficiencies compared to the Port Fuel Injection (PFI) supercharged approach. Several other papers also report efficiencies, as a function of equivalence ratio and ignition timing [56], as a function of the injection timing and intake manifold geometry for a PFI engine [60], as a function of the injection timing and injector location for a DI engine [61], etc. All of these papers show efficiency results above those typically reached with gasoline, but no direct comparisons are included [62].

The difference between the H₂ ICE and gasoline is the physical features between these two fuels. Hydrogen compared to gasoline fuel has the advantages of high flammability, low ignition energy, good homogenous combustion high octane number and high thermodynamic efficiency, as analyzed in most papers [63-65]. There is a small

ignition energy in a hydrogen-air mixture, the first draw-back regarding spark ignited (SI) H₂ ICE combustion are the backfire, pre-ignition and knocking; especially for a manifold injection H₂ ICE, the backfire is the first draw-back that should be overcome.

In the previous experiments, the issue regarding the spark ignition H₂ ICE combustion is backfire or pre-ignition occurring as a lean fuel/air ratio approaches stoichiometric which limits the torque output of the engine [66]. The backfire is the condition when the fresh charge of hydrogen is ignited in intake ports. Pre-ignition is the condition when the hydrogen charge is ignited after the intake valve closes and before the spark plug fires in the cylinder. It has been suggested in the literature [67] that backfire can be controlled by injecting the hydrogen only during the forward flow of air into the cylinder during the intake stroke, thus minimizing the fuel's exposure to being heated or coming into contact with hot spots or hot oil ash/residual in the combustion chamber.

Isadore and Frank [68] had detailed analysis of the flammability limits in hydrogen-air mixture. They concluded that the lean limit occurs at lower concentration as the mixture temperature increases with a linear relationship, while the pressure effect appears to be small. Keck [69] reports measurements in an optically accessible engine, operated on propane as well as hydrogen, and uses a turbulent model to compare predicted trends with experimentally observed trends. Using 3D-CFD-simulation, it is possible to gain insight of the processes that govern engine performance and emissions, as well as demonstrate the mixture formation both of intake and in-cylinder with respect to different engine speeds and equivalence ratios [70].

Combustion knock is one of the primary constraints limiting the performance of spark-ignition H₂ ICE, as it limits the torque output and efficiency. By understanding the

characteristics of combustion knock in a H₂ ICE will provide better techniques for its detection, prevention and control while enabling operation. Through comparisons with gasoline combustion knock, it was found that knock detection techniques used for gasoline engines, can be applied to a H₂ ICE as well after appropriate modifications.

Hydrogen's low ignition energy, high flame speed, and low energy density per unit volume presents IC engines with a number of challenges including well controlled combustion timing, rate of energy release, and power density. Meanwhile, hydrogen's broad flammability range and high auto-ignition temperature provide a great deal of flexibility to implement spark ignited combustion systems using high compression ratios (CR) and a wide range of equivalence ratios for lean combustion and emission control [71–73]. It is reported [74,75] that hydrogen as engine fuel has great potential for improving engine thermal efficiency due to its rapid combustion, which approaches the ideal constant-volume heat release combustion process.

Combustion knock results from the spontaneous ignition of a portion of the gas mixture in the combustion chamber ahead of the propagating flame. When this occurs, the rapid release of the chemical energy in the unburned mixture causes high local pressures and generates propagating pressure waves in amplitude of several bars across the combustion chamber. The large amplitude pressure waves of the hot combusted gases in the cylinder are the primary reason for mechanical engine failure through increased thermal and mechanical stress [76].

The pressure waves that result from combustion knock occur at frequencies that are acoustic vibration modes [77] of the chamber geometry. The mode frequencies can be predicted analytically for simple disk shaped combustion chambers while numerical

methods can be used for more complex shapes [78]. Scholl et al. [79] indicates the influence of combustion temperature, equivalence ratio, and levels of exhaust gas recirculation leading to shifts in the resonating frequencies of combustion knock.

There are several research theses concerned with hydrogen combustion in IC engines, of such indicating the knock free operation using stoichiometric mixtures at compression ratios (CR) of 11:1 as noted by Berckmuller [80]. Tang et al. [71] used lean mixtures at CR of 12.5:1 and 14.5:1 as did Smith et al. [81] without the occurrences of knock. The investigation on hydrogen combustion under higher pressures up to 1MPa was conducted by Bradley et al. [82]. Naber et al. [83], also presented some results of hydrogen auto-ignition and combustion under high pressure at diesel engine conditions.

In this thesis study, the performance and emission characteristics of a conventional eight cylinder spark ignition (SI) engine operated on hydrogen and gasoline are investigated experimentally.

The compressed hydrogen at 15 MPa is introduced to the engine adopted to operate on gaseous hydrogen by external mixing. A two-stage regulator is used to drop the pressure first to 300 kPa, then to atmospheric pressure. The variations of torque, power, brake thermal efficiency, and brake mean effective pressure, versus engine speed are compared for a carbureted SI engine operating on gasoline and hydrogen. Energy and exergy analyses are conducted for comparison purposes with varying volumetric efficiencies.

The test results demonstrated that power loss occurs at low speed hydrogen operation whereas high speed characteristics compete well with gasoline operation. Fast burning characteristics of hydrogen have permitted high speed engine operation. Finally,

both energy and exergy efficiencies of hydrogen fuelled engine is studied and compared with gasoline engine.

It must be mentioned that hydrogen's auto-ignition temperature is high (about 576°C), and it is impossible to bring hydrogen to its auto-ignition temperature by compression only. Thus, supportive ignition triggering devices should be used in the combustion chamber [84].

Das et al. [85], evaluated the potential of using hydrogen for small horsepower spark ignition (SI) engines and compared hydrogen fuelling with compressed natural gas (CNG). Another study dealt on certain drawbacks of hydrogen fuelled SI engines, such as high NO_x emission and small power output [86]. Das [87] determined the performance, emission and combustion characteristics of hydrogen fuelled SI and compressed ignition (CI) engines. Karim [88] reviewed the design features and the current operational limitations associated with the hydrogen fuelled SI engine. Li and Karim [89] investigated the onset of knock in hydrogen fuelled SI engine applications. Since the compression ratio as high as 29 was not enough to achieve ignition of hydrogen for a hydrogen fuelling CI engine, a comparative assessment showed that CI engines can be converted to operate on hydrogen–diesel dual mode without sacrificing the performance parameters [90]. Effects of compression ratio, equivalence ratio and engine speed on the performance and emission characteristics of a SI engine using hydrogen as a fuel was investigated by Al-Baghdadi [91]. The effect of methane and ethyl alcohol addition on the performance and emission characteristics of SI engines operating on fuel mixtures containing hydrogen was also investigated by some researchers [92,93].

The lower ignition energy of hydrogen makes the fuel–air mixture in the inlet manifold to get ignited by hotspots and this is called backfire [94]. Timed manifold injection has been found to be a good technique to avoid backfiring [95,96]. Another problem with hydrogen operation is the formation of NO at high loads. The peak cycle temperature shoots up whenever the load is increased, which tends to accelerate NO formation. Several techniques have been tried to inhibit NO formation. Some of them are: use of EGR, Turbo-charging with inter-cooling, addition of diluents or water injection along with the intake charge etc. [96–100]. Injection of water into the intake manifold has been found to be an effective way to reduce NO emission in SI (spark ignition) and CI (compression ignition) engines. About 50% reduction in NO has been reported with water injection in a gasoline-fuelled engine [101]. Increasing the intake charge humidity was also reported as an efficient technique to control NO emission [102]. Hot steam from a steam generator was mixed with the intake charge at different proportions and the effect on performance, emission and combustion parameters have been reported. A water/hydrogen mass ratio of 4:1 was reported as an optimum value for reducing NO_x emissions. Extremely fast burning of hydrogen leads to high rate of pressure rise, which leads to violent combustion (hydrogen knocking) [103].

Hydrogen knocking creates extremely high mechanical stresses and temperatures, which are also responsible for high NO_x emissions. Inlet charge temperature, compression ratio and spark timing have a pronounced effect on hydrogen knocking [104]. Adding diluents such as argon is also a method for suppressing knocking. Supplying more hydrogen and making the mixture richer also reduces the knocking tendency. However, the unburnt hydrogen can be trapped from the exhaust and can be

recycled [105]. The effect of spark timing on hydrogen combustion was studied and it was found that spark timing has a pronounced effect on the degree of constant volume combustion and thus affects thermal efficiency [106]. Reduction of nitric oxide emissions by retarding the spark timing with little sacrifice in thermal efficiency at an equivalence ratio of 0.43 in an in-cylinder injected hydrogen engine has been reported [107]. On the whole the problem of knocking and high NO_x emissions in hydrogen fuelled engines needs attention and use of diluents is a potential method to control them. Though the induction of hot steam into the manifold has been shown to reduce NO emissions, injection of water in the liquid form can lower charge temperatures significantly as the heat for vaporization can be extracted from the mixture. The effect of this method on performance, emissions and combustion has to be studied under a wide range of equivalence ratios. Since retardation of spark timing can also reduce NO_x emissions, combination of the two has potential to further reduce NO_x emissions [108].

Chapter 3

EXPERIMENTAL SETUP

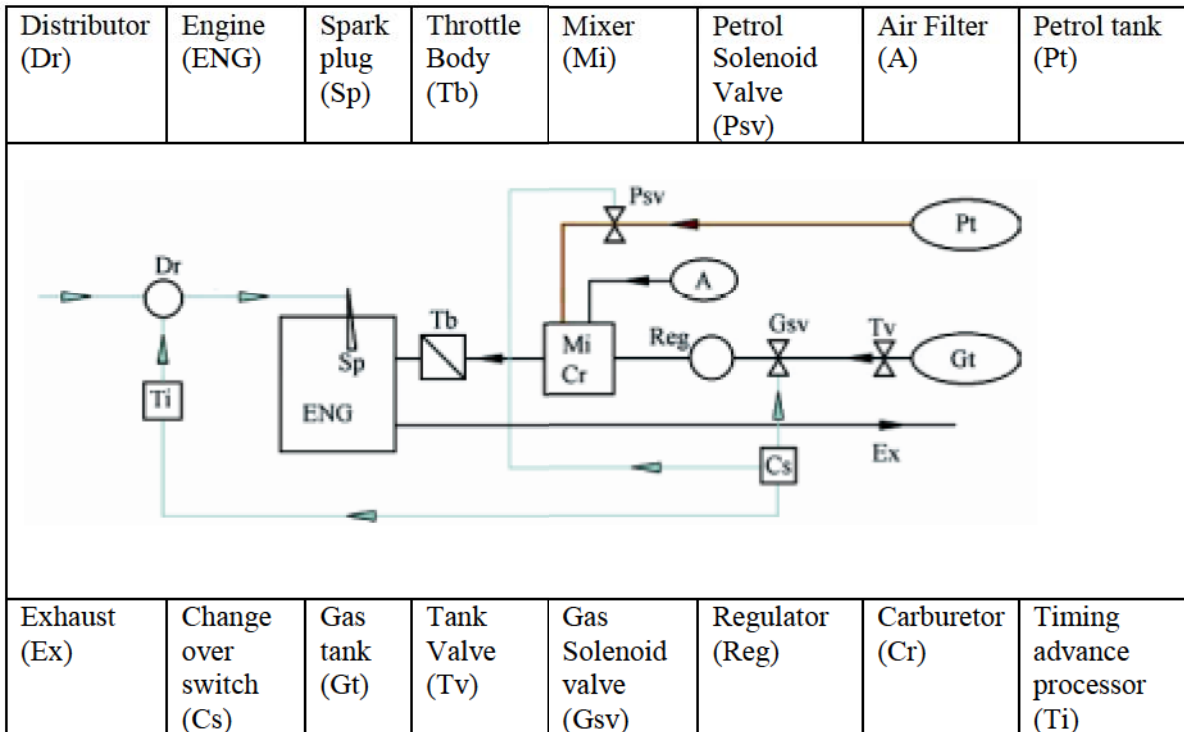
3.1 Introduction

In order to undertake a possibility of comparison between the two types of fuels to be accomplished for this thesis, the engine underwent an addition of some components for the means and purposes of fuel delivery. In this section, the method of converting this carbureted type engine is explained in much detail.

A similar type of conversion can be made via the installation of fuel injectors and direct injection methods, however, for this project the regulator, usually located below the carburetor where gasoline fuel is stored allowing for the mixture of the air to occur when the throttle body valves (butterfly) open through acceleration pedal connected via a steel wire. The diagram used to illustrate the setup and functionality of this concept is seen in Table 3.1, using this method of conversion would allow dual fuel distribution into the engine. This type of conversion uses a gas solenoid valve to allow the flow of the gaseous fuels into the regulator in a carburetor type engine and delivering the fuel to the mixer where it is then passed through the throttle body and into the intake manifold and finally the engine. This type of conversion is made for a natural gas vehicle, however, this same type of conversion can be applied for a hydrogen conversion, as both fuels are naturally aspirated when mixed with the air and into the intake manifold. Natural aspiration is used for safety precautions, and this also allows the fuel delivery from the gas mixer to the throttle body, such that if the fuel were to enter the engine at high

pressure it would not burn or would create a backfire that might lead to a dangerous situation such as engine failure.

Table 3.1: Natural gas conversion diagram for carburetor type engines.



Source: [109]

3.2 Engine Modifications and Parts Installation

In this section all the components and engine modification required for the conversion are described.

3.2.1 Engine Fluid Drain, Parts Removal and Installation

The gas tank is disconnected from the engine; this can be done by disconnecting the fuel line and capping it from the mechanical fuel pump, and the engine is left running until all the gasoline left in the fuel line, and carburetor are burned, this process takes

approximately 3-5 minutes. Similarly, the radiator coolant is drained to allow for radiator hose changes for the regulator.

After the fittings and the respective hoses have been installed back on the engine, on the carburetor remove and cap any vacuum lines, illustrated in Figure 3.1, as these are not necessary for the operation of the engine using hydrogen fuel.



Figure 3.1: vacuum lines removed and capped on the carburetor.

The TN2 regulator is now installed, as illustrated in Figure 3.2, the place chosen to put the regulator, it must be insured that the regulator is parallel to the vehicle; it can be placed close to the carburetor such that the fuel lines can be connected with ease. When installing the regulator, it is important that the bolts are not tightened too much, otherwise the threads will break. This precaution can be held for any fastenings being done on the vehicle, as some parts are mounted on the engine itself and is hard to replace or mount onto. After the installation of the regulator and the capping of the vacuum lines, the gas mixer assembly is installed. To install the gas mixer assembly the first part is the spacer, it is then held in place using a threaded rod and a bolt is installed to secure

it in place. Then the adapter is installed along with the gas mixer and the air filter and cover on top of the assembly, seen in Figure 3.3, ensuring the gaskets are in proper place. The hose from the regulator is installed to the gas mixer assembly; illustration is seen in Figure 3.4.



Figure 3.2: TN2 regulator installed parallel to the engine.



Figure 3.3: Gas mixer, air filter with cover, spacer and adapter assembly on top of the carburetor.



Figure 3.4: Hose connected from regulator to the mixer assembly, for hydrogen fuel.

The electrical component to power the regulator is the relay to be installed close to the regulator for ease of location, as seen in Figure 3.5.



Figure 3.5: Relay with all wires connected behind the regulator.

The relay is connected to the ignition switch and the oil pressure switch, on the relay the wires connected are the on position for the switch on Pin 30 using the yellow

wire, the ignition power on pin 86 using the blue wire, the crank on pin 85 using the red wire and to ground the relay and complete the circuit using pin 86 the black wire.

3.2.2 Tank Mount and Fuel Line Installation

The cylinder brackets used to hold the hydrogen tanks are the 9 inch CNG tank brackets modified to 10 -11 inch size to support the hydrogen tanks. The bracket sponges are removed and the brackets are widened and test fitted on the hydrogen tanks. There are 4 brackets being used to support the two tanks (Figure 3.6). After the modification is done for the brackets to support the hydrogen tank, two screws are welded on the bracket for easy fastening on board of the truck. After the welding, the brackets are cleaned and painted for aesthetics and installed securely in the bed of the truck shown in Figure 3.7.



Figure 3.6: Four mount brackets with welded screws on the brackets.



Figure 3.7: Hydrogen test tank with brackets installed at the back of the truck.

3.2.3 Combustion Aspects of Hydrogen in Spark Ignition Engine

Hydrogen is available in nature, but not in its natural state and the energetic cycle of hydrogen is shorter than fossil fuels, it does not pollute and it is carbon neutral when obtained from renewable sources of energy[111]. It is a great opportunity to use hydrogen in an internal combustion engine as a fuel, however the challenges of hydrogen fueling system for the engine and the control of the combustion in order to avoid the specific aspects of the abnormal combustion phenomena is order to obtain higher power and efficiency performances must be met. In Table 3.2, the physical and chemical properties of hydrogen and gasoline are compared.

Table 3.2: Properties of hydrogen and gasoline.

Property		Gasoline	Hydrogen
Molecular mass, [kg/kmol]		114	2.016
Theoretical air-fuel ratio, [kg/kg comb]		14.5	34.32
Density, at 0°C and 760 mm Hg, [kg/m ³]		0.735-0.760	0.0899
Flammability limits in air, at 20°C and 760 mm Hg	% vol.	1.48-2.3	4.1-75.6
	λ	1.1-0.709	10.12-0.136
Flame velocity in air ($\lambda = 1$), at 20°C and 760 mm Hg [m/s]		0.12	2.37
Octane Number		90-98	>130
Min. ignition energy in air [MJ]		0.2-0.3	0.018
Auto-ignition temperature, [K]		753-823	848-853
Lower Heating Value (gas at 0°C and 760mmHg)	Stoichiometric fuel-air mixture [KJ/m ³]	3,661	3,178
	[KJ/kg]	42,690	119,600

Source: [111]

The combustion of hydrogen carries some specific aspects such as the high pressure increasing rate due to the high combustion rate of hydrogen compared to the other fuels, as well as the spontaneous ignition (flow back) concerned with the relative air-fuel ratio mixture and the ignition energy. These aspects occur when the ignition delay is reduced and the combustion rate is high. At lean mixtures, these aspects disappear, however, the engine power per liter decreases significantly. Some methods that can be applied to avoid these combustion aspects are to remove any possible hot sources from the inside of the combustion chamber using cooled re-circulated exhaust gases or air. Another method that can be applied is by decreasing the heat release by decreasing the combustion rate and some modifications of the combustion chamber.

Chapter 4

ANALYSIS

4.1 Air Mass Estimation

In a port injected system, the reciprocating behavior of the cylinders is replaced by a continuously working volumetric pump that produces exhaust gases and torque; this is a mean value approach. The main continuous-time domain equation describing the air flow [110] models the air mass flow entering the intake manifold, through Equation (4.1) and the equation that would model the air mass flow leaving the intake manifold and entering the cylinders is given in Equation (4.2).

$$\dot{m}_\alpha(t) = c_d \cdot A(t) \cdot \frac{P_a}{\sqrt{R \cdot v_a}} \cdot \psi(p_a, p_m(t)) \quad (4.1)$$

$$\dot{m}(t) = \rho_m(t) \cdot \dot{V}(t) = \frac{P_m(t)}{R \cdot V_m} \cdot \lambda_l(p_m(t), \omega_e(t)) \cdot \frac{V_d}{N} \cdot \frac{\omega_e(t)}{2\pi} \quad (4.2)$$

The amount of fuel should be calculated according to the amount of air entering the cylinder. Since it is usually not possible to measure the mass flow at the intake of the cylinder, a model-based estimator is used to obtain this information. There are four possible cases that structure an air mass flow estimator [110], however depending on the available sensors. Using the case 1 scenario, the throttle angle is measured, and the corresponding throttle area $A(t)$ is multiplied with the discharge coefficient c_d . The rest of the manifold dynamics must be simulated using an open loop system, as measuring it is not usually possible. Using this method is the cheapest and the least precise, however,

using case 2 is similar to case 1 when the different ambient pressure p_a is measured. With this correct altitude compensation is possible. In case 3 the air mass flow \dot{m}_α entering the intake manifold is measured with an air mass flow sensor, usually mounted after the air filter, (see Figure 4.1) for a typical location of a thermistor mass air flow sensor.



Figure 4.1: Typical location of a mass air flow sensor.

In case number 4, the intake manifold pressure P_m is measured, and the relevant intake manifold temperature has to be estimated and the volumetric efficiency must be known with high precision. However, since the transient changes in the throttle area $A(t)$ are received with substantial delay, predicting the desired amount of fuel is made difficult. The air mass flow in the cylinder can also be calculated using four case scenarios in a discrete-time formulation. However, for this conversion the continuous-time formulation is chosen, as both methods use the ambient pressure to achieve the same results.

4.2 Kinetic Modeling of the Pre-flame Reactions

The processes of the combustion are produced through poly-chain reactions, in this type of system are influenced by pressure, temperature, concentration, activation energy parameters. Considering an elementary reaction where K_b , K_f are the kinetic

constants of the forward and reverse reactions velocities, and n_A , n_B , n_C , and n_D , are the concentrations of the correspondent species, a, b, c, d are the stoichiometric coefficients one can write [33]:

$$\frac{dn_A}{dt} = -K_b \cdot n_A^a \cdot n_B^b + K_f \cdot n_C^c \cdot n_D^d \quad (4.3)$$

Knowing the initial status of the system, the kinetic constants for the reactions' rates, the variables that define the system could be obtained after a time period (dt), the temperature, the pressure and the concentrations of considered species. By applying the model and Equation 4.3 the trend of the processes inside the engine cylinder during compression before the electric spark can be highlighted. For this model to be more accurate, the features required are: bore diameter, stroke length, compression ratio, the diameter of the inlet valve head, the diameter of the exhaust valve head, the opening of the inlet valve before TDC (Top Dead Center), the closure of the inlet valve after BDC (Bottom Dead Center), the opening of the exhaust valve before BDC, and the closure of the exhaust valve TDC.

4.3 Standardized Equation for Hydrogen Gas Densities for Fuel Consumption Applications

With the new technology and fuels in motor vehicles new methods of calculating fuel economy are established. Pressure, volume and temperature calculations are acceptable methods in calculating the fuel consumptions of hydrogen fuel in internal combustion engines and even fuel cells. By using these parameters the fuel consumption may be determined in an internal combustion engine using hydrogen fuel [111]. The temperature and pressure of the gas before and after usage within a storage tank are

known and the volume can be used in the consumption calculations. The method uses the density of hydrogen is also required for this calculation. Equation 4.4 illustrates the Younglove equation where p is the pressure, ρ is the molar density, T is the absolute temperature, R is the molar gas constant, and $G(i)$, n_j , m_i , and γ are constants that were determined from the available property data, written as a 32-term expression for pressure as a function of temperature and density for temperatures from 220 – 400K and pressures to 45MPa (6500psi) and 0.01% in density over the entire range of the calculation.

$$p = \rho RT + \sum_{i=1}^{19} G(i) \rho^{n_i} T^{m_i} + \sum_{i=20}^{32} G(i) \rho^{n_i} T^{m_i} \exp[\gamma \rho^2] \quad (4.4)$$

A common equation for the density of gases is based in the virial series, which has a statistical mechanical basis in terms of the relation between the number of particles, and particular gas density. The temperature-dependent virial equation is given as

$$z(p, T) = 1 + \sum_{i=2} B_i^*(T) p^{i-1} \quad (4.5)$$

where the $B_i^*(T)$ is the temperature dependent pressure virial coefficient and defined as:

$$B_i^*(T) = \sum_{j=1}^5 v_{ij} \left(\frac{T}{100K} \right)^{n_{ij}} \quad (4.6)$$

Combining with Equation 4.5 gives the following:

$$z(p, T) = 1 + \sum_{i=2}^6 \sum_{j=1}^2 v_{ij} \left(\frac{p}{1MPa} \right)^{i-1} \left(\frac{T}{100K} \right)^{n_{ij}} \quad (4.7)$$

By using this equation and the density constants, allows for the comparability of the compressibility factor. A general method for pressure, volume and temperature

calculations to determine the amount of hydrogen consumed is through the use of the following equation:

$$\Delta m = M \left[\rho_{final} (p_{final}, T_{final}) - \rho_{initial} (p_{initial}, T_{initial}) \right] V$$

$$\Delta m = \frac{MV}{R} \left[\frac{p_{final}}{T_{final} z(p_{final}, T_{final})} - \frac{p_{initial}}{T_{initial} z(p_{initial}, T_{initial})} \right] \quad (4.8)$$

where Δm is the mass of hydrogen consumed and M is the molar mass. Combined with the use of Equation 4.7, the compressibility factor is restricted to the T and p ranges for normal hydrogen from 200 to 400 K with pressures to 45 MPa, constant tables from yonglove equation and constant variables.

4.4 Thermodynamics of Internal Combustion Engine

This section explains the basic foundation of the thermodynamics without going into excessive detail. For the simulation of combustion-engine processes, the internal combustion engine is separated into a single component or partial system, and can be viewed as a closed or open thermodynamic system. To balance these systems the equation of continuity, the mass balance Equation 4.9 and the energy balance Equation 4.10 which uses the 1st law of thermodynamics with the energy flow Equation 4.11 for the open, stationary flooded flow system [112].

$$\frac{dm}{dt} = \dot{m}_1 - \dot{m}_2 \quad (4.9)$$

$$\frac{dU}{dt} = \dot{Q} + \dot{W} + \dot{E}_1 + \dot{E}_2 \quad (4.10)$$

$$\dot{E} = \dot{m} \left(h + \frac{c^2}{2} \right) \quad (4.11)$$

In the combustion chamber a closed thermodynamic system as illustrated in Figure 4.2 [112] is used and uses Equation 4.12 where no mass, and no enthalpy flows over the system limits. When the intake valves are open the system becomes an open thermodynamic system as illustrated in Figure 4.3.

$$\frac{dU}{dt} = \dot{Q} + \dot{W} \quad (4.12)$$

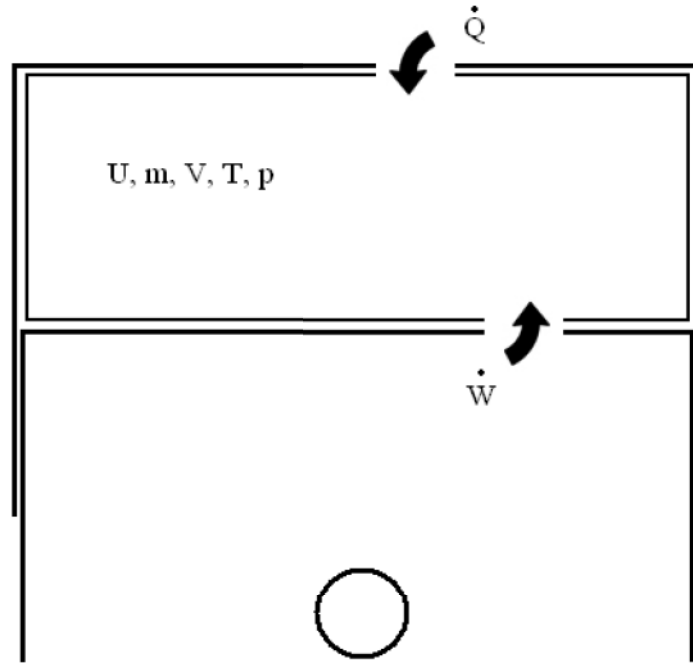


Figure 4.2: Closed thermodynamic system in a piston [112].

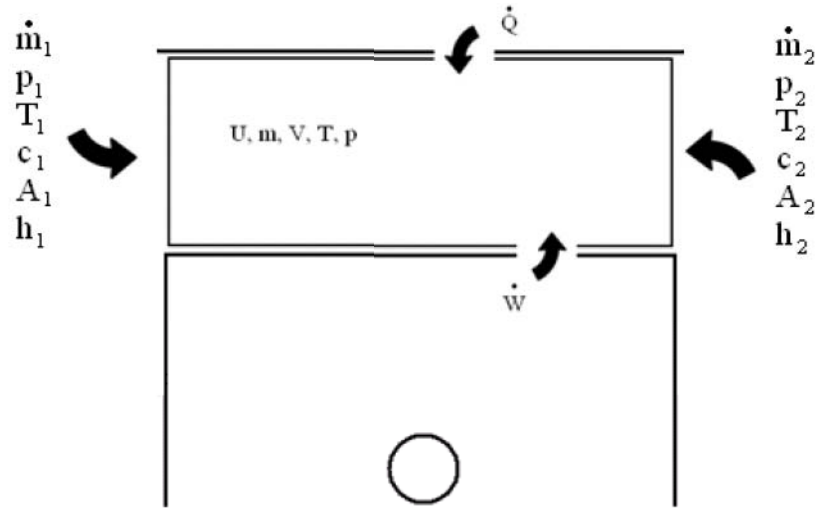


Figure 4.3: Open thermodynamic system in a piston [112].

By neglecting the friction or dissipation of the mechanical work into heat the volume work Equation 4.13 is used in the closed system. In the open system, the thermal energy transferred to the system and the intake is referred to as enthalpy, Equation 4.14. The thermal state Equation 4.15 ties together the pressure, temperature, and volume thermal conditions with the caloric state Equations 4.16, and 4.17 respectively.

$$\dot{W} = -p \frac{dV}{dt} \quad (4.13)$$

$$h = u + pv \quad (4.14)$$

$$f(p, T, v) = 0 \quad (4.15)$$

$$u = u(T, v) \quad (4.16)$$

$$h = h(p, T) \quad (4.17)$$

The inner energy as a function of temperature and volume and the enthalpy as a function of pressure and temperature can be viewed under ideal gases and using the thermal state Equation 4.18 to Equation 4.22. Since the inner energy of ideal gas is only

dependent on temperature, the caloric magnitudes of the ideal gas give the following equations:

$$pv = RT \quad (4.18)$$

$$du = c_v(T) dT \quad (4.19)$$

$$dh = c_p(T) dT \quad (4.20)$$

$$R = c_p(T) - c_v(T) \quad (4.21)$$

$$k = \frac{c_p}{c_v} \quad (4.22)$$

Under the consideration of enthalpy flows and the transferred kinetic energy to the system, the use of the energy balance of the open system Equation 4.23 can be used, and for stationary flooded open systems Equation 4.24 is used.

$$mc_v \frac{dT}{dt} + c_v T \frac{dm}{dt} = \frac{dQ}{dt} + \frac{dW}{dt} + \dot{m}_1 \left(h_1 + \frac{c_1^2}{2} \right) - \dot{m}_2 \left(h_2 + \frac{c_2^2}{2} \right) \quad (4.23)$$

$$\dot{m} \left[(h_2 - h_1) + \left(\frac{c_2^2}{2} - \frac{c_1^2}{2} \right) \right] = \frac{dQ}{dt} \quad (4.24)$$

For the outflow process the flow is assumed to be adiabatic and the velocity c_1 in the outflow cross section is calculated using:

$$c_1 = \sqrt{\frac{2k}{k-1} RT_0 \left[1 - \left(\frac{p_1}{p_0} \right)^{\frac{k-1}{k}} \right]} \quad (4.25)$$

along with the density ratio as given below:

$$\frac{\rho_1}{\rho_0} = \left(\frac{p_1}{p_0} \right)^{\frac{1}{k}} \quad (4.26)$$

resulting with the calculation and results for the mass flow rate are:

$$\dot{m} = A_1 \rho_1 c_1 \quad (4.27)$$

$$\dot{m} = A_1 \sqrt{\rho_0 P_0} \psi \left(\frac{P_1}{P_0}, k \right) \quad (4.28)$$

when equated resulting in Equation 4.29 the outflow function, dependent on the pressure ratio and the isentropic exponent.

$$\psi \left(\frac{P_1}{P_0}, k \right) = \sqrt{\frac{2k}{k-1} \left[\left(\frac{P_1}{P_0} \right)^{\frac{2}{k}} - \left(\frac{P_1}{P_0} \right)^{\frac{k+1}{k}} \right]} \quad (4.29)$$

4.5 Analysis of the Gas Exchange Stage (Backflow analysis)

During the gas exchange the energy balance equation on the expanding and contracting of the control volume in the in-cylinder gases is described as follows:

$$\left(h_i \dot{M}_i - \dot{Q}_{iv} - h_c \dot{M}_{ib} \right) = \frac{dU_c}{dt} + \dot{W}_p + \dot{Q}_c + \left(h_c \dot{M}_e - h_e \dot{M}_{eb} - \dot{Q}_{ev} \right) \quad (4.30)$$

where the intake (I) and exhaust (E) valves are present, as illustrated in Figure 4.4. The h_i is the specific stagnation enthalpy of the incoming gas and \dot{M}_i is the inlet valve mass inflow rate, h_c is the specific enthalpy of the in-cylinder gas, \dot{M}_{ib} is the intake valve mass backflow rate, \dot{Q}_{iv} is the heat transfer rate to the intake valve area, \dot{M}_e is the exhaust valve mass outflow rate, h_e is the specific stagnation enthalpy of the mixed exhaust gases, \dot{M}_{eb} is the mass backflow rate through the exhaust valve, and \dot{Q}_{ev} is the heat transfer rate to the exhaust valve area. If there is intake backflow, then an energy balance on the backflow zone is calculated using Equation 4.31 and illustrated in Figure 4.5. As

illustrated the total enthalpy H_{ib} of the backflow gas arises when the total internal energy change in the backflow zone and the work done in pushing back the fresh charge at the constant intake manifold pressure P_i is taken in the consideration.

$$(h_c \dot{M}_{ib} - \dot{Q}_{iv} - h_i \dot{M}_i) = \frac{dH_{ib}}{dt} \quad (4.31)$$

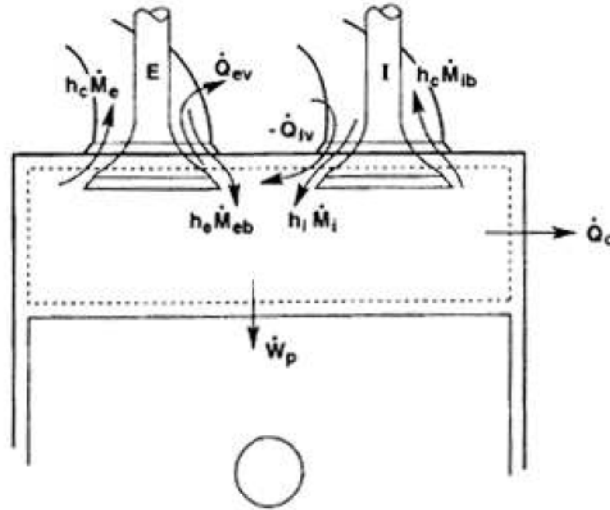


Figure 4.4: Energy balance on the in-cylinder gases with various terms [113].

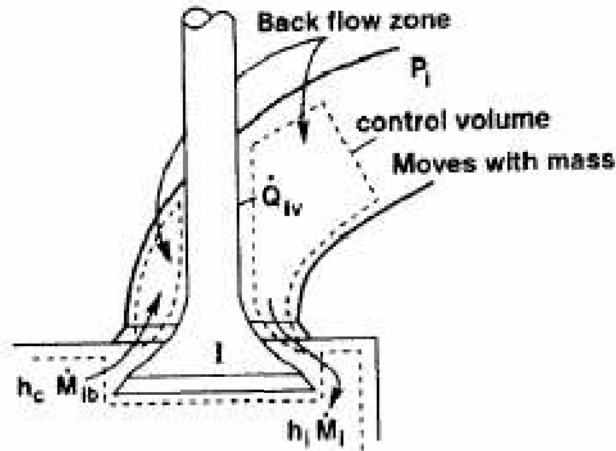


Figure 4.5: Energy balance of the backflow zone [113].

An energy balance is also made on the exhaust gas zone, Equation 4.32, as the total enthalpy H_e of the exhausted gas arises when the total internal energy change in the

backflow zone and the work done in pushing away the exhaust gas from the last cycle at the constant exhaust manifold pressure P_e is taken in the consideration, as illustrated in Figure 4.6.

$$\left(h_c \dot{M}_e - \dot{Q}_{ev} - h_e \dot{M}_{eb} \right) = \frac{dH_e}{dt} \quad (4.32)$$

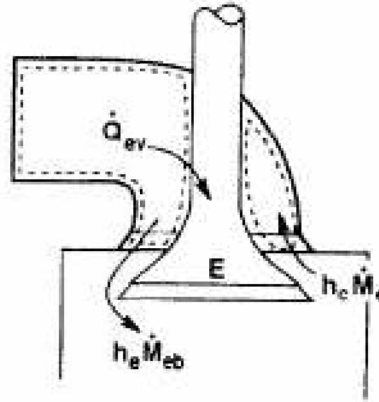


Figure 4.6: Energy balance on the exhaust gas zone [113].

The mass flow rates are determined using Equation 4.33 where C_d is a specified discharge coefficient and F is the mass flow rate for the isentropic flow. The upstream density ρ , contraction area A , upstream pressure P , downstream back pressure P_b , and gas specific heat ratio $\gamma = \frac{c_p}{c_v}$ can calculate the flow area using Equation 4.33 with an illustration in Figure 4.7. The flow routine provides for choked flow and accuracy at very low flow rates.

$$A_f = \pi \frac{D + D_i}{2} g = \pi \frac{D + D_i}{2} L \cos \theta \quad (4.33)$$

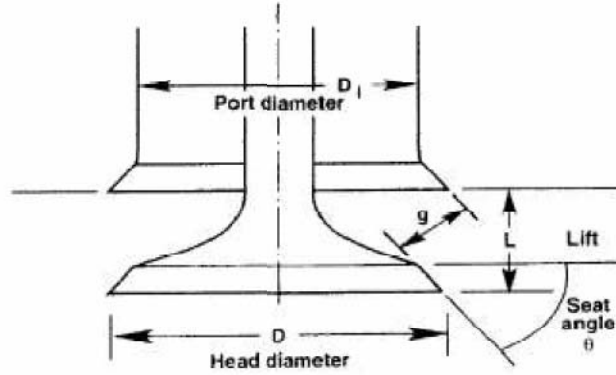


Figure 4.7: Typical inlet valve with various distances identified [113].

The mass balances are also required and the cylinder zone is calculated using Equation 4.34 and the intake backflow zone using Equation 4.35 and the exhaust gas using Equation 4.36. The valve flow heat transfer rates are found using Equation 4.37, where St_v is a user-specified Stanton number based on the velocity V_v for isentropic flow through the valve; ρ , c_p and T are the upstream density, specific heat and temperature; and A_v is the effective area for this heat transfer, specified by the user.

$$(\dot{M}_i - \dot{M}_{ib}) = \frac{dM_c}{dt} + (\dot{M}_e - \dot{M}_{eb}) \quad (4.34)$$

$$0 = \frac{dM_{ib}}{dt} + (\dot{M}_i - \dot{M}_{ib}) \quad (4.35)$$

$$(\dot{M}_e - \dot{M}_{eb}) = \frac{dM_e}{dt} \quad (4.36)$$

$$\dot{Q}_v = St_v V_v \rho c_p A_v (T - T_w) \quad (4.37)$$

4.6 Energy and Exergy Analyses

In this section the target engine being used to demonstrate the experimentation and data collection would be the use of the 1976 Chevrolet small block 350 5.7L 4-barrel Rochester carbureted V8 engine. The energy and exergy analyses comparison of this eight-cylinder, four-stroke spark-ignition engine using octane 95 gasoline fuel, was tested

under the performance of varying engine speed between 1200 and 2400 RPM. This allowed for a steady energy and exergy analyses comparison using the hydrogen fuel. The performance, fuel consumption and exhaust emissions of an internal combustion engine have been improved ever since the introduction and creation of these engines originating from the mid 20th century. Some of these improvements have not only been on the design aspect but also on both the engine performance and exhaust emissions. The octane rating of the gasoline fuel required by an engine is the measure of its resistance to detonation.

To calculate the energy and exergy analyses of this engine, the Ideal Otto Cycle method is used. An ideal Otto cycle has a compression ratio of 8, at the beginning of the compression process, the air is said to be at 100kPa and 17^oC and 800 kJ.kg of heat is transferred to air during the constant –volume heat addition process.

4.6.1 Experimental Setup and Testing Procedure

The test was performed on an eight-cylinder, four-stroke, Chevrolet small block 350CID 5.7 L spark ignition engine as seen in Figure 4.8, which originally requires 91-octane gasoline to operate. The 95-octane gasoline fuel was used in this experiment, and the schematic layout of the experiment is shown in Figure 4.9 and the final layout of the engine in a 1986 GMC Sierra 1500 truck for future work is seen in Figure 4.10, along with the details of the engine specifications are shown in Table 4.1. Furthermore, a schematic drawing of the experimental setup is drawn and divided into sub-components and analyzed using energy and exergy methods of analyses as seen in the following figures and experimental setup.



Figure 4.8: 1976 Chevrolet small block 350 5.7L V8.



Figure 4.9: Layout of the experimental apparatus.



Figure 4.10: Layout of the experimental apparatus in 1986 GMC Sierra 1500.

Table 4.1: The technical specifications of the Chevrolet 5.7L small block 350CID engine.

Engine Type	Chevrolet 5.7L small block 350CID
Cylinder number	8 Cylinders
Bore	4.000 inch (101.6 mm)
Stroke	3.48 inch (88.4 mm)
Firing Order	1-8-4-3-6-5-7-2
Compression Ratio	8:1
Maximum torque	160 ft.lbs at 3500 RPM
Maximum Power	120 HP
Engine Octane requirements	95 Octane on gasoline, 130 Octane on hydrogen

To analyze this engine in energy and exergy analyses, the engine is placed outside of the vehicle and many of the components required for the vehicle are not required when operating on an engine stand, therefore, these are not considered and only certain components of the engine are considered and analyzed. For this analysis the engine operating on gasoline fuel, and the engine as shown in Figures 4.11 and 4.12 on hydrogen fuel, shows the comparison of the components installed on the engine.



Figure 4.11: Engine on hydrogen components.

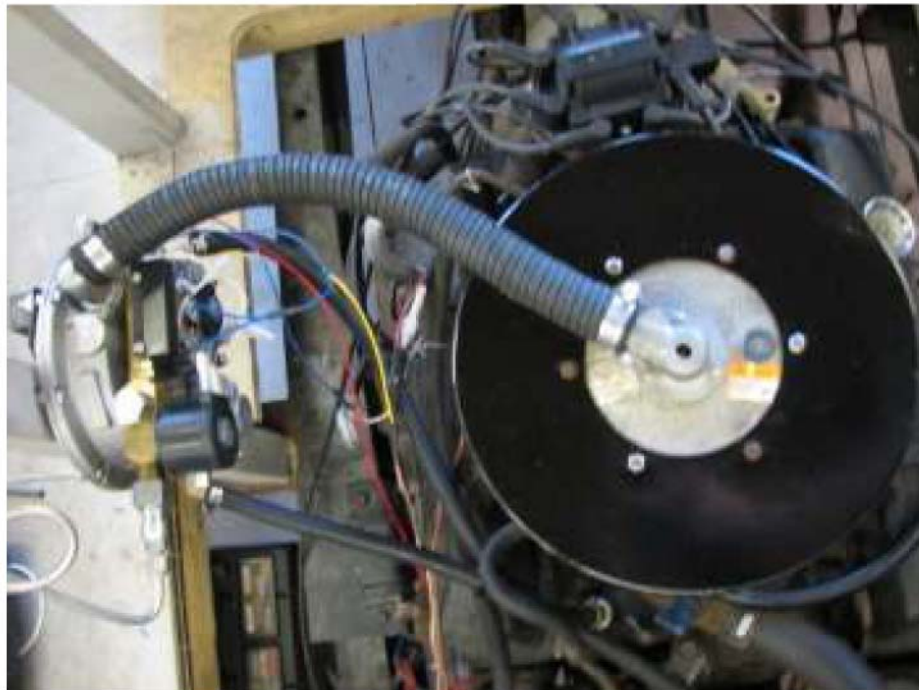


Figure 4.12: Engine on hydrogen components.

The layout of this experiment is seen in the two illustrations below in Figure 4.13 representing the engine on gasoline fuel and Figure 4.14 representing the engine on hydrogen fuel operations. The two illustrations shown below are divided into sub

components and the energy and exergy analyses of the engine based on the two fuels are analyzed, compared and a conclusion is drawn from this analyses.

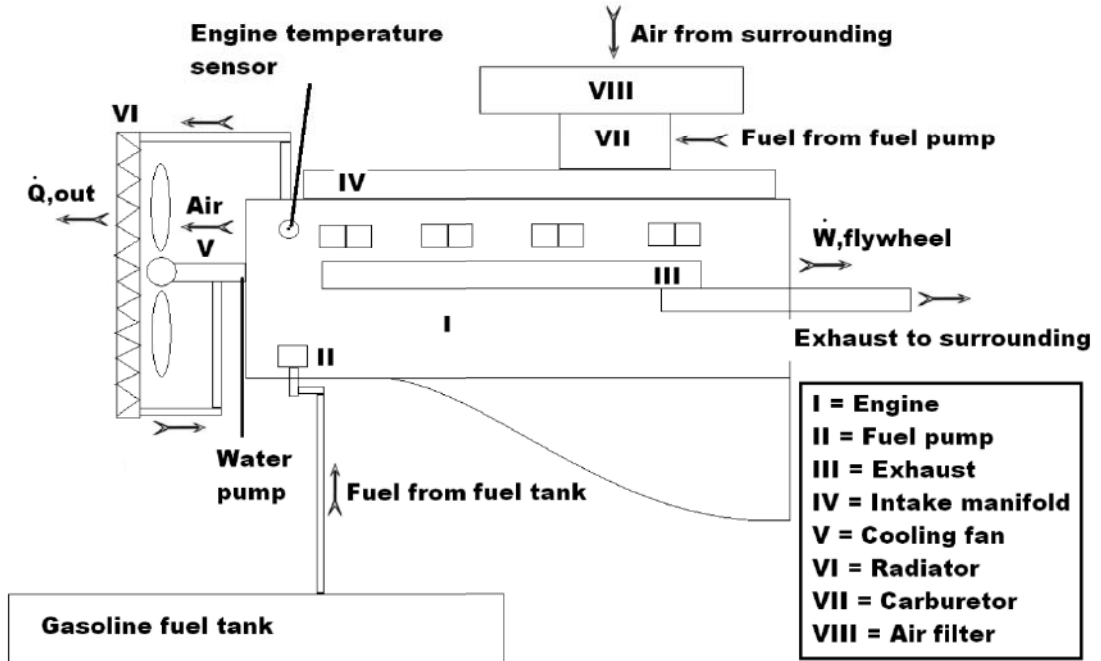


Figure 4.13: Illustration of engine on gasoline fuel operation.

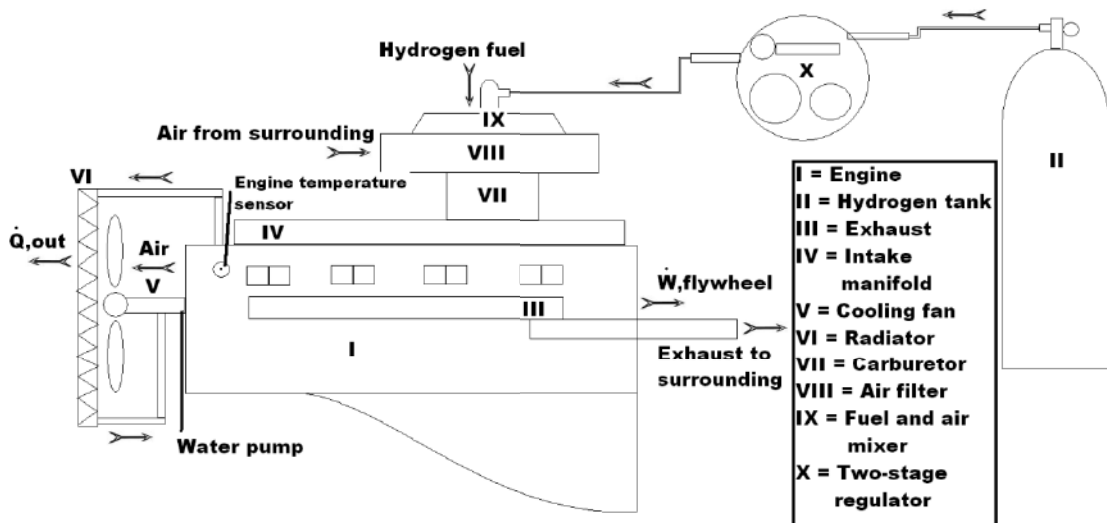


Figure 4.14: Illustration of engine on hydrogen fuel operation.

In the energy and exergy analyses using gasoline and hydrogen fuel in the experimental engine, only a few major components are analyzed which are essential to the operation of the engine. All other small components in the engine are considered to have about 80 - 85% efficiency towards the engine operation, not including transmission losses to the wheels [120]. Furthermore, the sub-components in the following figures are drawn with a schematic which would represent that system, for the ease of calculation purposes.

Using the Otto cycle [120], the net work output can be calculated, along with the thermal efficiency of the engine.

The energy balance equation for the combustion process, \dot{Q}_{loss} of approximately 62%, including \dot{W}_{sh} , shaft work, frictional losses, and heat losses is given in Equation 4.38. The energy losses in a typical vehicle are approximately 17.2% in standby/idle operations, as well as 2.2% loss for the accessories, 5.6% for the driveline losses, 2.6% aerodynamic drag losses, 4.2% rolling resistance, inertia and braking losses of 5.8%. All of these losses lead to this significant low efficiency from these engines [121]. The entropy balance equation as observed in Equation 4.39, is used for both the gasoline and hydrogen fuel where it is then used for calculating the overall thermal efficiency in Equation 4.40 and overall exergy efficiency in Equation 4.41. Similarly, the exergy balance equation as observed in Equation 4.42 is used for both the gasoline and hydrogen fuel, from which the overall exergy efficiencies are calculated. The energy efficiency of the gasoline fuel is seen in Figure 4.15 and the energy efficiency of the hydrogen fuel is seen in Figure 4.16. These two cases are compared and it is observed that the energy efficiency of the engine using hydrogen fuel is much lower than that of the gasoline fuel.

This is due to the physical properties of the hydrogen gas used as the fuel. Finally the exergy efficiencies are plotted as observed in Figure 4.17 for the gasoline fuel and compared with the exergy efficiency of the hydrogen fuel in Figure 4.18. This comparison demonstrates that the exergy efficiency of the engine running on the gasoline fuel is higher than if it were to run on hydrogen fuel.

$$\dot{m}_{a/f} h_{a/f} + \dot{W}_{sh} - \dot{m}_{ex} h_{ex} + \dot{Q}_{a/f} - \dot{Q}_{loss} = 0 \quad (4.38)$$

$$\dot{m}_{a/f} s_{a/f} + \dot{S}_{gen} - \dot{m}_{ex} s_{ex} + \frac{\dot{Q}_{a/f}}{T_0} - \frac{\dot{Q}_{loss}}{T_o} = 0 \quad (4.39)$$

$$\eta_{th} = \frac{\dot{W}_{net,out}}{\dot{m}_{fuel,actual} CV} \quad (4.40)$$

$$\eta_{ex} = \frac{\dot{W}_{net,out}}{\dot{m}_{fuel,actual} ex_{chemical}} \quad (4.41)$$

$$\dot{m}_{a/f} ex_{a/f} + \dot{E}x_{dest} - \dot{m}_{ex} ex_{ex} + \dot{Q}_{a/f} \left(1 - \frac{T_0}{T_i}\right) - \dot{Q}_{loss} \left(1 - \frac{T_0}{T_i}\right) = 0 \quad (4.42)$$

The energy and exergy efficiencies calculated are low for hydrogen fuel as compared to gasoline fuel. There are several reasons for the low efficiencies. This engine was designed specifically for gasoline fuel operations and not hydrogen. Furthermore, the mode of fuel delivery is mechanical and thus not appropriate for the gaseous hydrogen fuel. Lastly, to improve the efficiencies, this engine requires modifications that would incorporate the elimination of mechanical components for fuel delivery, air supply, exhaust stroke valves and spark timings.

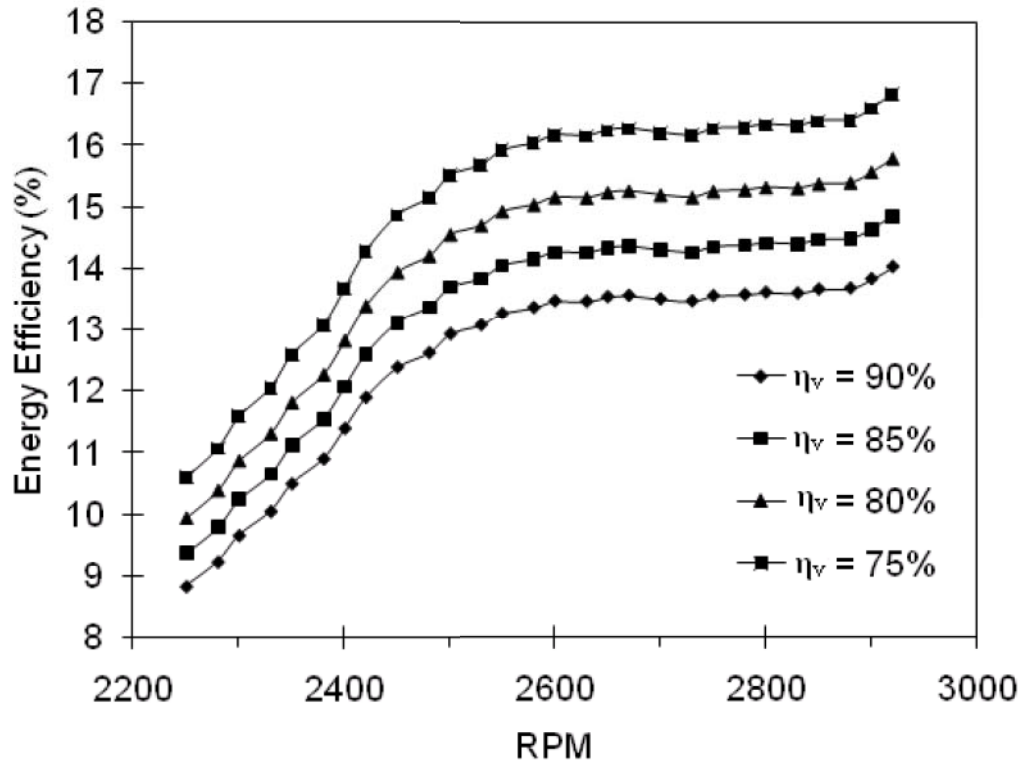


Figure 4.15: Energy efficiency of engine operating on gasoline fuel.

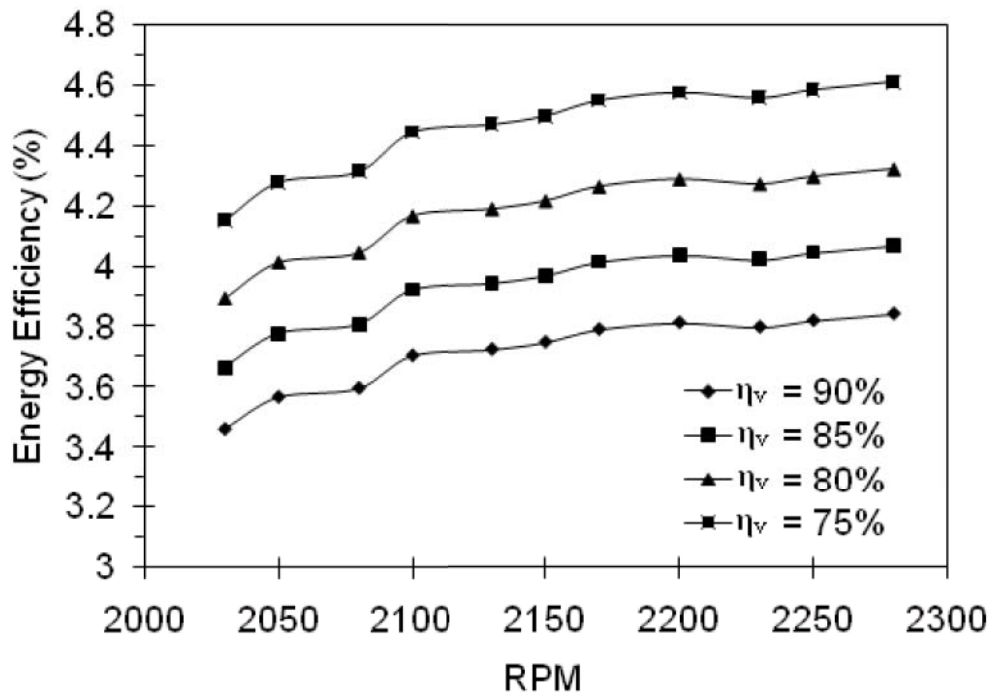


Figure 4.16: Energy efficiency of engine operating on hydrogen fuel.

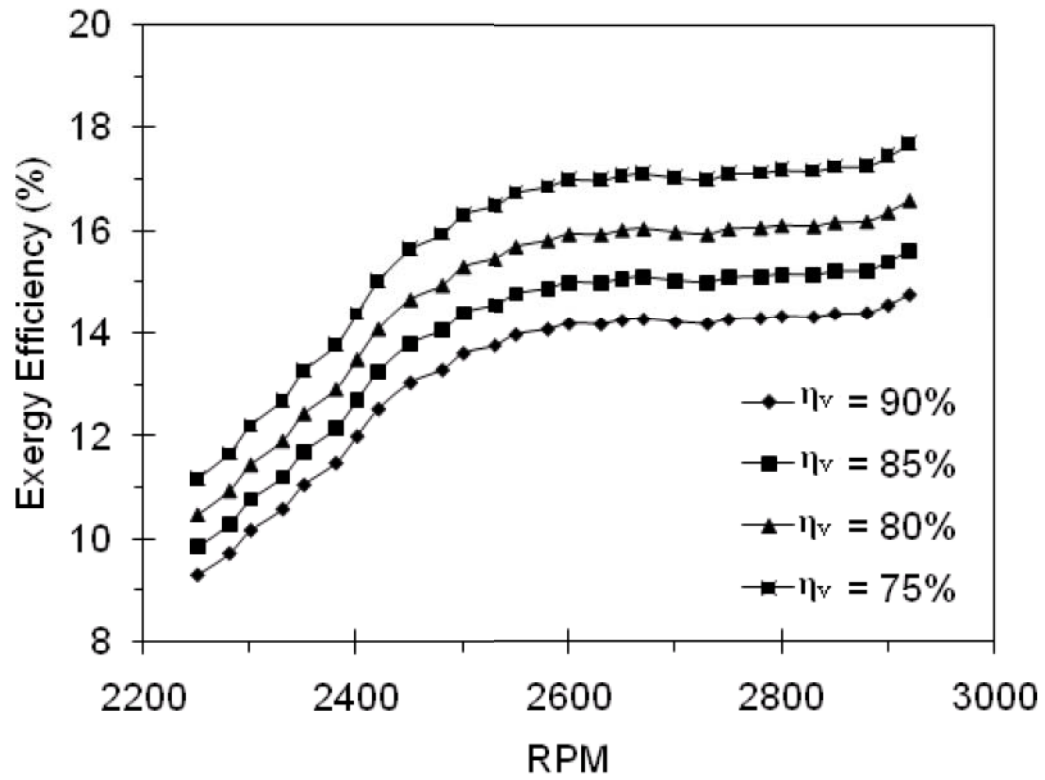


Figure 4.17: Exergy efficiency of engine operating on gasoline fuel.

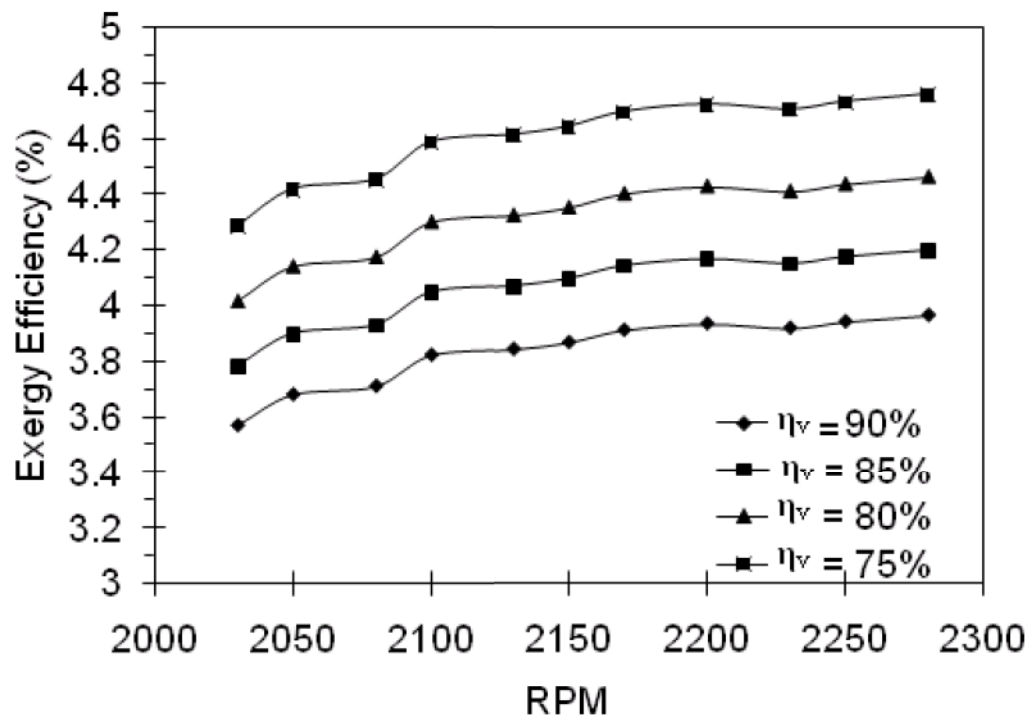


Figure 4.18: Exergy efficiency of engine operating on hydrogen fuel.

Although hydrogen fuel is not in the same state as of the gasoline fuel, when calculating for the efficiencies and using the Otto cycle, the energy density of both fuel differ, hydrogen has a lower volumetric energy density than gasoline. Also when calculating the efficiencies, the liquid, vapor and gaseous states were considered. Although for this analysis to be most accurate, temperature and pressure sensors are required to be placed at multiple entry and exit points. Once all of these data are collected a proper analysis can be done. Furthermore, additional study of hydrogen property is required under high pressures and natural aspiration pressures. As the above mentioned calculations and analyses, it shows that the hydrogen engine has lower exergy efficiency than that of the gasoline fuel. This is due to the energy density of the fuel and the gaseous state as compared to the liquid state of gasoline.

4.7 Fuel Economy and Engine Characteristics

In this section the fuel economy of both the hydrogen gas and the premium octane 95 gasoline fuel, are calculated and compared based on the performance of the engine and the conversion being done to it. Furthermore, in this chapter the power curves, and engine operating characteristics under various loads and volumetric efficiencies are compared and observed.

4.8 Fuel Economy Calculation for Gasoline Fuel

For the internal combustion engine, the optimum fuel along with the 5.7L V8 engine information are given below and shown in Figure 4.19.

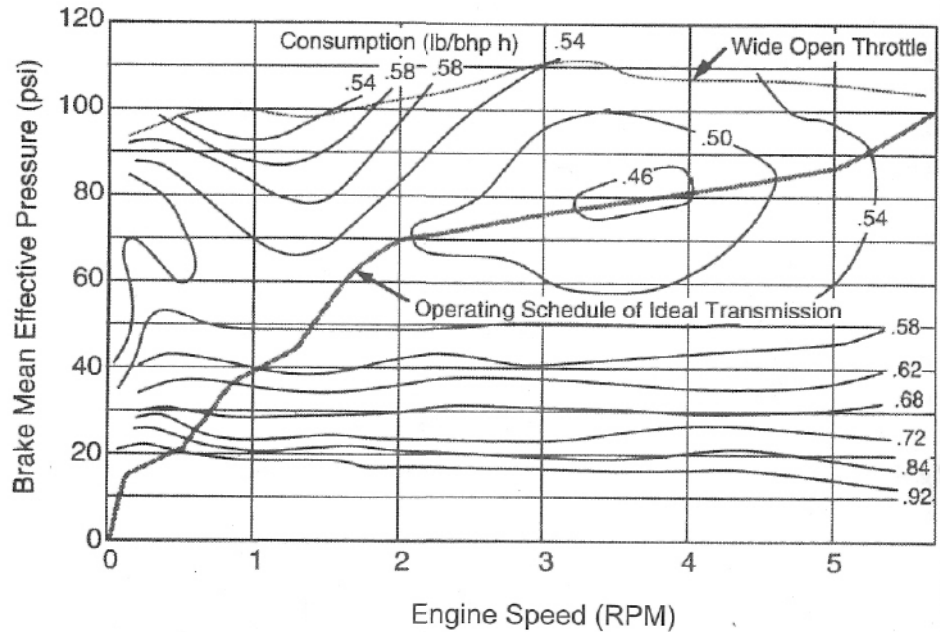


Figure 4.19: Specific fuel consumption map of a V8 engine [114].

The information known for the 1986 GMC Sierra 1500 truck has an air drag coefficient of 0.34. The truck with the new engine is weighted to approximately 3844 lbs (1,743.61 kg). The truck also has a frontal area of approximately 1.8581 m^2 , and the rolling radius and rolling resistance coefficient of the tires are 0.32 and 0.018, respectively. The final drive unit gear ratio, i_o is 3.76. It is also assumed that the transmission is a continuous variable transmission and the mechanical efficiency (η_t) is said to be 0.88.

The first calculation made is to find the gear ratio that provides the maximum fuel economy at a vehicle speed of 100km/hr, and then the fuel consumption of the car in liters per 100km with a mass density of the gasoline to be taken at 0.75 kg/L is calculated. It is first considered to determine the gear ratio that provides the maximum fuel economy at 100km/hr using Equation 4.43, where u_a is the speed of 100km/hr, “r” is

the rolling resistance coefficient of tires, i_o is the unit gear ratio, and n_p is the engine speed at the optimum fuel level.

$$i_g = 0.377 \frac{n_p r}{i_o u_a} \quad (4.43)$$

The power and force of friction are calculated using Equations 4.44 and 4.45 where P_e is output power, P_w is the aerodynamic and P_f the frictional power losses. P_w and P_f are calculated using Equations 4.45 and 4.46 through the frictional and aerodynamic forces.

$$P = \frac{1}{\eta_t} (P_f + P_w) = P_e \quad (4.44)$$

$$F_f = mgf \cos \alpha \quad (4.45)$$

$$F_w = \left(\frac{\rho}{2} \right) (C_D A_f u_a^2) \quad (4.46)$$

From Figure 4.19 using the actual power output from the engine, the optimum engine speed is determined to be at 1,600 RPM. Therefore, the gear ratio that would create the maximum fuel economy line is 0.4364 from the above made calculations. Calculating the specific fuel consumption using Equation 4.47, taking the mass density of octane 95 gasoline to be 0.75 kg/L, the following calculations are made.

$$Q = \frac{Pb}{1.02 \rho g u_a} \quad (4.47)$$

From Figure 5.1 the specific fuel consumption (b) is obtained from the known and calculated value P and is 0.4 lb/bhp.h (0.243 kg/kW.h). From Transport Canada website, the fuel economy of this vehicle is listed as 16L/100km for city driving conditions. With

the above calculations achieved results are very close, due to the age of the vehicle and the mileage taken on this vehicle the mileage calculated is 17.4L/100km.

4.9 Fuel Economy for Hydrogen Fuel

Considering the different properties of the two fuels of comparison, since hydrogen is stored in a compressed gas tank, the comparison of the two fuels would be the physical properties they are being stored. To obtain the fuel economy from the experimental setup, the measured fuel economy with respect to pressurized fuel vs. time is observed, and this also considers the losses of the fuel through the system and the unburned hydrogen fuel from the incomplete combustion to the hydrogen physical properties and the compression ratio of the engine is plotted in Figure 4.20.

Due to the limitations of the hydrogen gas and the current existing problem of premature detonation (backfire), the speeds chosen to do these calculations and collecting data were between 10 to 15km/hr.

For a 2,400 Psi hydrogen tank, it holds an approximate 0.5kg of fuel, equivalent to 1.89L of gasoline fuel. Hydrogen has 106.36 kcal/kg (191.3 Btu/lb) and it is considered that the engine is operating at 15% efficiency. Converting to km/L it yields that the fuel economy of the engine using hydrogen fuel is estimated to be approximately 4.15 km/L gasoline equivalent.

From an experimental run with the fuel onboard, to determine an approximation of the fuel usage, considering the difficulty with the calculation, the following data has been created with respect to the fuel left under pressure in the tank and time, as it is being used, this is seen in the graph in Figure 4.20.

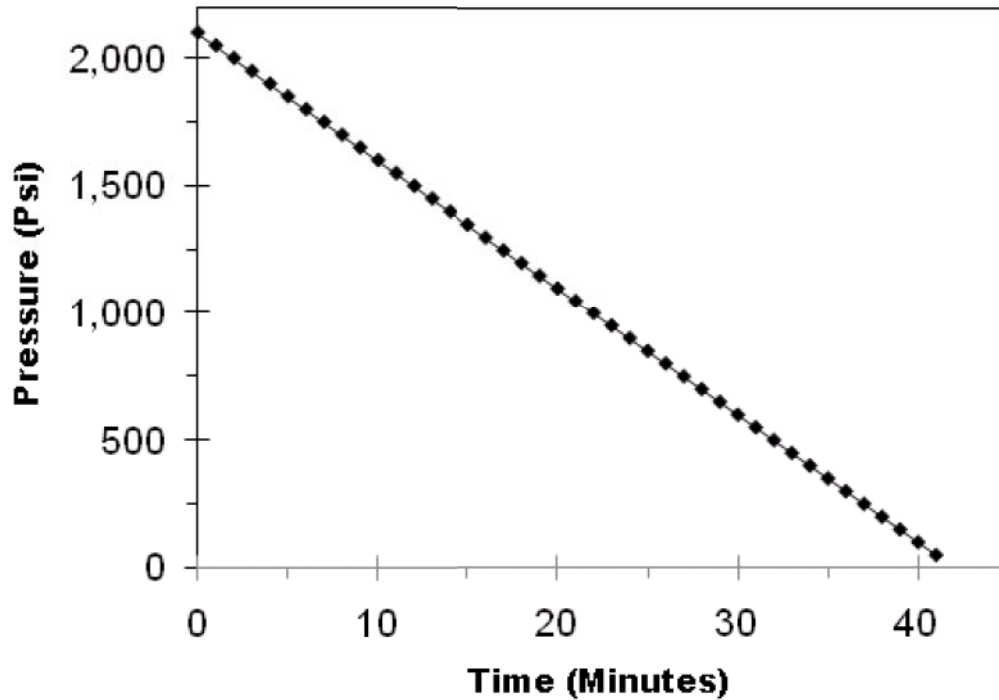


Figure 4.20: Pressure vs. time of hydrogen usage in a 5.7L V8.

Figure 4.20 shows the operation at 40min with 0.5kg of fuel that travelled a distance of 4.5km. This would yield a fuel economy of $4.5\text{km}/0.5\text{kg} = 4.5\text{km}/1.89\text{L} = 2.38\text{km/L}$ or $42.017\text{L}/100\text{km}$ of gasoline fuel equivalent.

When comparing the gasoline fuel and the hydrogen gaseous fuel together and calculating or measuring the fuel economy of both, it is noticed that considering the fuel densities and the method of each being stored, either in liquid state and the other in gaseous state, and the amount of hydrogen is required, the storage becomes an issue for the hydrogen fuel, and alternate methods must be taken into consideration for this storage problem as well as studying the different methods of improving the fuel efficiency and consumption of the engine.

The Brake Specific Fuel Consumption (BSFC) calculated using Equation 4.48 for both gasoline and hydrogen results in the following graphs in Figure 4.21 and 4.22 respectively for various volumetric efficiencies denoted as (η_v) [115].

$$bsfc = \frac{\dot{m}_{fuel,actual}}{P} \quad (4.48)$$

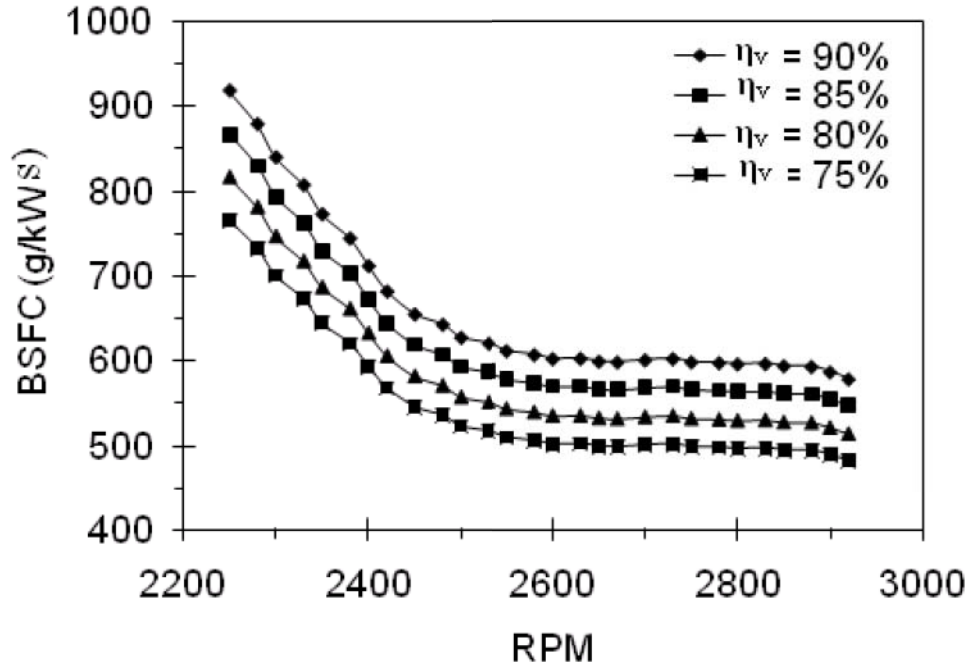


Figure 4.21: Brake specific fuel consumption for gasoline fuel.

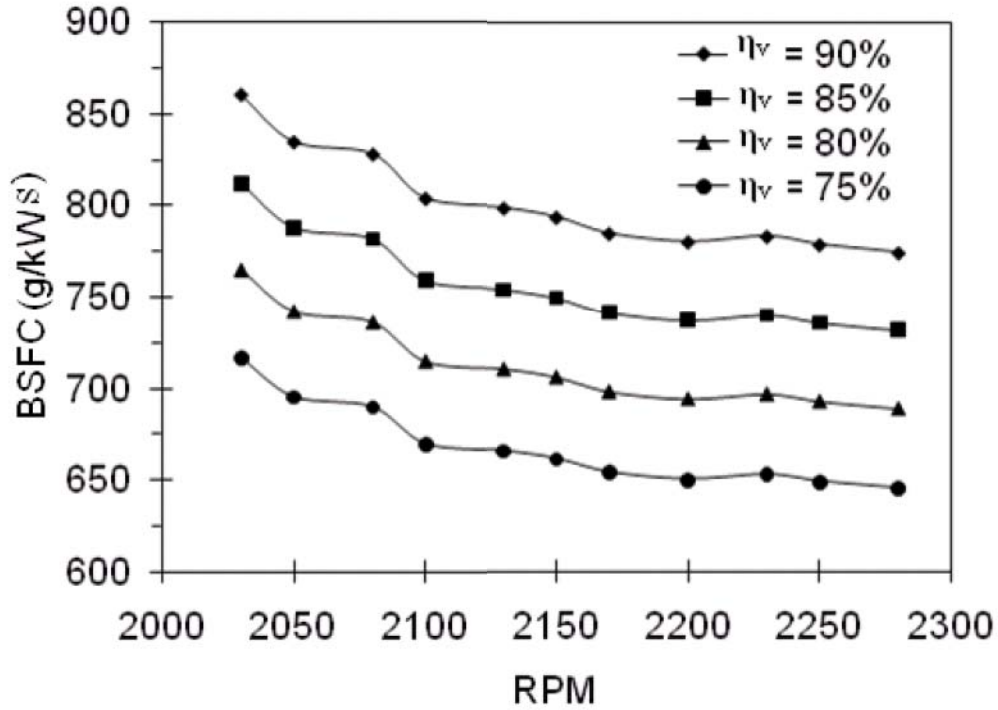


Figure 4.22: Brake specific fuel consumption for hydrogen fuel.

The $\dot{m}_{fuel,actual}$ is the mass flow rate of the fuel and P is the Power at the measured engine speed (RPM). To measure the $\dot{m}_{fuel,actual}$ Equation 4.49 is used, where the Air/Fuel ratio is obtained from the experimental setup. In Equation 4.50 where $\dot{m}_{air,actual}$ is the air mass flow rate obtained from the volumetric flow rate of the air multiplied by the standard condition of air at 69.2°F. The volumetric flow rate of air is calculated using the theoretical volumetric air flow rate multiplied by the volumetric efficiency, as seen in Equation 4.51. The theoretical volumetric air flow rate is obtained from the various engine speed (RPM) multiplied by the engine displacement ($E_{displacement}$) size 5.7L in Equation 4.52.

$$\dot{m}_{fuel,actual} = \frac{\dot{m}_{air,actual}}{AF_{ratio}} \quad (4.49)$$

$$\dot{m}_{air,actual} = \dot{V}_{air,actual} \rho_{air} \quad (4.50)$$

$$\dot{V}_{air,actual} = \dot{V}_{air,theoretical} \eta_{vol.} \quad (4.51)$$

$$\dot{V}_{air,theoretical} = RPM (E_{displacement}) \quad (4.52)$$

From these equations and various volumetric efficiencies the following graphs are obtained for both the gasoline and hydrogen fuel. Figure 4.23 is the gasoline mass air flow rate vs. engine speed. In Figure 4.24, the mass air flow rate of hydrogen is measured and plotted. Furthermore, in Figure 4.25 and 4.26 the mass fuel flow rate of gasoline and hydrogen respectively are measured and calculated. In Figure 4.27 the Air Fuel ratio (A/F_{ratio}) for both gasoline and hydrogen are plotted for the measured engine speed and are used for this experiment to differentiate the benefits of using both fuels.

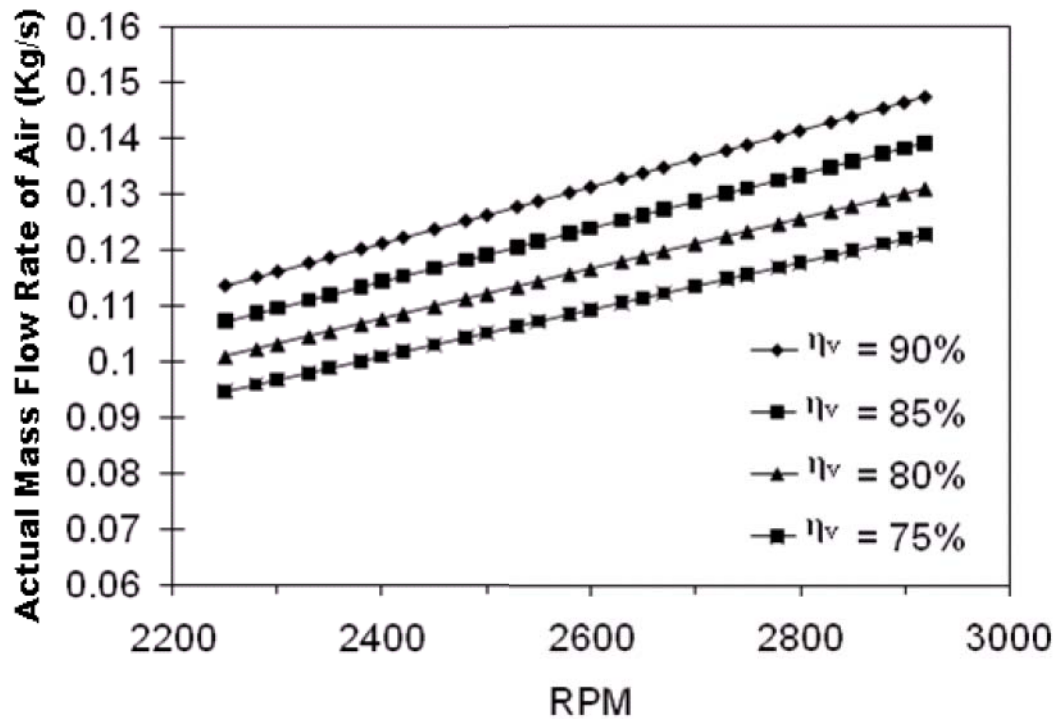


Figure 4.23: Gasoline mass air flow rate in 5.7L V8 engine.

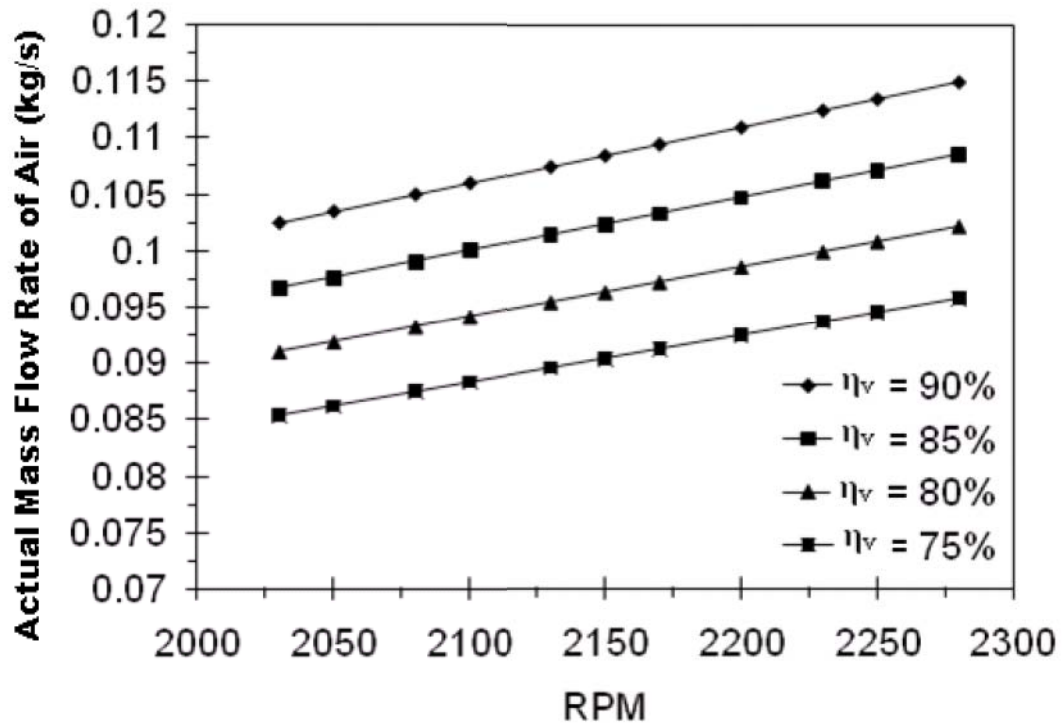


Figure 4.24: Hydrogen mass air flow rate in 5.7L V8 engine.

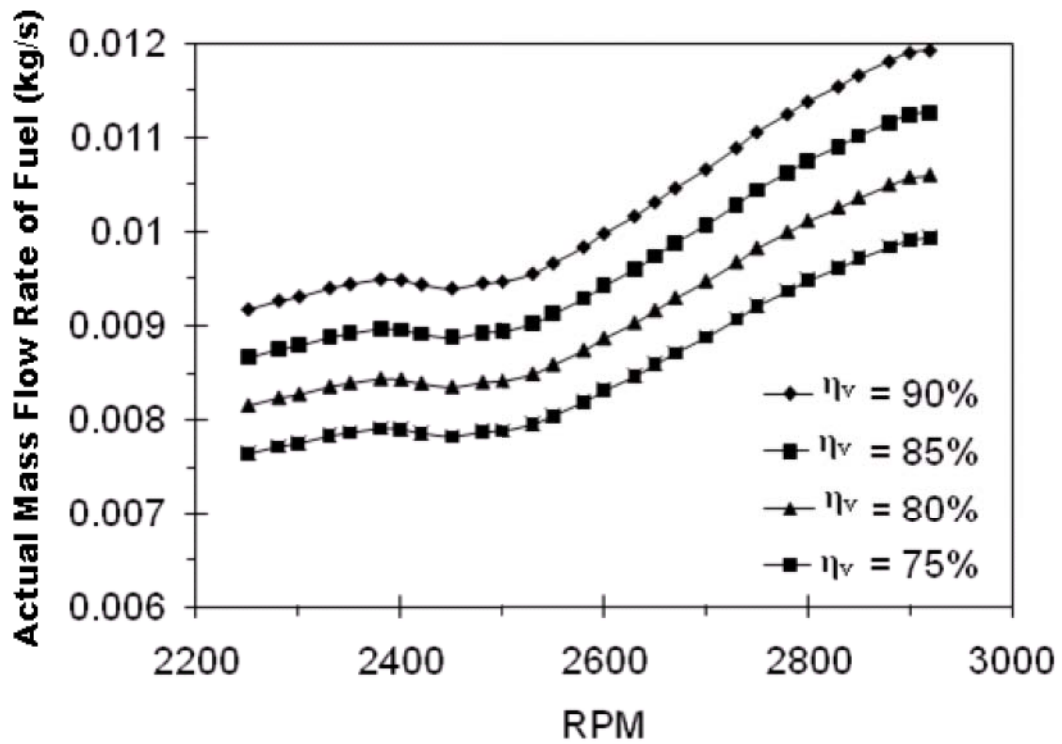


Figure 4.25: Gasoline mass fuel flow rate in 5.7L V8 engine.

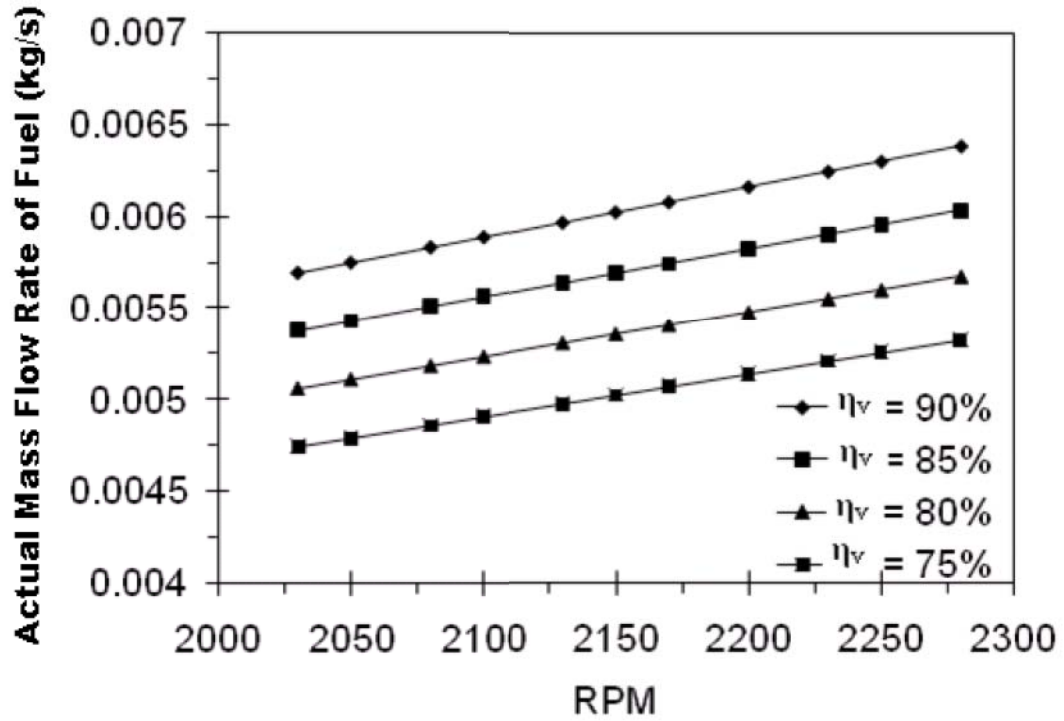


Figure 4.26: Hydrogen mass fuel flow rate in 5.7L V8 engine.

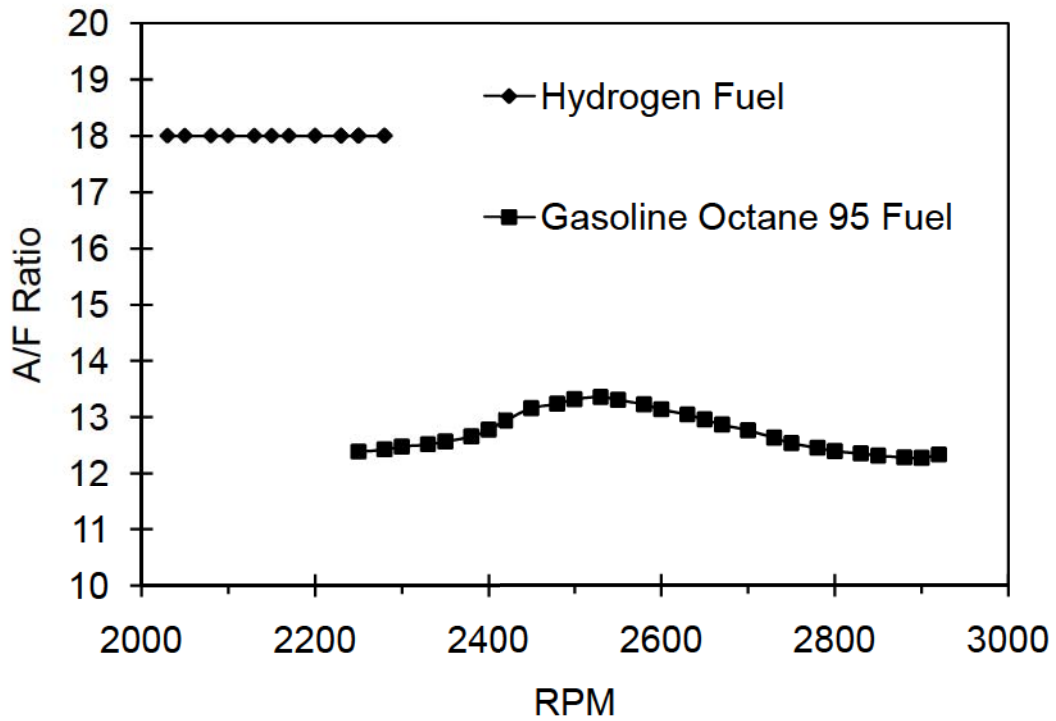


Figure 4.27: Air fuel ratio for both gasoline and hydrogen fuel under a range of RPM.

4.10 Engine Characteristics

The vehicle and engine at hand to be compared and analyzed is the 1986 GMC Sierra 1500, as observed in Figure 4.28, with a 1976 Chevrolet Small Block 350 5.7 L 4-barrel carburetor V8, as observed in Figure 4.29. This engine is operated via a 4-barrel carburetor that mixes the fuel with the air coming from the atmosphere as seen in Figure 4.30.



Figure 4.28: 1986 GMC Sierra 1500.

This 1986 GMC Sierra 1500 truck is a two wheel rear wheel drive with an 8' feet bed and single cabin, which makes it a reasonable work truck for its model year. The wheel base on this truck is 3.34 m (131.5 inches) [116], and the engine available for this truck was the 305 CID 5.0 L V8 4-barrel Rochester carbureted engine. The truck with the new engine is weighted to be at approximately 1,743.61 kg (3844 lbs).



Figure 4.29: 1976 Chevrolet small block 350 CID 5.7L V8.

The Chevrolet small block 5.7L 350 CID V8, has the physical dimensions of square 4.00 inch (102 mm) bore and 3.48 inch (88 mm) stroke [117], which produces after taking a dynamometer test approximately 120 HP and nearly 168 lb.ft of torque, as observed in Figure 4.31.



Figure 4.30: 4-barrel Rochester quadrajet M4MED carburetor.

The 4-barrel Rochester Quadrajets M4MED carburetor has a large 4-barrel carburetor that has a small primary side for fuel economy and good emissions, and a large secondary side for good performance. The Quadrajets carburetors have a maximum airflow of from 750-800 cfm. This is due to the secondary side of the Quadrajets, as it opens according to the airflow requirements of the engine, the same basic carburetor size can be used on a large range of engine sizes. On a mild 350 Chevrolet engine the air valve will never open all the way and this is due to the limitations of the motor, which can't use more than 600 cfm of airflow [117].

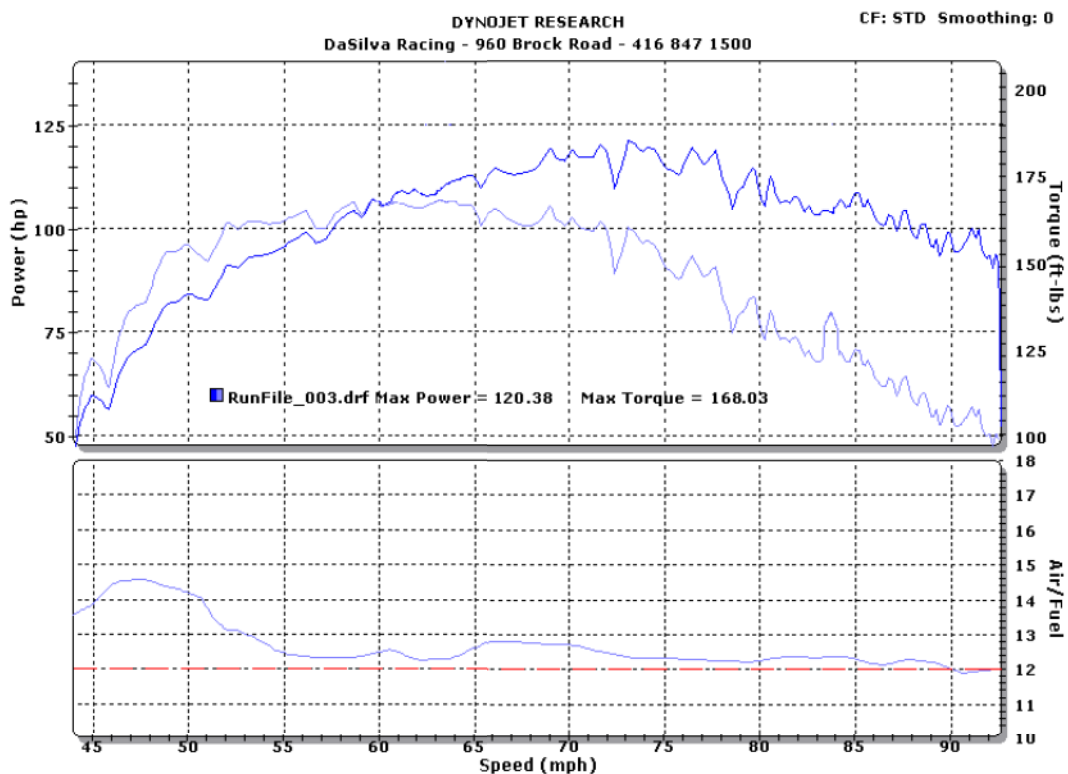


Figure 4.31: Results obtained from WinPEP7 DynoJet performance program.

The 1986 GMC Sierra 1500 was once more taken to the Dyno performance shop to be tested with the hydrogen fuel. A dynamometer or "dyno" for short, is a device for measuring force, moment of force (torque), or power. For example, the power produced

by an engine, motor or other rotating prime mover can be calculated by simultaneously measuring torque and rotational speed (rpm).

In addition to being used to determine the torque or power characteristics of a machine under test (MUT), dynamometers are employed in a number of other roles. In standard emissions testing cycles such as those defined by the US Environmental Protection Agency (US EPA), dynamometers are used to provide simulated road loading of either the engine (using an engine dynamometer) or full power-train (using a chassis dynamometer). In fact, beyond simple power and torque measurements, dynamometers can be used as part of a test-bed for a variety of engine development activities such as the calibration of engine management controllers, detailed investigations into combustion behavior and tribology, and the science and engineering of interacting surfaces in relative motion. It includes the study and application of the principles of friction, lubrication and wear.

The results obtained here are given in Figure 4.32; these directly cannot be compared to that of gasoline results, as the engine experienced premature detonations (backfire) with the hydrogen fuel. After further investigation it was noted that the hydrogen fuel brought the operating temperature of the engine higher than that of the gasoline fuel. Thus the results had shown in Figure 5.14 shows engine speed of up to 3000 RPM. The engine produced approximately 41 hp and 95 lb.ft of torque, much lower than the gasoline fuel.

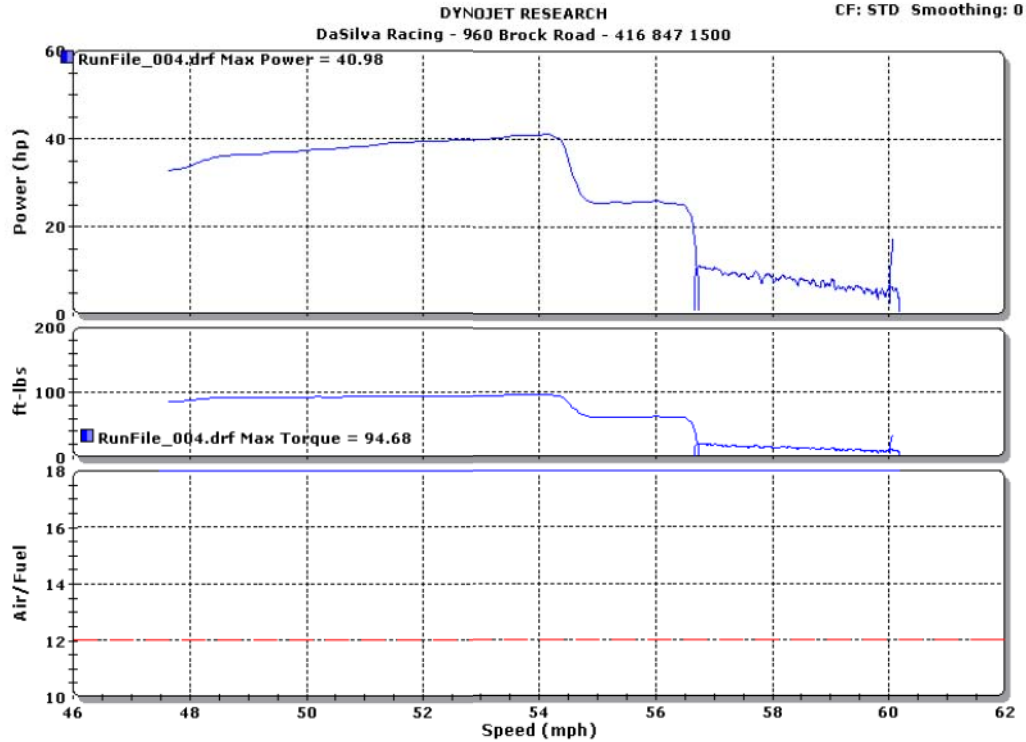


Figure 4.32: Hydrogen fuel results from the dynamometer.

The characteristics in between the hydrogen and gasoline fuel which regards to the noise level remained approximately the same. Furthermore, from the performance aspects the engine performed poorly with the hydrogen fuel than compared to the gasoline fuel. The reason behind this is that the hydrogen fuel has much lower ignition energy of $20\mu\text{J}$, compared to the gasoline fuel of $240\mu\text{J}$. The hydrogen fuel also has a theoretical explosive energy of $2.02\text{ (kg TNT/m}^3\text{ gas)}$ compared to the $44.22\text{ (kg TNT/m}^3\text{ gas)}$ of the gasoline fuel. However, the heating value of hydrogen (120 kJ/g) is higher than of the gasoline fuel (44.5 kJ/g). Thus it is more volatile and prompt to premature detonation (backfire) if the engine is not optimized for the hydrogen fuel.

Due to the limitation of the engine performance with the hydrogen fuel, the fuel economy calculations are from the engine operating at 3,000 RPM 2nd gear as shown in the previous section. For future work, the possibilities of eliminating premature

detonation (backfire/back flash) will be analyzed and a possible water injection will be introduced and the engine performance will be measured once more using the new system. Other possibilities include the components that are installed on the engine to burn the hydrogen fuel, will be analyzed. To develop this water injection kit, the six sigma methodologies are used, as it is shown in the next section.

The gasoline and hydrogen net power graph is seen in Figure 4.33 and the torque output on both fuels are seen in Figure 4.34, as both graphs are compared with various RPM range, which indicates the power output from both fuels.

The Brake Mean Effective Pressure (BMEP) for both hydrogen and gasoline are obtained and plotted in comparison with one another in Figure 4.35 and the BMEP is calculated from Equation 4.53. Torque is measured from the engine output from the dynamometer test runs using both gasoline and hydrogen fuels, and $E_{displacement}$ is the engine size of 5.7L, all multiplied by 1/100,000 to get the units in bar.

$$BMEP = \frac{Torque(2\pi)}{0.5E_{displacement}} \left(\frac{1}{100,000} \right) \quad (4.53)$$

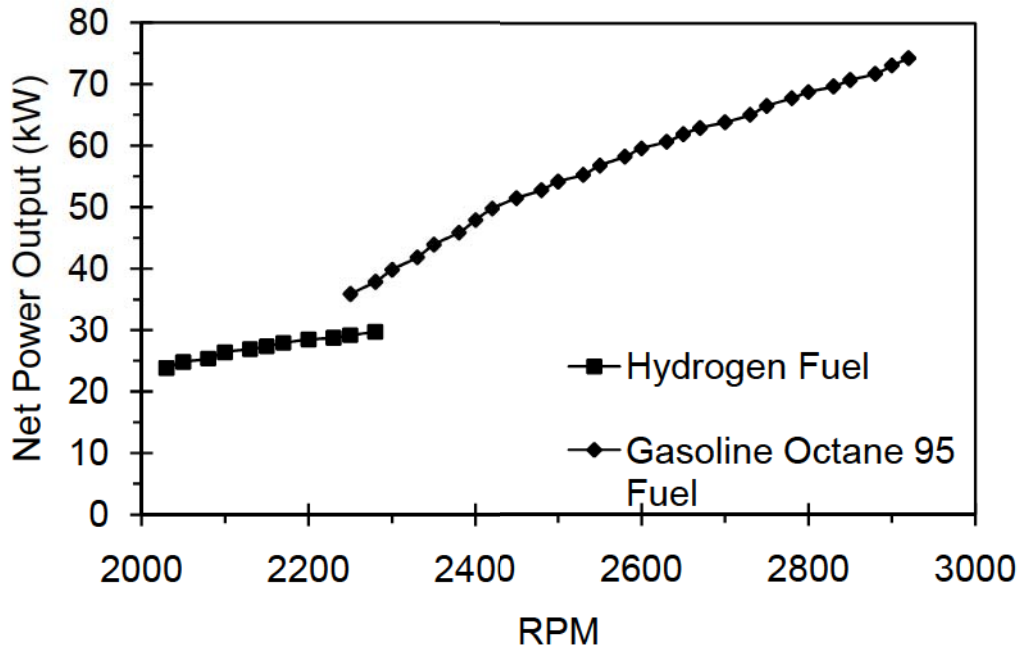


Figure 4.33: Hydrogen and gasoline fuel net power output graph.

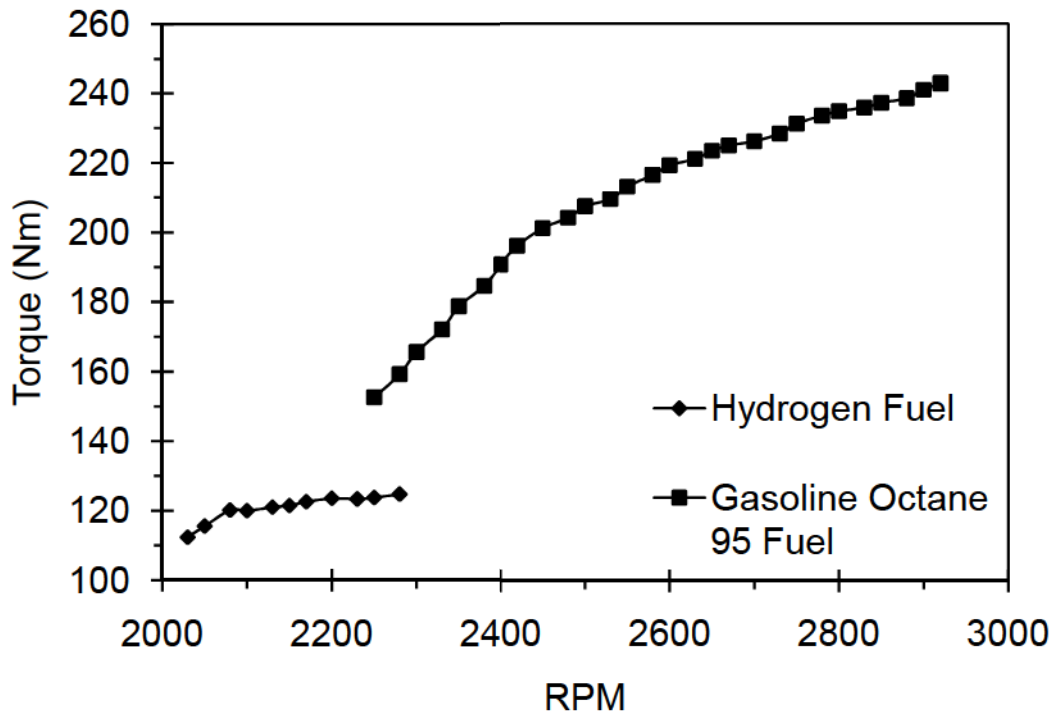


Figure 4.34: Hydrogen and gasoline fuel torque output graph.

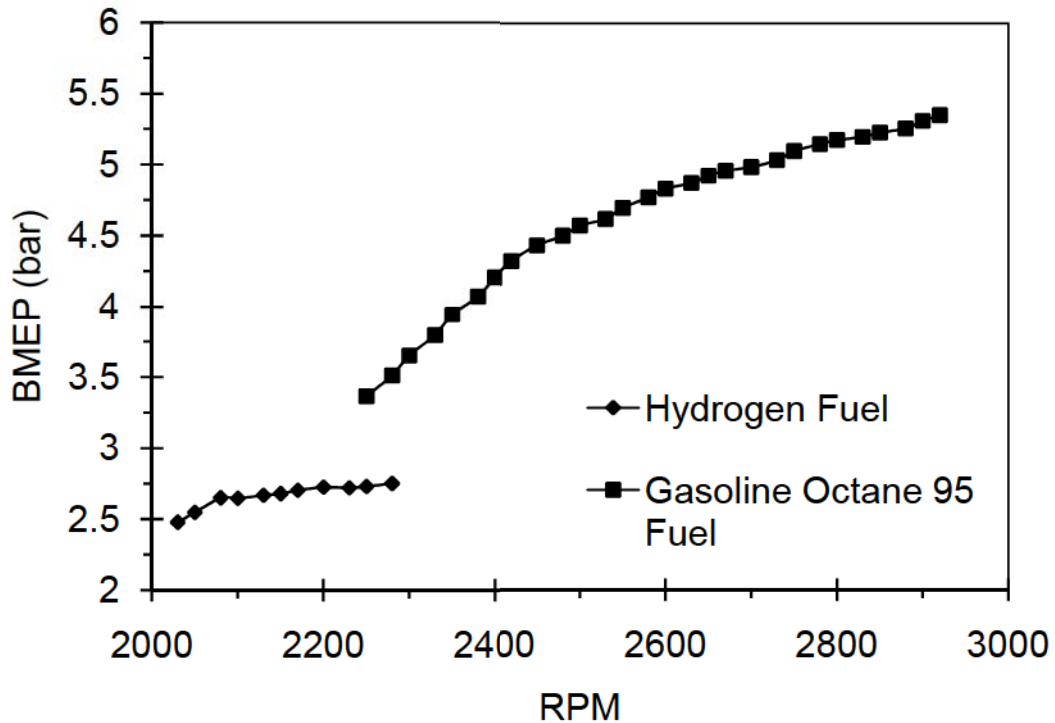


Figure 4.35: Brake mean effective pressure (BMEP) for both gasoline and hydrogen fuel.

The small block 5.7L Chevrolet V8 engine, demonstrates its abilities of running on both the gasoline and hydrogen fuels, however it is now comparable to demonstrate the benefits of running hydrogen over gasoline fuel, as observed in Table 4.2 and Appendix A for full report showing the emission test results for the gasoline. When compared to the emission test results for the engine running on hydrogen fuel, as observed in Table 4.3 and Appendix B for full report, it can be concluded that the carbon foot print can be reduced using this fuel. However, a sacrifice in fuel economy has to be made, and to be economically sensible, closer fueling stations are required, as this may add to the initial start-up costs of this hydrogen infrastructure.

Table 4.2: Emission test results running on gasoline fuel

	40 km/h			CURB IDLE		
	Limit	Reading	Result	Limit	Reading	Result
HC ppm	88	39	PASS	300	57	PASS
CO %	0.73	0.04	PASS	1.5	0.74	PASS
NO ppm	1523	536	PASS	N/A	N/A	N/A
	RPM	1493	VALID	RPM	1380	VALID
	Dilution	14.04	VALID	Dilution	14.49	VALID

Table 4.3: Emission test results running on hydrogen fuel

	40 km/h			CURB IDLE		
	Limit	Reading	Result	Limit	Reading	Result
HC ppm	88	N/A	N/A	300	N/A	N/A
CO %	0.73	N/A	N/A	1.5	N/A	N/A
NO ppm	1523	N/A	N/A	N/A	N/A	N/A
	RPM	0	VALID	RPM	0	N/A
	Dilution	N/A	N/A	Dilution	N/A	N/A

A few challenges had to be overcome for this conversion to take effect, and of such an adequate spacer as seen in Figure 4.36, had to be acquired for adapting the water nozzle, a two-fluid nozzle observed in Figure 4.37.



Location of the Water Nozzle

Figure 4.36: Water nozzle location on the spacer located on top of the carburetor.



Figure 4.37: Water nozzle with demonstration of the amount of water for injection.

Furthermore, to allow for the steam to exit the exhaust manifold quicker, dual exhaust headers were installed. With these after-market headers, the heat dissipated is much quicker, and thus heating up the spark plug wires much more quickly and even burning them. To overcome this problem a heat resistant covers that were installed as observed in Figure 4.38 to reduce the heat noise that caused the spark plug wires to burn and not spark accordingly with the distributor.



Figure 4.38: After-market headers with heat resistant covers for the spark plug wires.

Lastly, it was observed that there is unburned hydrogen fuel exiting the exhaust manifold when an idle air sample test was done, and this is caused by the limitations of the engine and its compression ratio along with the timing, although adjusted to the maximum limit without sacrificing more fuel usage. With hydrogen not requiring much energy to ignite, it is possible with the distributor operations that a small charge of spark is delivered and picked up by the neighboring spark plug wire during the combustion stroke, which would ignite the unburned fuel from the exhaust to ignite, causing post ignition. Along with the backflow of the fuel and air into the intake manifold a backfire is also experienced. To overcome this phenomenon as observed in Figure 4.39, the spark plug wires were modified to ground the excess charge from the exhaust stroke piston sparks and divert that away from the firing piston that gave that charge. This solved the

post-ignition problem as it was being faced before, while eliminating the backfire problem simultaneously.



Figure 4.39: Spark plug wire ground modification for post-ignition elimination.

Upon the successful conversion of this engine to operate on hydrogen fuel, there are several safety measures considered. The traditional spark plugs were replaced with platinum spark plugs, which withstand higher flame temperatures. This was done to ensure no damage is done to the engine during operation. Furthermore, a safety shut off switch was implemented in the cabin; in case of an emergency the operator is able to switch-off the regulator to stop the flow of hydrogen fuel to the engine. A fuse box was created in case of a power surcharge that would shut off fuel delivery in the regulator to the engine. Lastly, a hydrogen sensor is installed to warn the operator of a fuel leak.

Chapter 5

PARAMETRIC STUDY

5.1 Parameters Contributing to the Design of Water Injection

A primary objective is to determine decision support information for the selection of specific methods, for example choosing the number of runs, n , and the parameters used in the analysis. These methods could constitute an entire improvement system. Unlike randomization, a common aspect of all Design of Experiments (DOE) methods is the importance in identifying the Key Input Variable (KIV), a controllable parameter or factor whose setting is likely to affect at least one key output variable, and ranges for these factors. The preliminary identification of KIVs occurs from engineering judgment, and if poor choices of KIVs and ranges are identified, it is unlikely that the application of any DOE and Analysis of Variance (ANOVA) method will achieve the desired results.

Regression analysis refers to curve-fitting methods for predicting the average response performance for new combinations of factors, and understanding which factor changes in average outputs. In this study, the use of regression for predicting and performing hypothesis tests are conducted to identify the best sector of transportation that would most benefit from the use of hydrogen as its source of fuel, and lower CO₂ gas emissions.

Regression methods are the most widely used statistics or operations research techniques. Regression modeling is relevant where the response data is collected using a randomized experiment, or if it is obtained from an observational study. From this

analysis, the evaluation of regression models and its relation to design of experiments (DOE) and the analysis of variance, followed by multiple t-tests, is the primary hypothesis testing approach associated with regression [118].

The benefit of ANOVA followed by t-tests is that it can detect whether all data is noise with a regulated error rate, regardless of the number of coefficients of interest for testing. The steps involved in using the ANOVA method are to calculate the scaled input array matrix, creating the design matrix, calculating all quantities such as the sum of squares regression, the sum of squares error, degrees of freedom, the mean squared regression and the mean squared error, in the ANOVA table from the design matrix. Once the quantities are calculated, the terms in the model have a significant effect on the average response. Table 5.1 shows the ANOVA table and the p-value calculations. The number of factors in Table 5.1 is represented by the alphabetic text. There are aliases in the ANOVA table, which are thus shortened and listed in the table. This sequence is based on a fractional factorial array-based method, rather than a two sample t-test [119]. Main effect plots show means at the various levels of each factor, compared to the overall mean in the plot. In any regular fractional factorial design, uncorrelated estimates of the main effects are available. However, the main effects are aliased with certain interaction effects. If any of the interactions aliased with a main effect is active, the main-effect estimate will be biased. Usually, if a main effect is part of a significant contrast, the main effect is assumed to be significant. The effects in the alias string can be further explored in subsequent experiments, which are designed to "break the alias chain" by ensuring that effects of interest can be estimated and free of other effects. The parameters that are contributing to the design are listed below in the Table 5.1.

The main affecting factors are the location for the water pump and storage that can be installed in the vehicle, along with the power source for operating the water pump. These two parameters once finalized affect the water line length parameter, as the location will determine the total length of the water line. There are four more parameters that are not included in this parameter selection. These parameters are: water purity content percentage, the operating time for the engine, the operating temperature and the operating pressure. The parameters involved are associated with the eight principal parameters listed in the table above. These four functional parameters are independent of these eight principal parameters. However, they are co-related to each other, as once these eight parameters are designed, the four parameters will determine the final functionality of the water pump and the water delivery to the engine.

Table 5.1: Important parameters chosen for analysis.

Parameters	Parameter Title	Parameter Description
P1	Location	The location where the water tank, along with water pump are being installed
P2	Weight	The overall weight of the water tank with the water pump and power source powering the pump in the vehicle
P3	Control System (DAQ, Temperature Sensor connections)	The control system module, used to read the temperature amounts and store them on an onboard computer, is located in the cabin of the truck. However, the connectors must be shielded of any engine heat or noise that may disturb the data collection from the sensors. With this control system, the operation of the water pump is also controlled with a separate switch in the cabin, or a direct switch from the pump into the cabin.
P4	Water line length	This is the line that is connected from the water tank to the nozzle in the engine compartment, and this line is measured in accordance to passing the engine to avoid the heat in not changing the water temperature being delivered.

P5	Water Tank Size	The water tank determines the amount of water stored on board, and this is in accordance to the performance of the engine using the hydrogen fuel.
P6	Water Pump	The water pump must be submerged into the water tank in order to be functional, thus the dimensions of this pump and the output are very important to the overall functionality of the desired output.
P7	Water Nozzle	The location of the nozzle is very important as the water needs to get mixed with the hydrogen before it gets mixed with the oxygen. The water nozzle also has to be small such that there's a small amount of water being displaced into the engine.
P8	Power Source for water pump	This is the power required to make the pump operational, two options exist, one being the vehicle's battery power, and the switch to control the on and off position is implemented into the starter switch, or a solar panel with a separate operating switch .

5.2 QFD House of Quality

5.2.1 Interactions between parameters

The interactions between the parameters and the way they are related together are demonstrated in a house of quality QFD chart as shown in Figure 5.1. This chart demonstrates the importance of each parameter and their interactions with the other components installed. To allow for a clearance and ensuring that the required components to be installed are not interfering with one another, this design parameter is needed to ensure that there is no interference and leading the final design into succession.

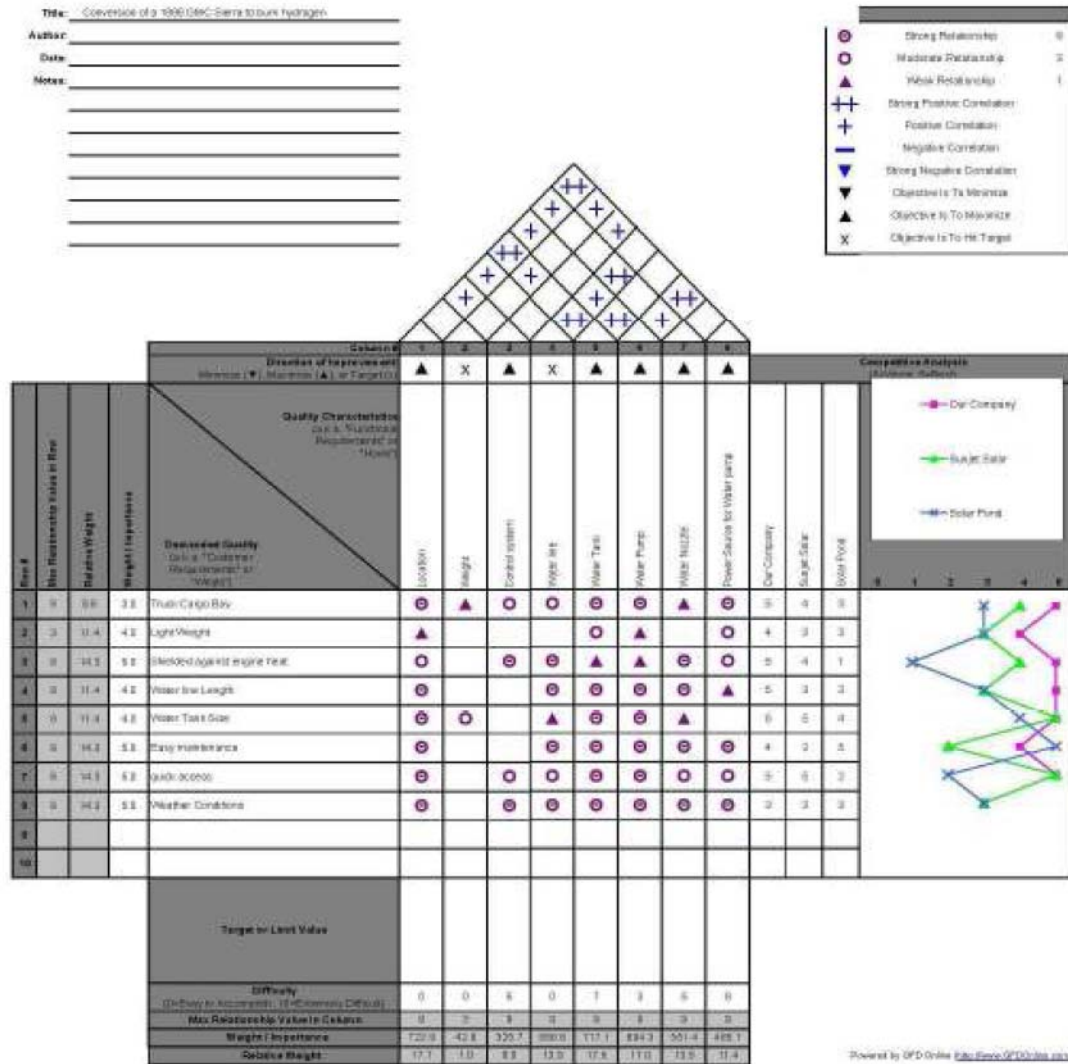


Figure 5.1: House of Quality QFD chart.

The formulation for the QFD and the ranking are formed is based upon the customer requirements and the affecting parameters that would determine the outcome of the final water pump and storage tank design. Furthermore, based upon a survey conducted and literature review research, these requirements were created. The survey conducted suggests that the customers are very specific about the location of the water tank being installed, as well as the ability to maintain, and accessing this water tank are very important factors.

5.2.2 Formulation of Rigidity Index

Rigidity is defined as the cost or difficulty of changes in a process, where it is determined by the number of decisions made over the total decisions. The Rigidity Index would determine the overall time that it would take and the flexibility available to complete the project. By having a lower rigidity index, more flexibility is provided to make changes earlier in the design stage. After the design stage, the flexibility is reduced and the cost of changes increases.

With this project, certain decisions and design parameters are fixed; therefore the rigidity index for this project has a set of start level where it cannot be altered. However, there still exist some decision criteria that would determine the final outcome of the project. The main factor for the Rigidity Index is the reduction of time while still having some flexibility to finish the design project. The rigidity index for Row 1 is formulated as:

$$RI_{R1} = \frac{\sum P_i}{\sum P_{\max}} \quad (5.1)$$

where P_i are values in the P columns and rows, {e.g. $P_1=0, P_2=1, \dots, P_8=1$ }, and P_{\max} is the maximum parameter value are achieved { $P_1=5, P_2=5, \dots, P_8=5$ }, totaling a value of 40, as observed in Table 5.2.

Table 5.2: Rigidity matrix parametric analysis.

Rigidity Matrix												
Parameters	P1	P2	P3	P4	P5	P6	P7	P8	Total	out of 40	RI - %	
P1	0	1	1	5	1	1	3	3	15	0.375	37.5	
P2	1	0	0	0	1	1	1	1	5	0.125	12.5	
P3	1	0	0	1	1	1	1	1	6	0.15	15	
P4	5	0	1	0	3	3	5	1	18	0.45	45	
P5	1	1	1	3	0	1	1	1	9	0.225	22.5	
P6	1	1	1	3	1	0	5	5	17	0.425	42.5	
P7	3	1	1	5	1	5	0	1	17	0.425	42.5	
P8	3	1	1	1	1	5	1	0	13	0.325	32.5	
Total	15	5	6	18	9	17	17	13	100	2.5	250	
out of 40	0.375	0.125	0.15	0.45	0.225	0.425	0.425	0.325				
RI - %	37.5	12.5	15	45	22.5	42.5	42.5	32.5				
Most important	5											
moderate	3											
Least important	1											
Not important	0											

From the Rigidity Index analysis and the house of quality customer requirement rating from Table 5.3, it is observed in the Table 5.4 below, on how the each decision criteria is affected by the made design parameters. Furthermore, it is also observed which decision criteria; customer requirement have a major effect to the outcome of the final design.

Table 5.3: Quality characteristics vs. demanded quality.

Demanded Quality (a.k.a. "Customer Requirements" or "Whats")	Quality Characteristics (a.k.a. "Functional Requirements" or "Hows")	Location	Weight	Control system	Water line	Water Tank	Water Pump	Water Nozzle	Power Source for Water pump
		Truck Cargo Bay	9	1	3	3	9	9	1
Light Weight	1	0	0	0	3	1	0	3	
Shielded against engine heat	3	0	9	9	1	1	9	3	
Water line Length	9	0	0	9	9	9	9	1	
Water Tank Size	9	3	0	1	9	9	1	0	
Easy maintenance	9	0	0	9	9	9	9	9	
quick access	9	0	3	3	9	9	3	3	
Weather Conditions	9	0	9	9	9	9	9	9	

Table 5.4: Customer requirements quality demand.

Demanded Quality (a.k.a. "Customer Requirements" or "Whats")	Quality Characteristics (a.k.a. "Functional Requirements" or "Hows")	Location	Weight	Control system	Water line	Water Tank	Water Pump	Water Nozzle	Power Source for Water pump	out of 40
Light Weight	0.125	0	0	0	0.375	0.125	0	0.375	0.125	
Shielded against engine heat	0.45	0	1.35	1.35	0.15	0.15	1.35	0.45	0.15	
Water line Length	4.05	0	0	4.05	4.05	4.05	4.05	0.45	0.45	
Water Tank Size	2.025	0.675	0	0.225	2.025	2.025	0.225	0	0.225	
Easy maintenance	3.825	0	0	3.825	3.825	3.825	3.825	3.825	0.425	
quick access	3.825	0	1.275	1.275	3.825	3.825	1.275	1.275	0.425	
Weather Conditions	2.925	0	2.925	2.925	2.925	2.925	2.925	2.925	0.325	

5.2.3 Decision Making Sequence

In the previous section the Rigidity Index is formulated and thus rearranged from lowest to highest, which would decrease the overall rigidity index and reduction of time to increase the flexibility of the project and thus allowance for making the decision of which parameter should be analyzed and installed to save time and cost as seen in Table 5.5. This is shown in the graph below, and some of these tasks can also be grouped together to reduce the overall time of the project to be finished.

Table 5.5: Ranked rigidity index percentage from lowest to highest.

RANKED			
Parameters	RI Total %	Parameters	Parameter Title
P2	12.5	P1	Location
P3	15	P2	Weight
P5	22.5	P3	Control System (DAQ, Temperature Sensor connections)
P8	32.5	P4	Water line length
P1	37.5	P5	Water Tank Size
P6	42.5	P6	Water Pump
P7	42.5	P7	Water Nozzle
P4	45	P8	Power Source for water pump

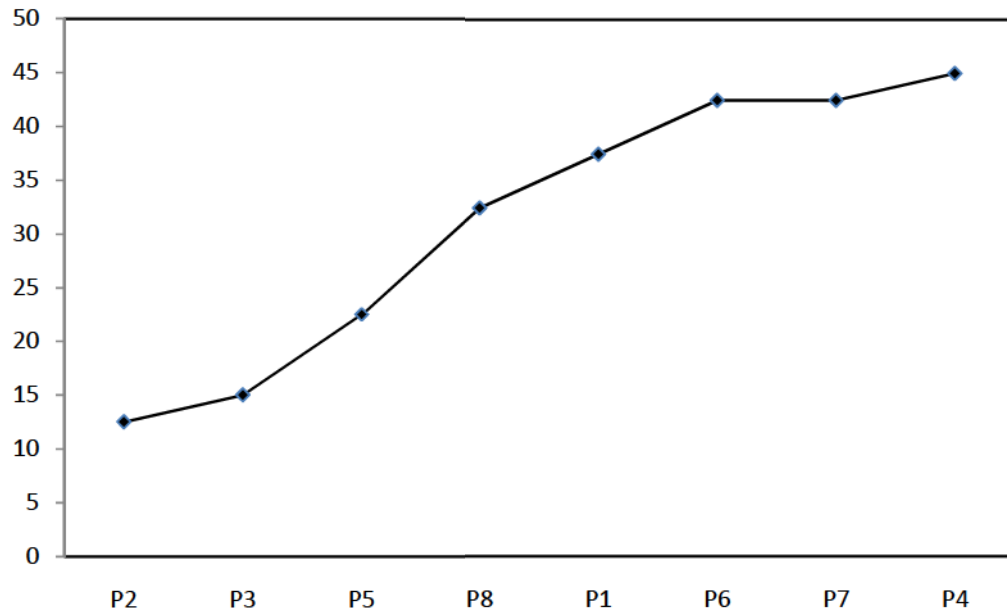


Figure 5.2: Variations of rigidity index.

The sequence in the above Figure 5.2 is used such that the weight parameter can be isolated and become independent of the outcome of the water pump and storage assembly. It is followed by the control system and this can be done simultaneously at the same time, while deciding the water tank size. This water tank size is dependent on the time of operation, and the surrounding temperature. There exists two sources of power to be delivered to the water pump, one being the existing car battery and the other is the proposed solar panel technology independent of the engine power control, however dependent to the control system parameter. In this case the control system parameter is considered first before the power source for the water pump is finalized. The location of mounting the water tank and the power source is very important and thus the reason for its high rigidity index value. After the location has been selected, a water pump is chosen, along with water nozzle to control the flow of water, while considering the total length of water line required pumping the water from the tank to the engine. The water line length is then affected by the location parameter and the water pump size.

5.3 TRIZ Methodology

5.3.1 - 39 Design Parameters

Some of the 39 Design Parameters that can be listed in this section are the Speed, which refers to the total speed of the water travelling, speed of the engine (RPM) and the speed of the vehicle. As well as, stress or pressure parameter, which refers to total pressure for the water to built up before it is injected to mix with the hydrogen fuel. Furthermore, temperature, referring to the overall temperature of the engine; for a higher engine temperature more water is required, and thus is an affecting factor. Lastly, Reliability, referring to the reliability of the water pump not failing during the engine operation; this could be caused through power failure, water line failure, and tank failure. Thus these factors affecting each other can also be contradicted using the TRIZ methodology and these related factors can be summed together for fewer amounts of experiments and further based analysis. For a more detailed explanation of these parameters please see Appendix C.

5.3.2 - 40 Inventive Principles

Some of the 40 inventive principles that can be listed in this section are the volume of the stationary object, which refers to the total volume of water travelling in the water lines. Area of the stationary object, this refers to the proposed area of the pump and the water tank. Furthermore, by using these 40 inventive principles, the principles that affect the outcome of the design can be determined. For a more detailed explanation and list of these principles please see Appendix D.

5.3.3 Axiomatic and Contradiction Matrix

The Axiomatic and Contradiction matrix shows a list of the principles that have the affecting parameters that contradict the overall design experimentation. For a complete contradiction matrix; below in Table 5.6 is a small portion of the contradiction matrix, highlighting the main affecting factors.

Table 5.6: Portion of TRIZ matrix.

<div style="border: 1px solid black; padding: 5px; display: inline-block;"> Worsening Feature Improving Feature </div>		Weight of moving object	Weight of stationary object	Length of moving object	Length of stationary object	Area of moving object	Area of stationary object	Volume of moving object	Volume of stationary object	Speed
		1	2	3	4	5	6	7	8	9
1	Weight of moving object	+	-	15, 8, 29, 34	-	29, 17, 38, 34	-	29, 2, 40, 28	-	2, 8, 15, 38
2	Weight of stationary object	-	+	-	10, 1, 29, 35	-	35, 30, 13, 2	-	5, 35, 14, 2	-
3	Length of moving object	-	-	+	-	15, 17, 4	-	7, 17, 4, 35	-	13, 4, 8
4	Length of stationary object	-	-	-	+	-	17, 7, 10, 40	-	35, 8, 2, 14	-
5	Area of moving object	-	-	-	-	+	-	7, 14, 17, 4	-	29, 30, 4, 34
6	Area of stationary object	-	-	-	26, 7, 9, 39	-	+	-	10, 11, 21, 27	-
7	Volume of moving object	-	-	-	-	-	-	+	-	29, 4, 38, 34

From the contradiction matrix, it is evident that the parameters 10, 11, 21, 27 are contradicting with the Volume of the stationary object with the area of the stationary object. The parameters 10, 11, 21 and 27 are subject to the Force applied from the vibration that the vehicle undergoes during operation, stress or pressure, is the pressure of the water accumulation that passes through the water lines and the nozzle and into the intake manifold. Power is the unit that provides the electricity required making the water pump operational, this is done through a solar panel attached to the rooftop of the vehicle

cabin. Lastly, Reliability is the principle that the designed water pump doesn't fail and provides the desired output.

5.4 Six Sigma Methodologies

In this section the methods of using six-sigma are covered, the first concept is the regression analysis, followed by Failure Mode Effect Analysis (FMEA), DOE, ANOVA, and Taguchi method. The water pump as shown in Figure 5.3, powered using solar panels as seen in Figure 5.4 are retrofitted into a water storage tank for the purpose of mounting it onto a vehicle.



Figure 5.3: Water pump [122].



Figure 5.4: Solar panel [122].

The water pump and solar panel have the following dimensions and data information as portrayed in Table 5.7.

Table 5.7: Water pump and solar panel data information

Pump Dimensions	2.375"L x 1.75"W x 3"H, 9.5"L cable
Solar Panel Dimensions	5.75"L x 4.875"W
Pump Mounting	place in water
Solar Panel Mounting	stake in ground, stand, or wall mount
Construction	plastic, glass
Maximum Flow	35 gph
Shipping Weight	1.36kg (3 lbs)

Source: [124]

5.5 Regression Analysis, Design of Experiments, and Analysis of Variation

In this part of the project, an estimated 4 factors that will be affecting the outcome of the desired performance on the water pump are the water concentration purity level, the time of operation, the operating pressure and the operating temperatures.

For this method, these factors are listed and analyzed, and from each factor it is found which factors will be affecting each other, through a derived regression analysis equation. These factors are listed below in Table 5.8 and analyzed using Excel to achieve the desired outcome for this solar powered water pump for a vehicle application. This custom made water pump to operate in the conditions of a vehicle atmosphere goes through a temperature change, water purity, vibration, along with the effects of water pressure delivery while securing an easy maintenance factor.

Table 5.8: Factor analysis using ANOVA method.

Analysis of Variance									
Source	DF	SS	MS	F	P				
A	1	32	32	0.962406	>0.1	accept			
B	1	21.125	21.125	0.635338	>0.001	accept			
C	1	2	2	0.06015	>0.1	accept			
D	1	15.125	15.125	0.454887	>0.1	accept			
AB	1	12.5	12.5	0.37594	>0.1	accept			
AC	1	3.125	3.125	0.093985	>0.1	accept			
AD	1	4.5	4.5	0.135338	>0.1	accept			
BC	1	2	2	0.06015	>0.1	accept			
BD	1	6.125	6.125	0.184211	<0.001	reject	Has an effect	B_1 X1	
CD	1	18	18	0.541353	<0.001	reject	Has an effect	B_2 X2	
ABC	1	0.125	0.125	0.003759	>0.1	accept			
ABD	1	24.5	24.5	0.736842	>0.1	accept			
BCD	1	84.5	84.5	2.541353	>0.1	accept			
ABCD	1	276.125	276.125	8.304511	>0.1	accept			
Error	16	532	33.25						
Total	31	1033.75	33.34677419						
			Y=15.875						

The regression equation for this analysis is then $Total = 15.9 - 2.00 A + 1.62 B + 0.50 C + 1.37 D$, and thus for this project, there are no affecting factors that create a huge impact to the desired outcome of the operation.

Using Minitab to generate the following data and from this data to create a regression equation as shown in Table 5.9.

Table 5.9: Regression analysis using total versus A,B,C,D factors.

Regression Analysis: Total versus A, B, C, D					
The regression equation is					
Total = 15.9 - 2.00 A + 1.62 B + 0.50 C + 1.37 D					
Predictor	Coef	SE Coef	T	P	
Constant	15.875	2.253	7.05	0.000	
A	-2.000	2.253	-0.89	0.394	
B	1.625	2.253	0.72	0.486	
C	0.500	2.253	0.22	0.828	
D	1.375	2.253	0.61	0.554	
S = 9.01136 R-Sq = 13.6% R-Sq(adj) = 0.0%					
Analysis of Variance					
Source	DF	SS	MS	F	P
Regression	4	140.50	35.12	0.43	0.783
Residual Error	11	893.25	81.20		
Total	15	1033.75			
Source	DF	Seq SS			
A	1	64.00			
B	1	42.25			
C	1	4.00			
D	1	30.25			

Using the DOE, ANOVA method from the Minitab program, it is possible to determine which factors are being affected. For the main effect for factor A, it is evident that this parameter creates an impact to overall outcome of the design feature as observed

in Figure 5.5. Using the DOE, and ANOVA function of Minitab, it is possible to determine the overall outcome of the design parameters and their affecting factors. It is observed that most of these factors are not affecting each other as observed in Figure 5.6.

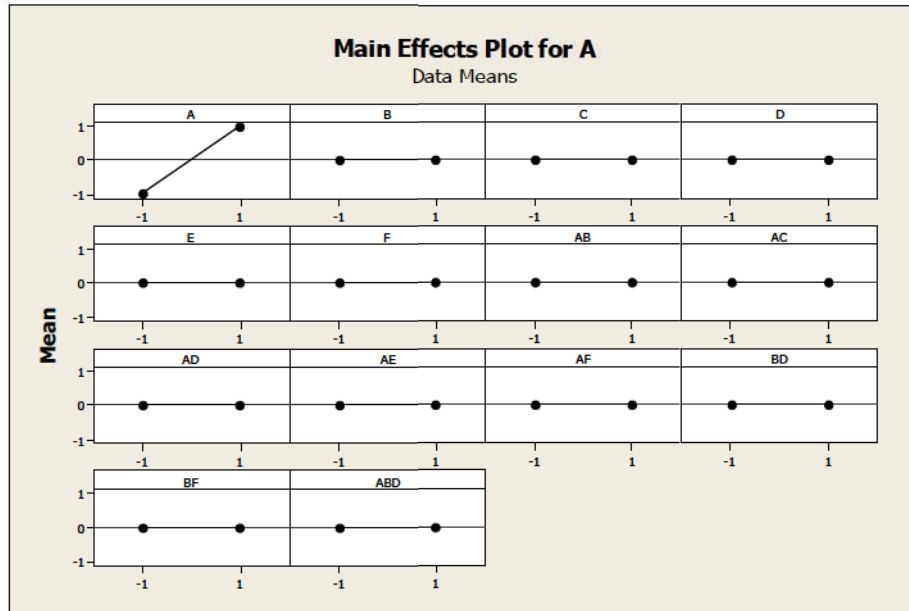


Figure 5.5: Main effect plot for A.

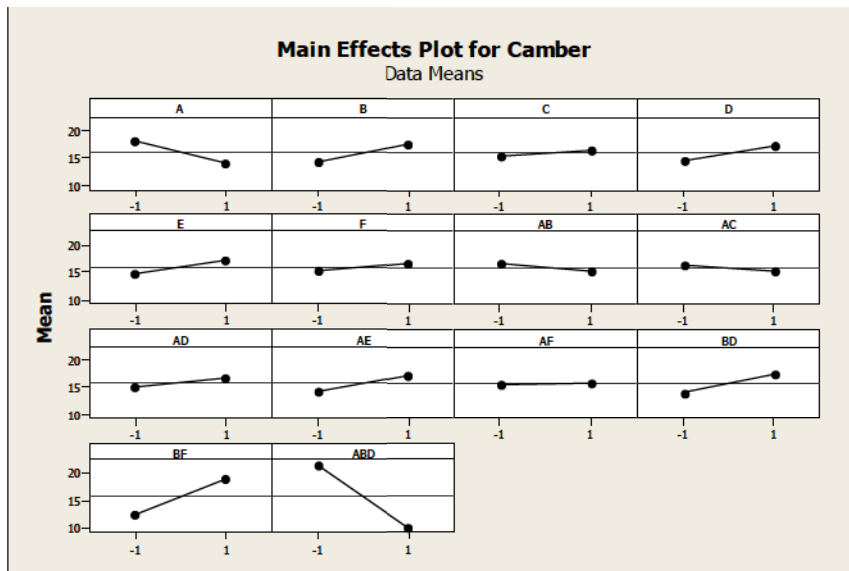


Figure 5.6: Main effect plot for total value.

From the Minitab program, there exists an option using all of the four-factors affecting the outcome of the design through the Taguchi method, and thus the main effect plots for the means are derived. This shows the extent of an affect each parameter has towards the outcome of the design. After the Taguchi method and the DOE and ANOVA analysis shown in the above Figure 5.7, the FMAE analysis is done in the next section.

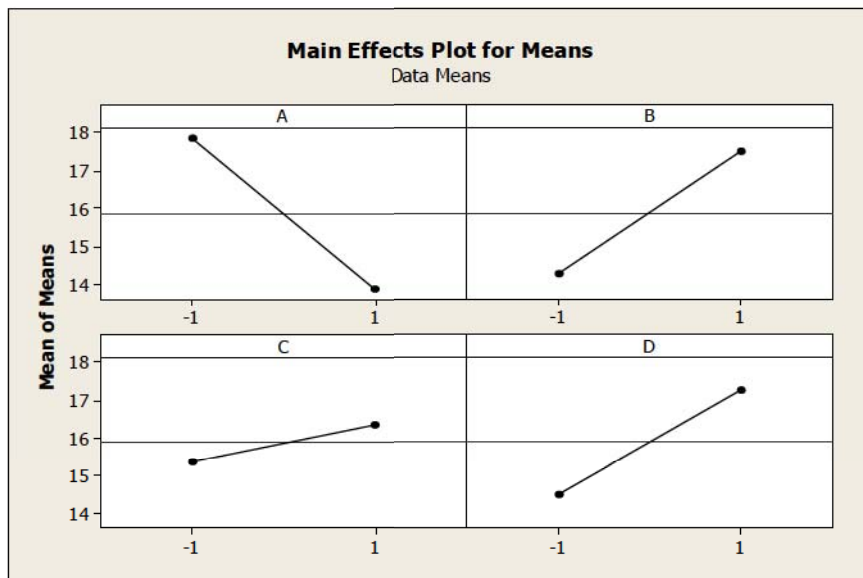


Figure 5.7: Main effect plot for means.

5.6 Failure Mode-Effect Analysis (FMEA)

5.6.1 FMEA analysis and poke yoke mistake proofing method

The FMEA analysis used in designing this water pump and water storage assembly to be implemented to achieve the desired outcome in the engine operation is discussed in this section, while water pump and water storage is demonstrated in Figure 5.8.

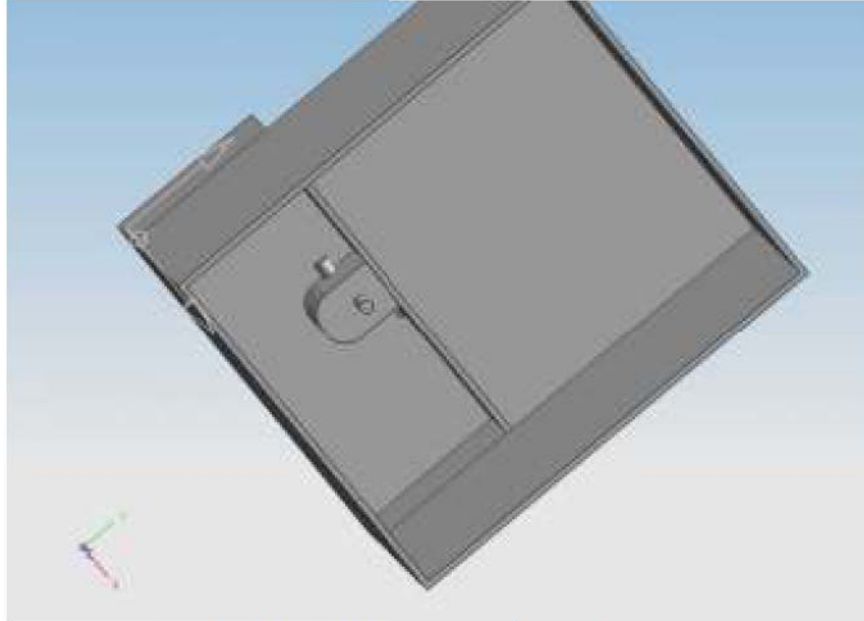


Figure 5.8: Water pump and water storage.

The FMEA analysis using the 10 failure modes that could occur for using this type of water pump and water storage is listed in Table 5.10. In this table a list of 10 failure modes are suggested and analyzed, as well as prevention methods has been discussed. Furthermore, the Risk Priority Number (RPN) has been calculated. It is observed that the water pump and solar panel mount failure have a high RPN number and must be analyzed in such a way that it is ensured no failure occurs during the operation. Poke Yoke method is used for five selected cases from the table in redesigning the equipment. The five cases chosen are:

- pump failure,
- pump mount failure,
- water tank mount failure,
- solar Panel mount failure, and
- control module failure.

5.6.2 Poke Yoke approach to the above mentioned five cases:

Pump failure

For the pump to fail there exists the problem of having the engine back flash, in which the water injection is the method of overcoming this initial problem. A method to overcome this failure is to have regular maintenance and ensuring the pump is clean and free of debris. Although this is mechanical related and the failure of the pump would be dependent on water quality and continuous power being delivered; however an alert message can be implemented to be delivered to the driver to notify the pump failure.

Pump mount failure

The mount that holds the pump in the water tank, would happen to fail, and this would cause the pump to move around excessively; this will also cause the water line to get disconnected resulting in not delivering water. Regular maintenance can prevent this from occurring; also a failsafe method would be to cushion the surrounding of the pump such that the pump would not be able to move around excessively until maintenance has taken place.

Water tank mount failure

The mount for the water tank that secures it to the bed of the truck that would happen to fail would cause many failures. One of the failures that would occur would be the detachment of the water line from the tank, power failure for the pump, possible detachment of the solar panel from the roof top, as well as it is a safety concern to the vehicle travelling behind. One way to allow more security and ensuring the water tank mount doesn't fail would be for regular maintenance on checking the mounts, as well as an additional bracket, similar to the type used for the hydrogen tank.

Solar panel mount failure

The mount for the solar panel failing, it would cause the failure of the water pump from operating, as well as creating a safety problem to the vehicle travelling behind. To make this a failsafe method would be to increase the number of fastening bolts from four to six to distribute the force in securing the solar panel evenly across the panel frame. Two straps can be implemented to ensure a safe and secure connection is made between the panels and cabin rooftop.

Control module failure

The control module that controls the pump speed, which is dependent on the engine operating temperature, as the engine temperature increases or works at higher RPM the control module, is responsible for adjusting the pump speed in accordance to deliver enough water to prevent the back flash being experienced. If for some reason this fails, then the engine would begin to experience back flashes, and this is not the desired outcome. One way to prevent this from occurring would be to implement an emergency alert to the driver to indicate the module has failed. Then the driver would be able to reduce engine RPM, and drive with caution until proper repairs have been made. To make this fail safe, there would be an implementation of a mechanical control valve that the operator can use to operate in case of a control failure. This can be located near the pump, and it requires the driver to make a stop to apply the manual adjustment. This ensures that the driver does not continue to drive.

Choosing one case of the five poke yoke designs, creating a closed-loop that has error detection and a compensation scheme module is for the control module failing in the water delivery system.

The close loop system design is to incorporate a manual control valve near the water tank, connected to the water line. This would require the driver to stop the vehicle and turn on this valve manually. This valve would be controlled mechanically to how much it can open and allow for a fixed operation point, which would work well at low and mid range RPM, however not suitable for high RPM operations. When this control module fails and the mechanical valve is operational, a yellow/amber blinking light is incorporated into the front dash panel of the vehicle to continuously alert the driver of the control system failure, until repairs have been made, then this light is set to off until a failure occurs.

Table 5.10: FMEA analysis.

Potential failure mode	Potential effect of failure	SEV	Current process controls					Recommended actions		Action results			
			Potential cause	Occur	Prevention	Detection	Det	R.P.N.	Recommended actions	Sev	Occur	Det	R.P.N.
Pump Fails	Engine back flash	10	Power failure	1	Regular maintenance	None	2	20	Backup power	10	1	2	20
			Dirt buildup	1	Regular maintenance	inspector	3	30	Maintenance	10	1	3	30
			Control system failure	1	Regular system check	Inspector	3	30	Regular maintenance	10	1	3	30
												0	
Tank Leaking	Water Depletion	9	Tank puncture	4	flying debris	Operator	3	108	plate cover	9	4	3	108
			Water Evaporation	1	High temperature	Operator	3	27	heating or cooling	9	1	3	27
Solar panel falling from roof	Injury	9	breaking panels and hitting others	8	Double Mounting	Operator	2	144	double mount	9	8	2	144
Water pump mount	Injury	9	breaking and flying out of truck	8	Double Mounting	Operator	2	144	double mount	9	8	2	144
Line Breaking	water leakage	9	Debris from road	1	Preventative MX	Cover	1	9	metal cover	9	1	1	9
			Catastrophic Mechanical Failure	1	Preventative MX	Operator	1	9	emergency shut off	9	1	1	9
Nozzle breaking	excessive pressure	8	System Failure	1	Preventative MX	Control System	1	8	emergency shut off	8	1	1	8

5.7 Detailed Design

In this section the design is explained in further details; the water pump and storage as shown in Figure 5.9 is designed in such a way that would fit in accordance to the modifications that has been done to the bed of the truck, as shown in Figure 5.10.

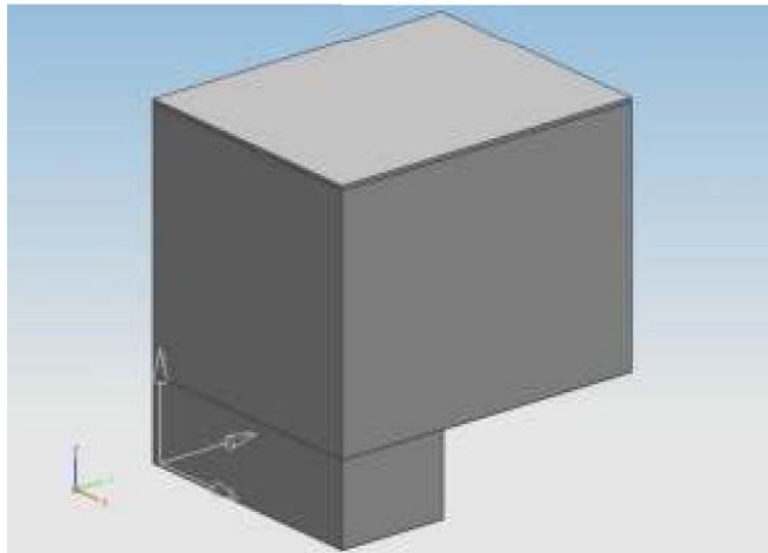


Figure 5.9: Water pump and water storage enclosure.



Figure 5.10: Water Storage and pump location.

The solar panels will be installed on the cabin roof, where the location is the most convenient to both the water pump and the gathering of solar energy to operate the pump. A switch to power the pump can also be wired and delivered into the cabin, and this location serves the purpose of having a shorter wiring throughout the installation. This is a good place to mount the water pump and water storage tank, as to this would be a great access point, as required by the customer from the QFD analysis. This location also serves for easy access for pump maintenance, and also the mounting of this tank to the board provides additional support in ensuring the tank is securely placed in the vehicle.

5.8 Designs for Excellence

The design for excellence methodology (commonly known as Design for X) is divided into the design for reliability, maintainability, manufacturing and assembly, as well as designs for environmentally benign, and design for life cycle. In this section the design for manufacture and assembly is discussed.

Design for manufacture and assembly consists of the ability to easily manufacture and assemble this water pump and storage tank into the vehicle. From Figure 5.11, it shows the water pump mounted to the bottom of the tank, and this design is to minimize the assembly required for inserting this water pump in the tank. The water tank as shown in Figure 5.12, show that there is a hole with an inserted power cable that enters the tank to the water pump, this is one of the two steps required for installing the water pump into the tank.

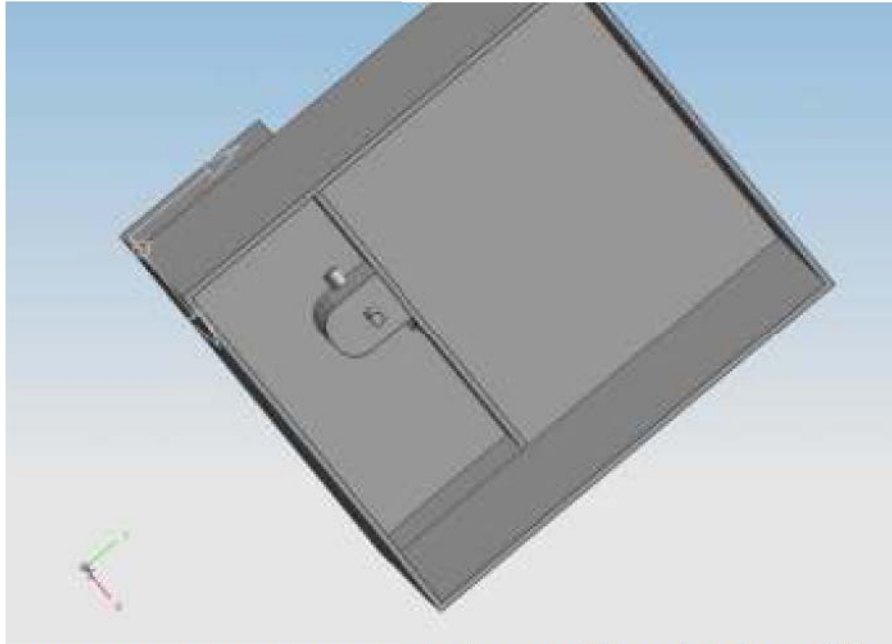


Figure 5.11: Pump mounted to the bottom of the tank in the middle.

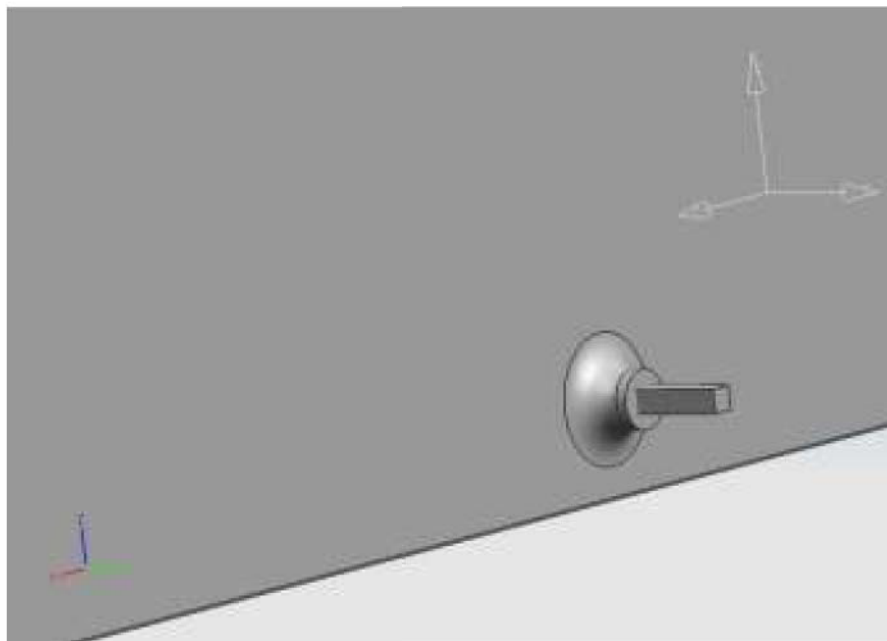


Figure 5.12: Power cable and sealant for allowing the power cable to enter the tank.

To minimize the design for manufacturing, a mold will be created, and the method of injection molding is used to make this water tank from plastic. This would also reduce the setup time and costs required in making this water tank. The design

consists of a detachable top cover which allows for easy access to the pump, and maintenance, as well as filling the tank with water, as illustrated in Figure 5.13.

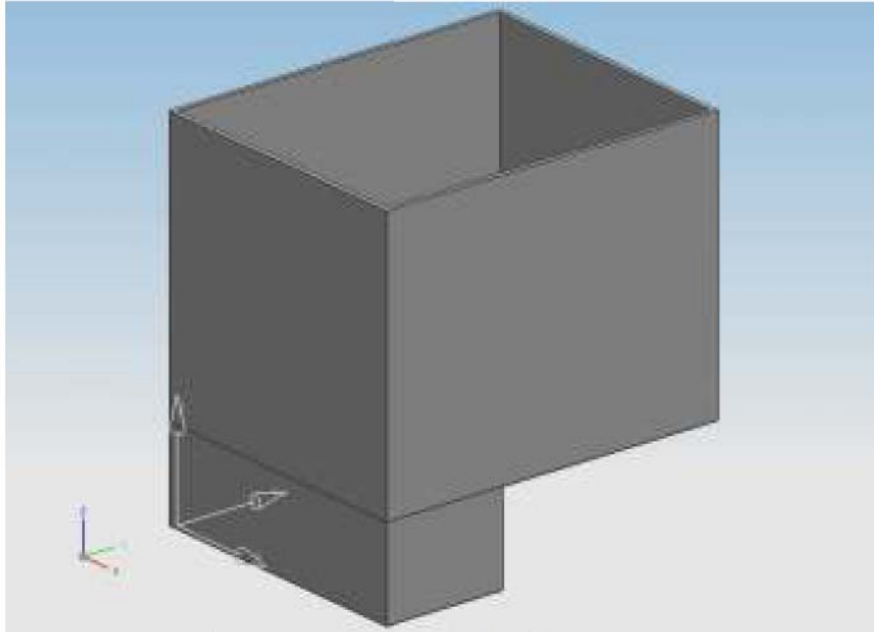


Figure 5.13: Water tank with open top.

5.9 Axiomatic Design

Using Axiomatic Design to determine the design and understanding of the product, through manufacturing and production it is defined as sets of processes and activities that transform the customer's wants, or requirements into design solutions. A more detailed Functional Requirement customer specification can be seen in the house of quality matrix. There are two design axiom methods that can be implemented in a design process. The first axiom method is the independence axiom, in which the independence of the functional requirements is maintained. The second axiom method is the information axiom, in which the information content in a design is minimized.

5.9.1 Axiom 1

The design process involves three mappings between four domains; the first mapping involves the mapping between critical-to-satisfaction customer attributes and the functional requirements. A functional requirement is a solution-neutral, that is, design-parameter-independent, describing the functionality of a system. Functional specifications are established and used regardless of the design parameters used. This can be done through a Quality Function Deployment. As described in the previous sections the design parameters and the customer requirements this axiom can be achieved using the QFD, house of quality method. After defining the design parameters and the customer requirements, a physical mapping can be constructed, in which a matrix can be formed. However without being able to write the mapping mathematically, the transfer function can be derived from physics or identified empirically using regression and DOE, as seen in the previous sections of this report.

5.9.2. Axiom 2

This axiom deals with design information content complexity, which is a function of the number of functional requirements and design parameters and their variations. In this axiom it is easier to have an idea about complexity by shaping where it does exist and how it affects the design rather than what it really means. Complexity is defined as a quality of an object, and in this case that would be the process that design provides. The amount of complexity encountered in a functional requirement is related to the probability of meeting its mapped to the design principles successfully. A relationship from this has been shown throughout the report.

Chapter 6

CONCLUSIONS AND RECOMMENDATIONS FOR FUTURE WORK

6.1 Conclusions

The purpose of this thesis study was to convert a 1986 GMC Sierra 1500 pickup truck to burn hydrogen fuel using the Internal Combustion Engine that burned gasoline as a fuel. A major objective of this conversion was to reduce CO₂ emissions and contribute to the reduction of greenhouse gases and to help the environment by using renewable sources of energy. To convert the GMC Sierra from burning gasoline to hydrogen by using the same Internal Combustion Engine, many aspects had to be considered. Of such aspects before the conversion could take place, the type of conversion kit required to do this conversion was a Natural Gas conversion kit, due to budget and time limitations, different measures of actions were taken.

Upon the conversion of this vehicle to operate on hydrogen fuel, multiple knocks and backfires were observed. This was later discovered that the backfire was a post ignition problem that lowered the power output of the engine. To overcome this problem timing of the spark ignition was considered as well as the air/fuel ratio were considered. Furthermore, a water injection kit was designed and developed for increasing the power output of the engine using the hydrogen fuel. This water injection requires more in depth study that is outside of the scope of this thesis study. To fully eliminate these post ignition phenomena, the spark plug wires modification was proposed and installed on the vehicle that would ground the unnecessary charge from the distributor during the exhaust

stroke. A further analysis and emission tests showed that there is un-burned hydrogen fuel that is being dissipated into the atmosphere. The cause of this problem is due to the lower compression ratio for this engine that was specifically designed for gasoline fuel type operations. For a better compression ratio a diesel engine best suits the scenario for a more complete burn of the hydrogen fuel, which would significantly improve the mileage for this vehicle operating on such fuel. Although hydrogen fuel as compared to the gasoline fuel seems to be unfavorable, there are a few investigations and modifications that need to be investigated. The benefits of using hydrogen need to be considered along with the modes of fuel delivery and compression ratio that is most advantageous for this fuel.

Hydrogen fueled vehicles will be part of the future; however at this point further studies are required to allow for a higher efficiency and modes of fuel delivery and fuel storage that would improve the fuel economy mileage of the vehicle along with application that is being used as compared to the gasoline fuel. To allow for this to become a reality more fueling station infrastructures are required to be built for this purpose to make this economically and practically sensible to make hydrogen powered vehicles as part of a solution to the high energy demand.

The following are the main findings of this thesis study.

- For a better fuel mileage a better mode of fuel delivery is required.
- Backfire or post ignition can be overcome with lower electric charge for hydrogen fuel.
- Water injection and gas re-circulation will help improve engine power output and increase fuel economy.

- To use hydrogen fuel more efficiently a new engine design and modes of fuel delivery are required.

6.2 Recommendations for Future Work

Any future work that might undergo for the conversion of the 1986 GMC Sierra would be to re-design an engine that is more efficient and deliver more power output. Since the development of internal combustion engines in 1886, the basics of combustion remains the same, it is time for a new engine design to appear and replace the conventional engines existing today.

Future work with this 1986 GMC Sierra would involve the re-design of the vehicle dynamics for less air drag and more aerodynamics leading to an improvement of fuel economy. An increase in power is expected when the engine used methods of fuel injection and modes of super chargers and turbo charger using hydrogen fuel. With direct injection the efficiency and fuel economy will increase. Thus more fuel can be stored on-board resulting shorter fueling times. In addition, the lower fuel consumption would result in lowered operating cost user.

Furthermore, to make an engine more efficient and powerful, the number of mechanical parts needs to be reduced. If the air delivery and fuel delivery are electronically controlled and not reliant on the mechanical components to deliver the air/fuel mixture into the cylinders, this will increase the performance of the engine as well. The idea of fuel and air delivery inside the cylinder chambers needs to be analyzed and from this a unique engine design can be derived, even replacing the conventional combustion in an engine.

One of the most effective ways of getting more power from an engine is to increase the amount of air and fuel that it can burn. Some methods are to increase the number of cylinders or make the cylinder bore diameter bigger. However these methods can be costly; a turbo charger or compressor is a simpler and more compact method of adding power to the engine.

Turbochargers can be also be used for the gas re-circulation and steam entrapment from the exhaust, and by condensing that steam back into water it can be used to feed the engine for a better compression ratio and a more complete burn of the hydrogen fuel. Overall, turbo-charging is advantageous for this system, and safer as ice formation during cold weathers can be eliminated coming from the exhaust.

Lastly, a corrosion study should be done to analyze the amount of corrosion created due to the combustion process of hydrogen. Also, a further analysis should be done for the quality of water from the exhaust pipe for environmental studies.

To allow for a complete burn a cold air intake should be introduced into the system and further analyzed to compare the difference between cold air and warm air. This will improve the performance of the vehicle and possible fuel economy.

REFERENCES

- [1] United Nations Statistics Division, September 2007. “Environmental Indicators, CO₂ Emissions”. Canada (available online at http://unstats.un.org/unsd/environment/air_co2_emissions.htm)
- [2] Cherry J., 2008, “Airports – Actions on climate change”. Airports Council International Canada: Montreal, presentation (available online at <http://www.icao.int/env/meetings/Giacc/Aci.pdf>)
- [3] Fuel Cell Markets Ltd., 2010, “Advantages and Benefits of Fuel Cell and hydrogen technologies.” Fuel Cell Markets the bridge to sustainable energy. UK (available online at http://www.fuelcellmarkets.com/fuel_cell_markets/5,1,1,663.html#H2)
- [4] Bloustein E.J., 2006, “Hydrogen Safety, New Jersey Hydrogen Learning Center”, USA: New Jersey (available online at <http://policy.rutgers.edu/CEEEP/>)
- [5] Linde Group, 2009, “Hydrogen Material Safety Data Sheet” The Linde Group. USA: New Jersey, Datasheet (available online at http://msds.lindeus.com/files/msds/Linde_H2_gas___US.pdf)
- [6] Bellis M., 2008a, “Christian Huygens (1629 – 1695)” About.com: Inventors, USA: New York (available online at http://inventors.about.com/library/inventors/bl_huygens.htm)
- [7] Bellis M., 2008b, “The History of Automobile.” About.com: Inventors, USA: New York (available online at <http://inventors.about.com/library/weekly/aacarssteama.htm>)
- [8] Cleveland C. J., 2006. “Otto, Nikolaus August”. The Encyclopedia of earth USA: Boston (available online at http://www.eoearth.org/article/Otto,_Nikolaus_August)

- [9] Cleveland C. J., 2006a. "Lenoir, Jean Joseph Etienne." The Encyclopedia of earth USA: Boston (available online at http://www.eoearth.org/article/Lenoir%2C_Jean_Joseph_Etienne)
- [10] Holt D. J., 2005, "100 Years of Engine Developments", SAE International, USA: Warrendale
- [11] Cleveland C. J., 2006b. "Benz, Karl Friedrich. The Encyclopedia of earth USA: Boston (available online at http://www.eoearth.org/article/Benz%2C_Karl_Friedrich)
- [12] Cleveland C. J., 2006c. "Daimler, Gottlieb. The Encyclopedia of earth USA: Boston (available online at http://www.eoearth.org/article/Daimler%2C_Gottlieb)
- [13] Hydrogen Engine Center (HEC), 2008. "4.9L Hydrogen ICE". Hydrogen Engine Center, Canada: Trois Rivieres. Datasheet (available online at <http://www.hydrogenenginecenter.com/userdocs/HEC649I-CLB-Oxx-Power.pdf>)
- [14] Murray R.G. 1971. "Hydrogen Internal Combustion Engine." U.S. Patent 3572297, filed January 26, 1970, and issued March 1971.
- [15] Eisele E., Binder K., Drexl K. 1978 "Combustion Process for externally controlled reciprocating piston." U.S. Patents 4086878, filed April 15, 1976, and issued May 2, 1978.
- [16] Erren R. A. 1939. "Internal Combustion Engine using hydrogen as fuel." U.S. Patents 2183674, filed September 10, 1936 and issued December 1939.
- [17] Watanabe K. 1985. "Internal Combustion engine of hydrogen gas." U.S. Patents 4508064, filed September 28, 1982 and issued April 2, 1985.

- [18] Quigley R. E., Centerville Jr., Medisch G. N. 1969 “Hydrogen-oxygen fuel Internal Combustion engine.” U.S. Patents 3471274, filed October 28, 1966 and issued October 1969.
- [19] Meyer S. 1994 “Hydrogen gas fuel management system for an Internal Combustion Engine.” U.S. Patents 5293857, filed June 24, 1992 and issued March 15, 1994.
- [20] Anderson H. P. 2000 “Hydrogen powered vehicle, Internal Combustion Engine and spark plug for use.” U.S. Patents 6119651, filed December 23, 1998 and issued September 19, 2000.
- [21] Salimi F.; Shamekhi A. H.; Pourkhesalian A. M., “Role of mixture richness, spark and valve timing in hydrogen-fuelled engine performance and emission International Journal of Hydrogen Energy” 2009, 34 (9), pp. 3922-3929
- [22] Tang X, Kabat DM, Natkin RJ, Stockhausen WF, Heffel JW. “Ford P200 hydrogen engine dynamometer development”, SAE paper, 2002-01-0242.
- [23] Verhelst S, Sierens R, Verstraeten S. “A critical review of experimental research on hydrogen fueled SI engines.” SAE paper, 2006-01-0430.
- [24] Fagelson J.J., McLean W.J., de Boer P.C.T. “Performance and NO_x emissions for spark-ignited Combustion engines using alternative fuels – quasi one-dimensional modeling. I. hydrogen fueled engines.” Combustion Science and Technology 1978; 18:47–57.
- [25] Prabhu-Kumar GP, Nagalingam G, Gopalakrishnan KV. “Theoretical studies of a spark-Ignited supercharged hydrogen engine.” International Journal of Hydrogen Energy 1985; 10:389–97.

- [26] Ma J, Su Y, Zhou Y, Zhang Z. "Simulation and prediction on the performance of a vehicle's hydrogen engine." *International Journal of Hydrogen Energy* 2003;28:77–83.
- [27] Verhelst S, Verstraeten S, Sierens R., 2006, "Development of a simulation code for hydrogen fuelled SI engines." In: *Proceedings ASME Spring Technical Conference*, Aachen, May 8–10.
- [28] Drew A. N., Timoney D. J., Smith W. J., 2007 "A simulation and design tool for hydrogen SI engine systems-validation of the intake hydrogen flow model." *International Journal of Hydrogen Energy*; 32:3084–92.
- [29] Knop V., Benkenida A., Jay S., Colin O., 2008, "Modeling of combustion and nitrogen oxide formation in hydrogen-fuelled internal combustion engines within a 3D CFD code." *International Journal of Hydrogen Energy*; 33:5083–9.
- [30] Cox K. E., Williamson K. D., 1979, "Its Technology and Implications," *International Journal of Hydrogen*, Vol. IV. CRC Press, Boca Raton, Florida.
- [31] Bockris J. O'M., 1980 "Energy Options." Wiley, New York.
- [32] North D.C., 1992 "An investigation of hydrogen as an internal combustion fuel," *International Journal of Hydrogen Energy*, Volume 17, Issue 7, Pages 509-512.
- [33] Cruver P. C., 1989 "Hydrogen: tomorrow's limitless power source". *Futurist*, 24-26.
- [34] McCarty R. D., Hord J. and Roder H. M., 1981 "Selected Properties of Hydrogen (NBS Monograph 168)".
- [35] Huang F. F., 1988 "Engineering Thermodynamics", 2nd ed. Macmillan, New York.
- [36] Stone R., 1985 "Introduction to Internal Combustion Engines." Macmillan, New York.

- [37] Furuhashi S., Fukuma T., Kashima T., 1984 “Liquid hydrogen fuel supply system to hot surface ignition turbocharged engine”, in Cryogenic Processes and Equipment Conf. 1984, New Orleans (9-14 December 1984) pp. 105-113. ASME, New York.
- [38] Petkov T. I., Barzev K. N., 1987 “Some aspects of hydrogen application as a supplementary fuel to the fuel-air mixture for internal combustion engines.” International Journal of Hydrogen Energy 12, 633-638.
- [39] Leading by CO₂ example. 2009 “Editorial, Automotive engineering international”; AEI
- [40] Fuel cells. Cover story, Engine technology international; June 2007.
- [41] Davidson D., Fairlie M., Stuart AE. 1986 “Development of a hydrogen-fueled farm tractor.” International Journal of Hydrogen Energy; 11:39–42.
- [42] Olavson L.G., Baker N.R., Lynch F.E., Meija L.C. 1984 “Hydrogen fuel for underground mining machinery”. SAE, paper 840233.
- [43] Tang X., Kabat D.M., Natkin R.J., Stockhausen W.F., Heffel J. 2002 “Ford P2000 hydrogen engine dynamometer development.” SAE, paper 2002-01-0242.
- [44] Heffel J.W., Johnson D.C., Shelby C. 2001 “Hydrogen powered Shelby Cobra: vehicle conversion.” SAE, paper 2001-01-2530.
- [45] Smith J.R., Aceves S., Van Blarigan P. 1995 “Series hybrid vehicle and optimized hydrogen engine design.” SAE, paper nr 951955.
- [46] Verhelst S., Sierens R. 2001 “Aspects concerning the optimization of a hydrogen fueled engine.” International Journal of Hydrogen Energy;26:981–5.
- [47] Berckmuller M., Rottengruber H., Eder A., Brehm N., Elsasser G., Muller-Alander G. 2003 “Potentials of a charged SI-hydrogen engine.” SAE, paper nr 2003-01-3210.

- [48] Project coordinator motor vehicles and road transport. TUV Rheinland E.V. for the Federal Ministry for Research and Technology. 1990 “Alternative energy sources for road transport – hydrogen drive test.” Technical report, TU V Rheinland.
- [49] Jing-Ding L., Ying-Qing L., Tian-Shen D., 1986, “Improvement on the combustion of a hydrogen fueled engine.” *International Journal of Hydrogen Energy*;11:661–8.
- [50] Guo L.S., Lu H.B., Li J.D., 1999, “A hydrogen injection system with solenoid valves for a four cylinder hydrogen-fueled engine.” *International Journal of Hydrogen Energy*; 24:377–82.
- [51] Natkin R.J., Tang X., Boyer B., Oltmans B., Denlinger A., Heffel J.W., 2003, “Hydrogen IC engine boosting performance and NOx study.” SAE, paper nr 2003-01-0631.
- [52] Rottengruber H., Berckmuller M., Elsasser G., Brehm N., Schwarz C., 2004 “A high-efficient combustion concept for direct injection hydrogen internal combustion engine.” In: 15th World hydrogen energy conference, paper nr 28J-01. Yokohama, Japan.
- [53] Heffel J.W. 2003 “NOx emission reduction in a hydrogen fueled internal combustion engine at 3000 rpm using exhaust gas recirculation”. *International Journal of Hydrogen Energy*; 28:1285–92.
- [54] Verhelst S., Sierens R. 2007 “Combustion studies for PFI hydrogen IC engines.” SAE, paper 2007-01-3610.
- [55] Bleechmore C., Brewster S. 2007 “Dilution strategies for load and NOx management in a hydrogen fueled direct injection engine.” SAE, paper nr 2007-01-4097.

- [56] Subramanian V., Mallikanjuna J.M., Ramesh A. 2007 “Effect of water injection and spark timing on the nitric oxide emission and combustion parameters of a hydrogen fueled spark ignition engine.” *International Journal of Hydrogen Energy*;32:1159–73.
- [57] Welch A., Mumford D., Munshi S., Holsbery J., Boyer D., Younhins M., Jung H. 2008 “Challenges in developing hydrogen direct injection technology for internal combustion engines.” SAE, paper 2008-01-2379.
- [58] Kiesgen G., Kluting M., Bock C., Fischer H. 2006 “The new 12-cylinder hydrogen engine in the 7 series: the H₂ ICE age has begun.” SAE, paper 2006-01-0431.
- [59] Eichlseder H., Wallner T., Freymann R., Ringler J. 2003 “The potential of hydrogen internal combustion engines in a future mobility scenario.” SAE, paper 2003-021-2267.
- [60] Sierens R., Verhelst S. 2003 “Influence of the injection parameters on the efficiency and power output of a hydrogen fueled engine.” *Transactions of the ASME. Journal of Engineering Gas Turbines Power*; 125:444–9.
- [61] Wallner T., Nande A.M., Naber J. 2005 “Evaluation of injector location and nozzle design in a direct-injection hydrogen research engine.” SAE, paper 2008-01-1785.
- [62] Verhelst S.; Maesschalck P.; Rombaut N.; Sierens R. 2009 “Efficiency comparison between hydrogen and gasoline, on a bi-fuel hydrogen/gasoline engine” *International Journal of Hydrogen Energy*, 34 (5), pg. 2504-2510
- [63] Negurescu N., Pana C., Ginu M., Soare D. 2006 “Aspects regarding the combustion of hydrogen in spark ignition engine.” SAE paper 2006-01-0651.
- [64] Sierens R., Verhelst S. 2001 “Experimental study of a hydrogen fueled engine.” *Transaction of ASME Journal of Engineering Gas Turbines Power*;123:211–6.

- [65] Fushui L. 2004 “CFD study on hydrogen engine mixture formation and combustion.” Gottingen: Cuvillier Press.
- [66] Tang X.G., Daniel M.K., Robert J.N. “Ford P2000 hydrogen engine dynamometer development.” 2002 SAE paper no. 2002-01-0242.
- [67] Swain M.R. 1996 “Design and testing of a dedicated hydrogen fueled engine.” SAE paper no. 961077.
- [68] Isadore L.D., Frank E.B. 1958 “Survey of hydrogen combustion properties.” Supersedes NACA research memorandum E57D24, Report 1383.
- [69] Keck JC. 1982 “Turbulent flame structure and speed in spark-ignition engines.” Process Combustion Institute;145:1–66.
- [70] Liu X., Liu F., Zhou L., Sun B., Schock H. J., 2008 “Backfire prediction in a manifold injection hydrogen internal combustion engine” International Journal of Hydrogen Energy 33 (14), pg. 3847-3855
- [71] Tang X., Kabat D.M., Natkin R.J., Stockhausen W.F., Heffel J.W. 2002 “Ford P2000 hydrogen engine dynamometer development.” SAE 2002-01-0242.
- [72] Tang X., Natkin R.J. 2003 “Hydrogen IC engine boosting performance and NO_x study.” SAE 2003-01-0631.
- [73] Jing-Ding L., Ying-Qing L., Tian-Shen D. 1986 “Improvement on the combustion of a hydrogen fueled engine.” International Journal of Hydrogen Energy;11(10):661–8.
- [74] White C.M., Steeper R.R., Lutz A.E. 2006 “The hydrogen-fueled internal combustion engine: a technical review.” International Journal of Hydrogen Energy; 31(10): 1292–305.

- [75] Sierens R., Verhelst S. 2001 “Experimental study of a hydrogen fuelled engine.” *Journal of Engineering Gas Turbines Power*;123(1):211–16.
- [76] Szwaja S.; Bhandary K.R.; Naber J.D. 2007 “Comparisons of hydrogen and gasoline combustion knock in a spark ignition engine.” *International Journal of Hydrogen Energy*, 32 (18), pg. 5076-5087
- [77] Brunt M., Pond C., Biundo J. 1998 “Gasoline engine knock analysis using cylinder pressure data.” SAE 980896.
- [78] Worret R., Bernhardt S., Schwarz F., Spicher U. 2002 “Application of different cylinder-pressure-based knock detection methods in spark ignition engines.” SAE 2002-01-1668.
- [79] Scholl D.J., Stockhausen W.F., Russ S.G. 1997 “Detection of spark knock oscillations: dependence on combustion temperature”. SAE 970038.
- [80] Berckmüller M. 2003 “Potentials of a charged SI-hydrogen engine.” SAE 2003-01-3210.
- [81] Smith J.R., Aceves S., Blarigan P.V. 1995 “Series hybrid vehicles and optimized hydrogen engine design.” SAE 951955.
- [82] Bradley D., Lawes M., Kexin L., Verhelst S., Wooley R. 2007 “Laminar burning velocities of lean hydrogen–air mixtures at pressures up to 1.0MPa.” *Combust Flame*; 149(1,2):162–72.
- [83] Naber J.D., Siebers L.D. 1998 “Hydrogen combustion under diesel engine conditions.” *International Journal of Hydrogen Energy*; 23(5):363–71.

- [84] Kahraman E.; Ozcanli S. C.; Ozerdem B. 2007 “An experimental study on performance and emission characteristics of a hydrogen fuelled spark ignition engine” *International Journal of Hydrogen Energy*, 32 (12), pg. 2066-2072
- [85] Das L.M., Gulati R., Gupta P.K. 2000 “A comparative evaluation of the performance characteristics of a spark ignition engine using hydrogen and compressed natural gas as alternative fuels.” *International Journal of Hydrogen Energy*;25(8):783–93.
- [86] Mars A., Haks A. 2003 “A prediction study of a spark ignition supercharged hydrogen energy.” *Energy Conver Manage*; 44(20):3143–50.
- [87] Das L.M. 2002 “Hydrogen engine: research and development” (R&D) programs in Indian Institute of Technology (IIT). Delhi *International Journal of Hydrogen Energy*; 27(9):953–65.
- [88] Karim G.A. 2003 “Hydrogen as a spark ignition engine fuel.” *International Journal of Hydrogen Energy*; 28(5):569–77.
- [89] Li H., Karim G.A. 2004 “Knock in spark ignition hydrogen engine.” *International Journal of Hydrogen Energy*; 29(8):859–65.
- [90] Homan H.S. 1978 “An experimental study of reciprocating internal combustion engines operated on hydrogen”. PhD thesis, Cornell University.
- [91] Mars A. 2004 “Effect of compression ratio, equivalence ratio and engine speed on the performance and emission characteristics of a spark ignition engine using hydrogen as a fuel.” *Renewable Energy*; 29(15):2245–60.
- [92] Li H., Karim G.A. 2005 “Exhaust emissions from an SI engine operating on gaseous fuel mixtures containing hydrogen.” *International Journal of Hydrogen Energy*;30(13–14):1491–9.

- [93] Mars A. 2000 “Performance study of a four-stroke spark ignition engine working with both of hydrogen and ethyl alcohol as supplementary fuel.” *International Journal of Hydrogen Energy*; 25(10):1005–9.
- [94] Lee J.T., Kim Y.Y., Lee C.W. 2001 “An investigation of a cause of backfire and its control due to crevice volumes in a hydrogen fuelled engine.” *Transactions of ASME*; 123:204–10.
- [95] Das L., Rohit Gulati M., Gupta P.K. 2000 “Performance evaluation of a hydrogen fuelled spark engine using electronically controlled solenoid actuated injection system.” *International Journal of Hydrogen Energy*; 25(8):569–79.
- [96] Lee S.J., Yi H.S, Kim E.S. 1995 “Combustion characteristic of intake port injection type hydrogen fuelled engine.” *International Journal of Hydrogen Energy*;20(4): 317–22.
- [97] James W.H. 2003a “NO_x emission and performance data for a hydrogen fuelled internal combustion engine at 1500 rpm using exhaust gas recirculation.” *International Journal of Hydrogen Energy*; 28(8):901–8.
- [98] James W.H. 2003b “NO_x Emission reduction in a hydrogen fuelled internal combustion engine at 3000 rpm using exhaust gas recirculation.” *International Journal of Hydrogen Energy*; 28(11):1285–92.
- [99] Das L.M. 2002 “Near term introduction of hydrogen engines for automotive application.” *International Journal of Hydrogen Energy*; 27(5):479–87.
- [100] Mars A. 2003 “A prediction study of a spark ignition supercharged hydrogen engine.” *Energy Conversion and Management*; 44:3143–50.
- [101] Lanzafame R. 1999 “Water injection effects in a single cylinder CFR engine.” SAE paper 1999-01-0568.

- [102] Morse N.T., Brueckner S.R., Bohac S.V. 2002 “Effect of fuel humidity on the performance of a single cylinder research engine operating on hydrogen”. SAE paper 2002-01-2685.
- [103] Bohacik T. 1996 “Constant volume adiabatic combustion of stoichiometric hydrogen oxygen mixtures.” *Journal of Renewable Energy* 1996;9:1254–7.
- [104] Hailin L., Karim G.A. 2004 “Knock in spark ignition hydrogen engine.” *International Journal of Hydrogen Energy*; 29(8):859–65.
- [105] Hailini L., Karim G.A, 2002 “The performance of hydrogen oxygen SI engine.” SAE paper 2002-21-2688.
- [106] Toshio S., Nakajima Y., Fatakuchi T. 2000 “Thermal efficiency analysis in a hydrogen premixed combustion engine.” *SAE Rev* 2000;21:177–82.
- [107] Homan H.S., McLean W.J., De Boer P.C.T. 1983 “The effect of fuel injection on NOx emissions and undesirable combustion for hydrogen fuelled piston engines.” *International Journal of Hydrogen Energy*; 8(2):131–46.
- [108] Subramanian V.; Mallikarjuna J.M.; Ramesh A. 2007 “Effect of water injection and spark timing on the nitric oxide emission and combustion parameters of a hydrogen fuelled spark ignition engine.” *International Journal of Hydrogen Energy*, 32 (9), pg. 1159-1173
- [109] Studies of natural gas conversion and dual fuel systems, 2008, private communication, Shiraz, Iran
- [110] Guzzella L., Onder C.H. 2004 “Introduction to modeling and control of internal combustion engine systems” book (pp. 24, and 182). Germany: Springer-Verlag Berlin Heidelberg


- [111] SAE International, 2006, "Hydrogen IC Engines" (pp. 45, 51), USA: SAE International
- [112] Merker G.P. , Schwarz C., Stiesch G., Otto F. 2006 "Simulating Combustion" (pp. 12-14) Germany: Springer-Verlag Berlin Heidelberg
- [113] Lumley J.L. 1999 "Engines an introduction" (pp. 34, 35, 218-220) USA: Cambridge University Press
- [114] Gillespie, T. D. 1992. "Fundamentals of Vehicle Dynamics." SAE International. USA: Warrendale
- [115] Basshuysen R.V., Schafer, F. 2004 "Internal Combustion Engine Handbook, basics, components, systems, and perspectives." SAE International. Warrendale, PA, USA.
- [116] Customer Guide Automotive, 2009 "1990-1998 GMC Sierra: Full Review", how stuff works. (available online at <http://consumerguideauto.howstuffworks.com/1990-to-1998-gmc-sierra-6.htm>)
- [117] Kit cars USA, 2009 "The Chevrolet small block V8 through the years" Hot Rod Magazine yearbook, USA
- [118] Allen T. T., 2006. "Introduction to Engineering Statistics and Six Sigma Statistical Quality Control and Design of Experiments and Systems." Germany: Springer-Verlag London Limited
- [119] Yang K., El Haik B. S., 2003 "Design for Six Sigma. A Roadmap for Product Development. "(McGraw-Hill, 2003) USA: New York
- [120] Cengel Y. A., Boles Michael A., (2002) Thermodynamics, An engineering approach 4th edition. New York: McGraw Hill Higher Education.

[121] Advanced Technologies and Energy Efficiency 2010 “Where does the energy go?”
Fuel Economy Guide, USA: Gaithersburg, MD (available online at
<http://www.fueleconomy.gov/FEG/atv.shtml>)

[122] Best Nest, 2009 “SunJet 150 Mini-Solar Pump Kit” Water Gardens USA:
Cincinnati, OH (<http://www.bestnest.com/bestnest/RTProduct.asp?SKU=STI-21410R01>)

Appendix A

Emission test results running on gasoline fuel





Certificate Number:
176 381 5825

ONTARIO DRIVE CLEAN PROGRAM

VEHICLE EMISSIONS INSPECTION REPORT

Test Date/Time: Nov 12, 2008 @ 17:46:10

ONTARIO MINISTRY OF THE ENVIRONMENT

VEHICLE INFORMATION

Year: 1986	Make: GMC	Model: PICKUP
VIN: 2GTDC14H3G1500604	Engine Size: 05.0L	Cylinders: 08
GVWR: 2722 kg	Estimated Test Weight: 2268 kg	Inspection Type I


ASM 2525/CURB IDLE TAILPIPE EMISSIONS INSPECTION

	40 km/h			CURB IDLE		
	Limit	Reading	Result	Limit	Reading	Result
HC ppm	88	39	PASS	300	57	PASS
CO %	0.73	0.04	PASS	1.5	0.74	PASS
NO ppm	1523	536	PASS	N/A	N/A	N/A
RPM	1493	VALID		RPM	1380	VALID
Dilution	14.04	VALID		Dilution	14.49	VALID

EMISSIONS CONTROL SYSTEMS INSPECTION

Air Injection System:	N/A
Exhaust Gas Recirculation System:	N/A
Positive Crankcase Ventilation System:	N/A
Catalytic Converter:	N/A
Fuel Evaporative System:	N/A
Thermostatic Air Cleaner System:	N/A
Gas Cap Pressure Test:	PASS
Fuel filler integrity check:	N/A


OVERALL TEST RESULT: PASS



POSTAL CODE: N/A PROGRAM AREA: N/A REPAIR COST LIMIT: N/A

THANK YOU FOR YOUR CONTRIBUTION TO CLEAN AIR. BRING THIS REPORT TO REGISTER YOUR VEHICLE. IT IS VALID FOR ONE YEAR. THIS TEST DETERMINES COMPLIANCE WITH TAILPIPE EMISSIONS LIMITS AT THE TIME OF THE TEST. BY LAW ALL EMISSIONS CONTROL EQUIPMENT MUST BE INSTALLED AND FUNCTIONING AT ALL TIMES.

FOR PIO USE ONLY



RJXN56MGBXFUN8YWRXTF

KIOSK SECURITY CODE

ZEAN37

DRIVE CLEAN FACILITY

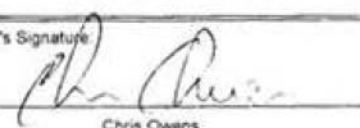
DCF NAME: Durham Auto Works ADDRESS: 40 Russett Ave, Unit A Oshawa ON L1G 3R5 PHONE: (905) 576-5406 INSPECTOR ID: 7993	REPORT NUMBER: 020416 DCF NUMBER: 1890 ANALYZER NUMBER: A1763 SOFTWARE VERSION: 4.54
---	---

VEHICLE EMISSIONS INSPECTION QUESTIONS

For additional information, please contact the Drive Clean Call Centre

1-888-758-2999
www.driveclean.com

Inspector's Signature:



Chris Owens


217 725

Appendix B

Emission test results running on hydrogen fuel

ONTARIO DRIVE CLEAN PROGRAM VEHICLE EMISSIONS INSPECTION REPORT

Test Date/Time: Aug 19, 2009 @ 15:32:21




ONTARIO MINISTRY OF THE ENVIRONMENT

VEHICLE INFORMATION						
Year: 1986	Make: GMC	Model: PICKUP				
VIN: 2GTDC14H3G1500604	Engine Size: 05.7L	Cylinders: 08				
GVWR: 2722 kg	Estimated Test Weight: 2268 kg	Inspection Type: I				

ASM 2525/CURB IDLE TAILPIPE EMISSIONS INSPECTION							EMISSIONS CONTROL SYSTEMS INSPECTION	
	40 km/h			CURB IDLE				
	Limit	Reading	Result	Limit	Reading	Result		
H/C ppm	88	N/A	N/A	300	N/A	N/A	Air Injection System:	N/A
CO %	0.73	N/A	N/A	1.5	N/A	N/A	Exhaust Gas Recirculation System:	N/A
NO ppm	1523	N/A	N/A	N/A	N/A	N/A	Positive Crankcase Ventilation System:	N/A
	RPM	0	BYPASS	RPM	0	N/A	Catalytic Converter:	N/A
	Dilution	N/A	N/A	Dilution	N/A	N/A	Fuel Evaporative System:	N/A
							Thermostatic Air Cleaner System:	N/A
							Gas Cap Pressure Test:	PASS
							Fuel filler integrity check:	N/A

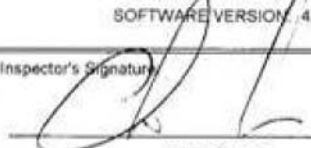
OVERALL TEST RESULT: INCOMPLETE



POSTAL CODE: N/A PROGRAM AREA: N/A REPAIR COST LIMIT: N/A

Exhaust + sample too diluted - will not pick anything from tailpipe

DRIVE CLEAN FACILITY	
DCF NAME: Durham Auto Works	REPORT NUMBER: 021744
ADDRESS: 40 Russell Ave, Unit A Oshawa ON L1G 3R5	DCF NUMBER: 1890
PHONE: (905) 576-5406	ANALYZER NUMBER: A11763
INSPECTOR ID: 7993	SOFTWARE VERSION: 4.54

VEHICLE EMISSIONS INSPECTION QUESTIONS	Inspector's Signature
For additional information, please contact the Drive Clean Call Centre 1-888-758-2999 www.driveclean.com	 Chris Owens

Appendix C: TRIZ Methodology, 39 Design Parameters

Parameter 1. Weight of moving object:

This is the weight of the overall vehicle.

Parameter 2. Weight of stationary object

The total weight of the water pump.

Parameter 3. Length of moving object

the total length of the water to travel to the engine

Parameter 4. Length of stationary object

The total length of the water line

Parameter 5. Area of moving object

The total area of the engine compartment

Parameter 6. Area of stationary object

The area of the pump and the water tank being mounted

Parameter 7. Volume of moving object

This refers to the volumetric space of the engine bay

Parameter 8. Volume of stationary object

This refers to the total volume of water travelling in the water lines

Parameter 9. Speed

This refers to the total speed of the water travelling, speed of the engine (RPM) and speed of the vehicle.

Parameter 10. Force (intensity)

The amount of force required to inject the water.

Parameter 11. Stress or pressure

The total pressure for the water to be, before it is injected to mix with the fuel.

Parameter 12. Shape

The overall shape of the water pump design

Parameter 13. Stability of the object's composition

The ability of the water pump to withstand corrosion

Parameter 14. Strength

The strength of the brackets supporting the water pump during operation.

Parameter 15. Duration of action of moving object

The duration of the water pump being active during engine operation.

Parameter 16. Duration of action by stationary object

The duration of the water pump being supported by the brackets

Parameter 17. Temperature

The overall temperature of the engine

Parameter 18. Illumination Intensity

Not required

Parameter 19. Use of energy by moving object

The energy required to power the water pump

Parameter 20. Use of energy by stationary object

The energy required to keep water from freezing during winter conditions.

Parameter 21. Power

The power output from the engine

Parameter 22. Loss of Energy

The loss of energy due to the operation of all the components in the vehicle.

Parameter 23. Loss of substance

The material composition of water introduction into the engine.

Parameter 24. Loss of information

The loss of information through the installed wires from the excess heat coming from the engine.

Parameter 25. Loss of Time

The time to deliver the water if information is lost.

Parameter 26. Quantity of substance/the matter

The amount of water available in the tank.

Parameter 27. Reliability

The reliability of the water pump not failing during the engine operation

Parameter 28 Measurement accuracy

The accuracy of temperature, water pressure, fuel pressure and engine temperature readings.

Parameter 29. Manufacturing precision

Not required (as this deals with the pump manufacturing)

Parameter 30. Object-affected harmful factors

Too much vibration, would affect the delivery of the water

Parameter 31. Object-generated harmful factors

The excess heat generated would alter the outcome of the results

Parameter 32. Ease of manufacture

Would refer to the finished product and how easily it can be replicated.

Parameter 33. Ease of operation

Refers to the easy operation of the water pump after installation.

Parameter 34. Ease of repair

How easily the water pump can be repaired. Space, tools requirements are the factors involved.

Parameter 35. Adaptability or versatility

This refers to how adaptable the water pump can be with a different system.

Parameter 36. Device complexity

How complex the design can be and this would affect the ease of reparability

Parameter 37. Difficulty of detecting and measuring

The factors affecting the measurements of the water remaining in the tank, the water pressure, and water delivery to the engine.

Parameter 38. Extent of automation

This refers to the automation to the point that it can be turned on by a switch and the programmed electronics would follow the sequences.

Parameter 39. Productivity

The productive outcome of the water pump installed and the achieved desired outcome.

Appendix D: TRIZ Methodology, 40 Incentive Principles

Principle 1. Segmentation

- A. Divide an object into independent parts.
 - *Pump, water line, wiring, water tank*

Principle 2. Taking out

- A. Separate an interfering part or property from an object, or single out the only necessary part (or property) of an object.
 - Includes wiring and water lines getting in the way of the engine operation

Principle 3. Local quality

- A. Change an object's structure from uniform to non-uniform, change an external environment (or external influence) from uniform to non-uniform.
 - Location of where the water lines are being mounted away from the engine

Principle 4. Asymmetry

- A. A. Change the shape of an object from symmetrical to asymmetrical.
 - The water lines should be the same from the tank to the engine

Principle 5. Merging

- A. Bring closer together (or merge) identical or similar objects, assemble identical or similar parts to perform parallel operations.
 - Merging all the wiring together

Principle 6. Universality

- A. Make a part or object perform multiple functions; eliminate the need for other parts.

Principle 7. "Nested doll"

- A. Place one object inside another; place each object, in turn, inside the other.
 - Location of the pump inside the engine bay

Principle 8. Anti-weight

- A. To compensate for the weight of an object, merge it with other objects that provide lift.
- B. To compensate for the weight of an object, make it interact with the environment (e.g. use aerodynamic, hydrodynamic, buoyancy and other forces).

Principle 9. Preliminary anti-action

- A. If it will be necessary to do an action with both harmful and useful effects, this action should be replaced with anti-actions to control harmful effects.
- B. Create beforehand stresses in an object that will oppose known undesirable working stresses later on.

Principle 10. Preliminary action

- A. Perform, before it is needed, the required change of an object (either fully or partially).
 - *Pre-clean the mounting area*
- B. Pre-arrange objects such that they can come into action from the most convenient place and without losing time for their delivery.
 - *Arrange all the parts to be installed*

Principle 11. Beforehand cushioning

- A. Prepare emergency means beforehand to compensate for the relatively low reliability of an object.

Principle 12. Equipotentiality

- A. In a potential field, limit position changes (e.g. change operating conditions to eliminate the need to raise or lower objects in a gravity field).

Principle 13. 'The other way round'

- A. Invert the action(s) used to solve the problem (e.g. instead of cooling an object, heat it).
- B. Make movable parts (or the external environment) fixed, and fixed parts movable).

Principle 14. Spheroidality - Curvature

- A. Instead of using rectilinear parts, surfaces, or forms, use curvilinear ones; move from flat surfaces to spherical ones; from parts shaped as a cube (parallelepiped) to ball-shaped structures.

Principle 15. Dynamics

- A. Allow (or design) the characteristics of an object, external environment, or process to change to be optimal or to find an optimal operating condition.

Principle 16. Partial or excessive actions

- A. If 100 percent of an object is hard to achieve using a given solution method then, by using 'slightly less' or 'slightly more' of the same method, the problem may be considerably easier to solve.

Principle 17. Another dimension

- A. To move an object in two- or three-dimensional space.

Principle 18. Mechanical vibration

- A. Cause an object to oscillate or vibrate.
- B. Increase its frequency (even up to the ultrasonic).

Principle 19. Periodic action

- A. Instead of continuous action, use periodic or pulsating actions.

Principle 20. Continuity of useful action

- A. Carry on work continuously; make all parts of an object work at full load, all the time.

Principle 21. Skipping

- A. Conduct a process, or certain stages (e.g. destructible, harmful or hazardous operations) at high speed.

Principle 22. "Blessing in disguise" or "Turn Lemons into Lemonade"

- A. Use harmful factors (particularly, harmful effects of the environment or surroundings) to achieve a positive effect.
- B. Eliminate the primary harmful action by adding it to another harmful action to resolve the problem.

Principle 23. Feedback

- A. Introduce feedback (referring back, cross-checking) to improve a process or action.
- B. If feedback is already used, change its magnitude or influence.

Principle 24. 'Intermediary'

- A. Use an intermediary carrier article or intermediary process.
- B. Merge one object temporarily with another (which can be easily removed).

Principle 25. Self-service

- A. Make an object serve itself by performing auxiliary helpful functions

Principle 26. Copying

- A. Instead of an unavailable, expensive, fragile object, use simpler and inexpensive copies.
- B. Replace an object, or process with optical copies.

Principle 27. Cheap short-living objects

- A. Replace an inexpensive object with a multiple of inexpensive objects, comprising certain qualities (such as service life, for instance).

Principle 28 Mechanics substitution

- A. Replace a mechanical means with a sensory (optical, acoustic, taste or smell) means.
- B. Use electric, magnetic and electromagnetic fields to interact with the object.

Principle 29. Pneumatics and hydraulics

- A. Use gas and liquid parts of an object instead of solid parts (e.g. inflatable, filled with liquids, air cushion, hydrostatic, hydro-reactive).

Principle 30. Flexible shells and thin films

- A. Use flexible shells and thin films instead of three dimensional structures

- B. Isolate the object from the external environment using flexible shells and thin films.

Principle 31. Porous materials

- A. Make an object porous or add porous elements (inserts, coatings, etc.).

Principle 32. Color changes

- A. Change the color of an object or its external environment.
- B. Change the transparency of an object or its external environment.

Principle 33. Homogeneity

- A. Make objects interacting with a given object of the same material (or material with identical properties).

Principle 34. Discarding and recovering

- A. Make portions of an object that have fulfilled their functions go away (discard by dissolving, evaporating, etc.) or modify these directly during operation.

Principle 35. Parameter changes

- A. Change an object's physical state (e.g. to a gas, liquid, or solid).
- B. Change the concentration or consistency.
- C. Change the degree of flexibility.

Principle 36. Phase transitions

- A. Use phenomena occurring during phase transitions (e.g. volume changes, loss or absorption of heat, etc.).

Principle 37. Thermal expansion

- A. Use thermal expansion (or contraction) of materials.
- B. If thermal expansion is being used, use multiple materials with different coefficients of thermal expansion.

Principle 38. Strong oxidants

- A. Replace common air with oxygen-enriched air.
- B. Replace enriched air with pure oxygen.
- C. Expose air or oxygen to ionizing radiation.
- D. Use ionized oxygen.
- E. Replace ozonized (or ionized) oxygen with ozone.

Principle 39. Inert atmosphere

- A. Replace a normal environment with an inert one.
- B. Add neutral parts, or inert additives to an object.

Principle 40. Composite materials

- A. Change from uniform to composite (multiple) materials.